Project Title:

Innovative compact HYbrid electrical/thermal storage systems for low energy BUILDings

Project Acronym:

HYBUILD

Grant Agreement Nº: 768824

Collaborative Project

Deliverable Report

Deliverable Number:

D6.3

Deliverable title:

Report of the energy performance analysis after intervention

Related task:	T6.1: IPMPV Guideline for HYBUILD project. T6.2: Installation of the measurement system for the pre-intervention monitoring T6.3: Installation & commissioning T6.4: Monitoring and evaluation after installation
Lead beneficiary:	NOBATEK/INEF4
Authors and institutions:	Saed Raji (NBK), Aurélien Henon (NBK), Baptiste Durand-Estebe (NBK), Gabriel Zsembinszki (UDL), Luisa F. Cabeza (UDL), David Vérez (UDL), Àlex Florensa (ALM), Chryso Heracleous (UCY), Chrysanthos Charalambous (UCY), Venizelos Efthymiou (UCY), Aimilios Michael (UCY), Federico Trentin (EURAC), Mattia Dallapiccola (EURAC), Werner Pink (PINK)
Due date:	March 31st, 2022

This project has received funding from the European Union's Horizon 2020 research and innovation programme *under grant agreement No 768824.*
The content of this document reflects only the author's view and the Commission is not responsible for any use that may be made of the information it contains.

DOCUMENT STATUS HISTORY		
Date	Description	Partner
23/03/22	Review draft	NBK
31/03/22	Reviewed	UDL, R2M, COMSA
01/04/22	Final	NBK
30/05/22	Amendments to Expert Comments	NBK
15/09/22	Final. Included last demo results.	NBK, UDL, UCY, COMSA

Table of contents

1 EXECUTIVE SUMMARY

1.1 Description of the deliverable content and purpose

This document provides the synthesis of the main results from the HYBUILD demonstration activities: details on the demonstration installations, collected data sets, components analysis, and the evaluation of the Key Performance Indicators (KPI) selected for the project (deliverable D1.3). The pre-intervention monitoring was conducted during the baseline period of the HYBUILD project meaning before the installation of the HYBUILD systems in the three demo sites; these results and the corresponding methodology have already been presented in D6.2. The monitoring plan for each demo site was discussed and validated by demo sites' owners and all the partners involved in the definition and production of KPIs for the project.

The **Key Performance Indicators** (KPI) are proposed on the basis of the seven indicators which have been selected and precisely described in deliverable D1.3. Their calculation for each demonstration installation represents an important result for the assessment of the HYBUILD systems; they are to be considered also with the perspective of the current TRL of the system and its respective components.

A one-year pre-intervention monitoring period had been carried out in Aglantzia and Langenwang demo sites, and 7 months in Almatret demo site (though both winter and summer conditions are represented). The HYBUILD systems implementation was carried out by end of 2020 for the continental demo site and end of 2021 for the Mediterranean demo sites, as described in deliverable D6.1.

Sections 2 presents an update of the installation and commissioning activities on each demonstration site during the last months of the project.

Section 3 presents the data and corresponding energy analysis at component level.

Section 4 describes the current status of the Key Performance Indicators (KPI) to be calculated. This result is in some cases limited by the final readiness level of the technology. Indeed some KPI are not relevant in the cases the technology does not work yet as well as initially expected at the start of the project.

1.2 Relation with other activities in the project

The activities presented in this deliverable are a consequence of the definition of the measurement and evaluation plan in task 6.1.

The results here, and especially the ones described in section 6 (post-intervention), have been obtained in the context of task 6.4 (monitoring and evaluation after installation).

Of course, all the measurements and monitoring activities are deeply dependent on the technical details of the implementation of the demonstrators, in task 6.3.

1.3 Acronyms and Abbreviations

DHW	Domestic Hot Water
GA	Grant Agreement
HDD	Heating Degree Days
IPMVP	International Performance Measurement and Verification Protocol
KPIs	Key Performance Indicators
MAE	Mean Average Error
M&V	Measurements and Verification
RH	Relative Humidity
ROI	Return on Investment
T	Temperature
DL	Data Logger
ACS	Adaptive Comfort Standard
sMFH	small Multi Family House
HP	Heat Pump
RPW-HEX	Refrigerant-Phase change material-Water HEat eXchanger
SH	Space Heating
SC	Space Cooling
PV	Photovoltaic
BESS	Battery Energy Storage System
SoC	State of Charge
SC(el)	Self-consumption (electric)
SS(el)	Self-sufficiency (electric)
SR(el)	Share of Renewables (electric)
SYS	System
DHN	District Heating Network
PCOP	Period Coefficient of Performance
PPF	Period Performance Factor

1.5 Key performances indicators (KPIs)

Following the methodology described in Deliverable 1.3 (Requirements: Key performance Indicators, system components and performance targets), and considering the HYBUILD main objectives for Mediterranean and Continental HYBUILD systems, the KPIs selected by the project partners are:

- KPI.1 – Thermal energy storage density
- KPI.2 – Seasonal energy performance
- KPI.3 – Share of renewable and self-consumption
- KPI.4 – Energy savings and CO_2 emission savings
- KPI.5 – Compactness
- KPI.6 – Flexibility
- KPI.7 – Return on Investment

For the complete description of the KPIs, the authors refer to D1.3 to evaluate the link between the KPIs and the monitoring system.

Table 1. Relevant KPIs with the corresponding HYBUILD objectives

	HYBUILD objectives	KPI
1	Increase of thermal energy storage density	KPI.1
2	Expected energy and CO_2 emissions reduction ranging from 20% to 40% depending on the configuration and contexts	KPI.2, 3 and 4
3	Increase of seasonal performance of the heating and cooling system	KPI.2
4	Easy to integrate and compact solution into existing building	KPI.5
5	ROI of 8 years for building non-connected to DHC and 15 years for buildings connected to DHC	KPI.7
6	Superior energy performance contributing to the energy system flexibility	KPI.6

2 Commissioning update on the three demo sites

The commissioning of the demonstration installations has been described in deliverable 6.1 submitted on September 30th, 2021.

During the following months, improvements and finetuning activities have continued in order to achieve demonstrators operating as initially expected and gather data as relevant as possible. This section summarizes the installation activities with a special emphasis on the work done over the last months of the project.

2.1 General overview of the demonstration sites

The three demo sites in HYBUILD have been designed according to two different hybrid energy production concepts:

- The Mediterranean concept, for the demo sites in Almatret and Aglantzia (Figure 1).
- The continental concept, for the demo site in Langenwang (Figure 2).

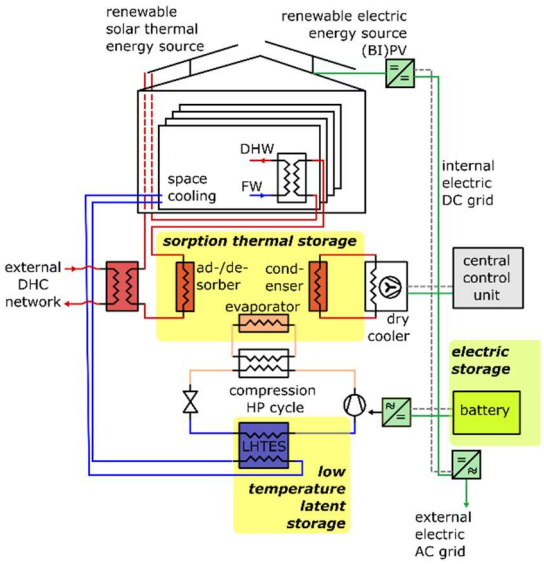

Figure 1. HYBUILD Mediterranean concept

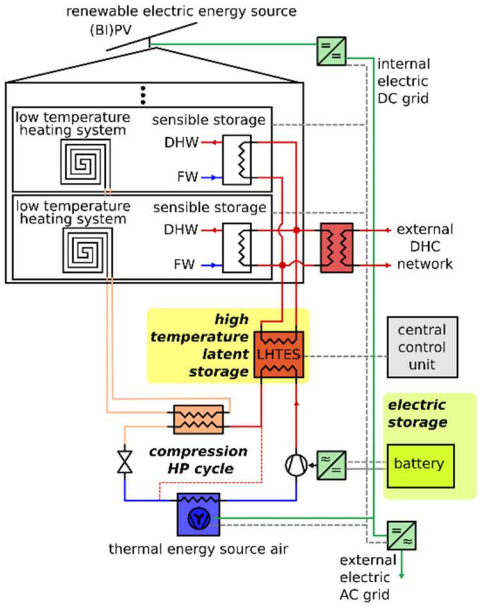

Figure 2. HYBUILD continental concept

2.2 Commissioning of the demonstrator in Almatret

Figure 3. Almatret demo site building

- **Climate:** Mediterranean
- **Site description**: Residential house in Almatret
- **Date of construction**: 1970
- **Current use of the building**: Residential
- **Area**: 107 m^2

In the Almatret demo site, the Mediterranean system is installed and tested. The system contains Fresnel solar collectors to capture the solar thermal energy, photovoltaic (PV) panels to produce electricity from solar radiation, a low temperature storage tank with phase change material (PCM) in thermal contact with the evaporator of the compression system (heat pump), and a sorption thermal storage system thermally connected with the solar thermal collectors and with the condenser of the compression system.

The installation and commissioning started during summer 2021 and is still ongoing.

2.2.1 Description of the installation works

Although the core part of the system installed at the Almatret demo site is identical with the general layout of the Mediterranean system, the actual system includes some particularities that resulted from the adaptation of the system to the local conditions. Specifically, since the building in Almatret to which the system was connected is the house where the doctor lives with his family, it was considered necessary to maintain the current gas-boiler as a back-up to assure uninterrupted supply of both DHW and heating during the period corresponding to the system installation and commissioning. For the same reason, the current heating system based on hot water radiators connected to the gas-boiler was also maintained to provide heating in winter, instead of installing an additional heating system connected to the HYBUILD heat pump. Therefore, the current heating system was connected to the buffer tank of the HYBUILD system through a heat exchanger, to reduce the gas consumption for heating by exploiting the heat produced by the Fresnel solar collectors. The detailed P&ID diagram of the Mediterranean system adaptation to Almatret demo is shown in Figure 4.

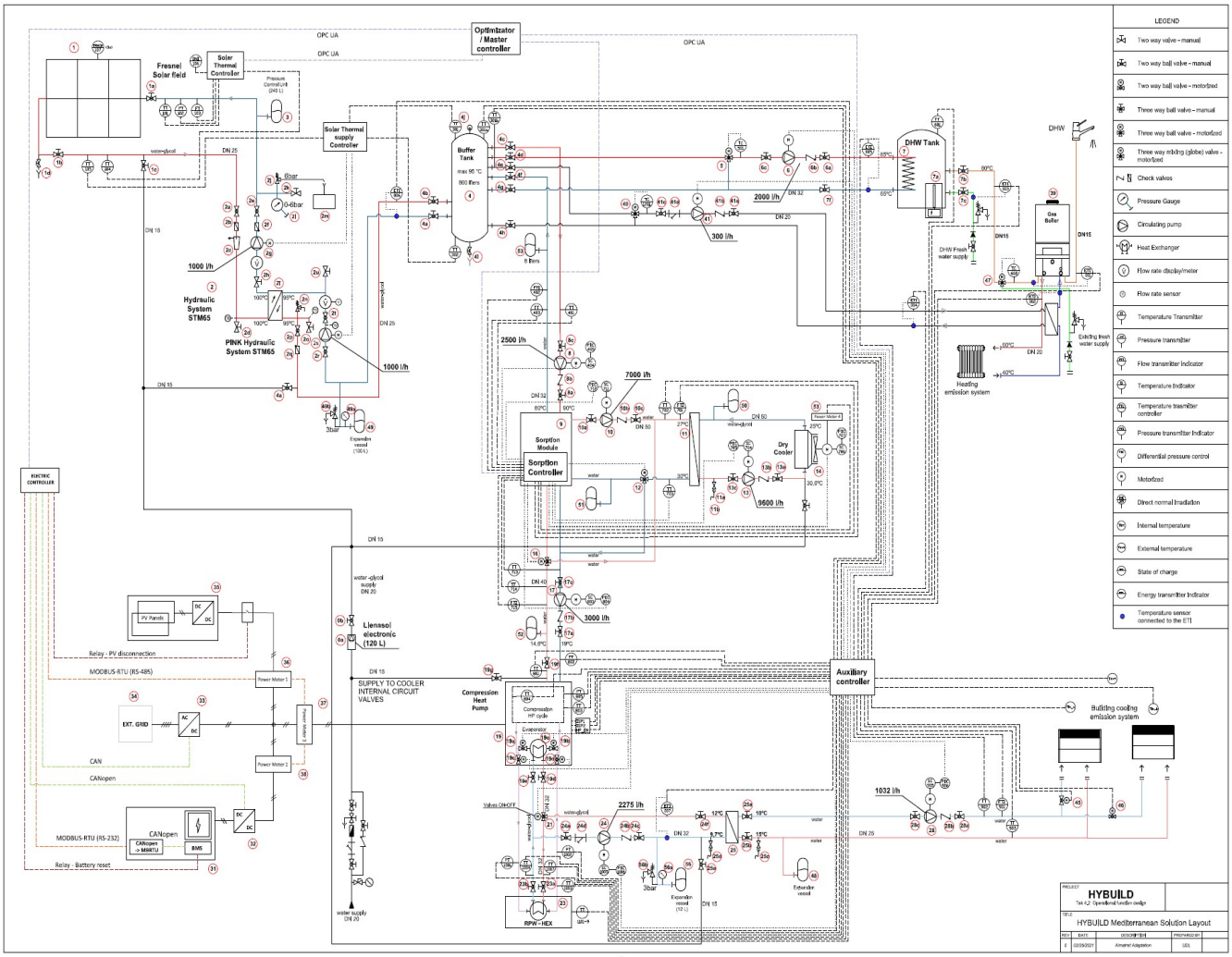

Figure 4. P&ID of the system installed at the Almatret demo site

Installation works actually started well before the commissioning of the system. First of all, the municipality of Almatret built the HYBUILD equipment room, partially funded by HYBUILD and partially from their own funding. Since the building didn't have any cooling system installed prior to HYBUILD system installation, a cooling system using fan-coils was designed and installed during the first half of 2020. The cost of this installation was entirely covered by Almatret municipality from own funding. A schematic of the cooling system is shown in Figure 5.

Moreover, the Fresnel solar collectors, provided by the former project partner Fresnex, were shipped to Almatret and placed in the intended location in September 2019. A total of 6 modules were provided, with a total surface area of mirrors of 60 m^2 and with a receiver placed at the middle of the mirrors in the north-south direction.

A schematic view of the on-site location of the different equipment and components related to the Almatret demo installation and commissioning is shown in Figure 6. As seen in the figure, HYBUILD demo is located very close to the demo of another H2020 project, Innova MicroSolar (grant agreement N° 723596), which also have a field of Fresnel solar collectors that was already installed on-site when HYBUILD project started. This fact put some constraints on the location of the location of different components of the HYBUILD system, such as the Fresnel collectors, PV panels, and dry cooler.

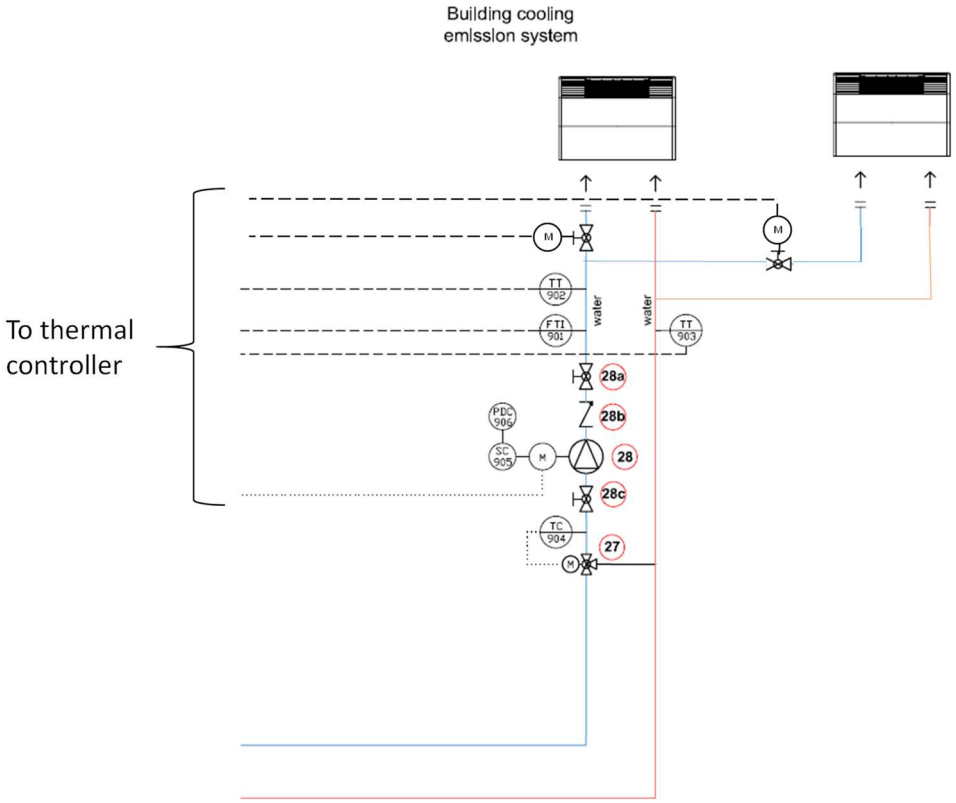

(a)

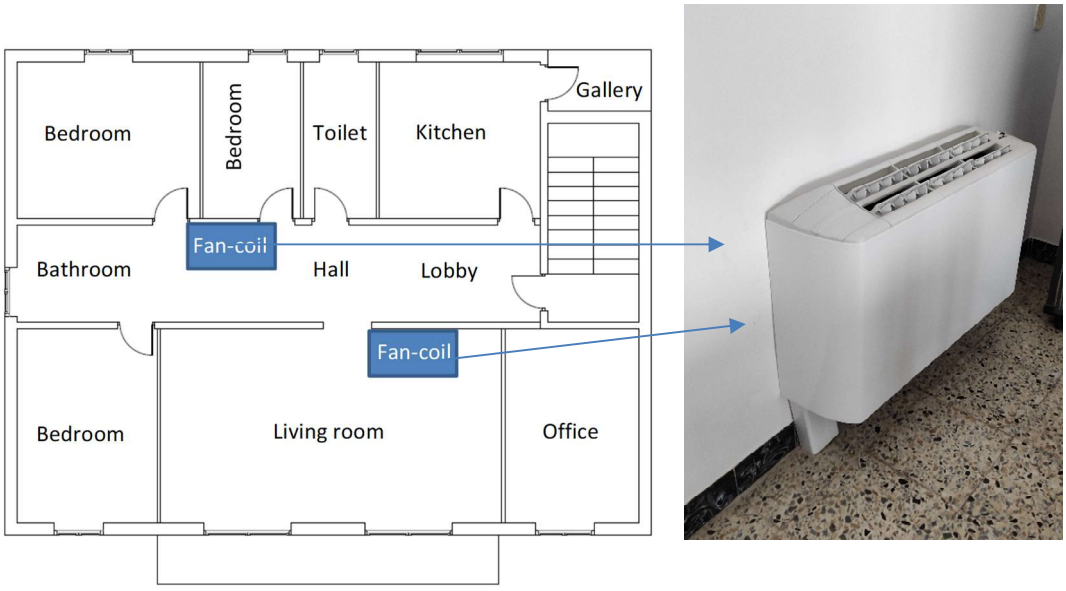

(b)

Figure 5. Details on the cooling system: (a) schematic of the fan-coils connection and (b) location of the fan-coils

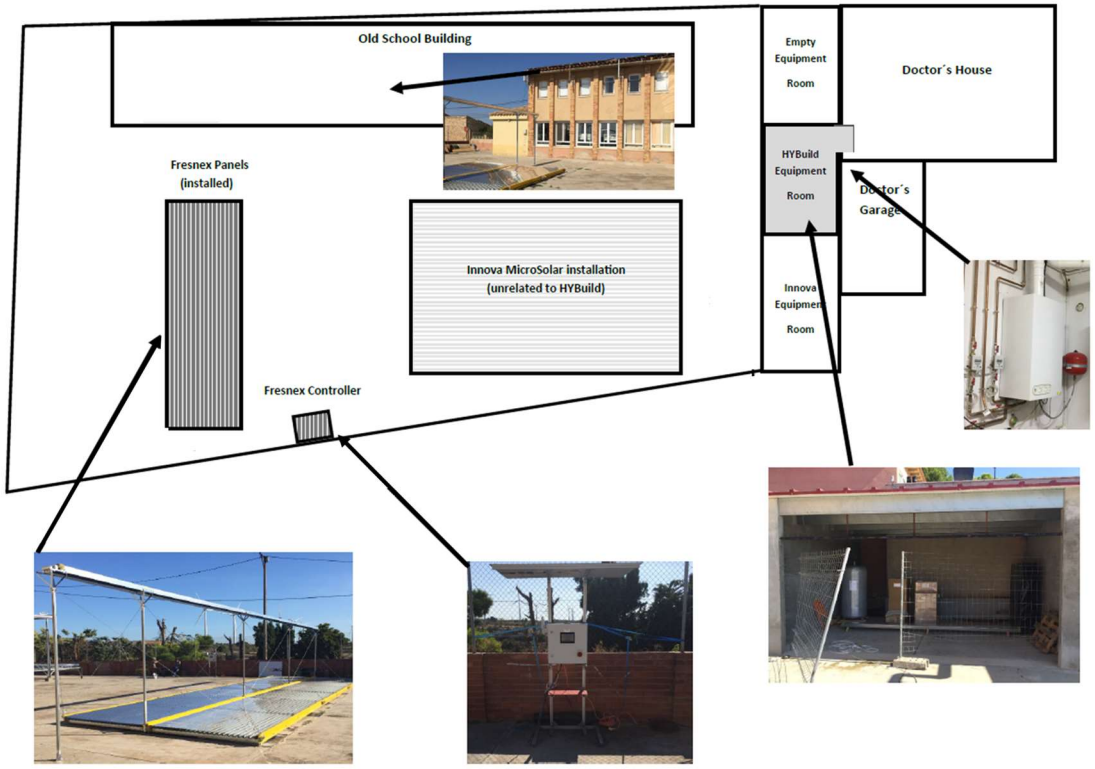

Figure 6. On-site location of the different equipment and components in Almatret

Other equipment that was also shipped to Almatret in September 2019 were the following system components provided by PINK: buffer tank (VarioStar - Vario 800), DHW tank (HDSW160), solar pump station (STM65) for the solar thermal field, pumping station (Grundfos ALPHA1 25-40 180) for the connection between the buffer tank and the DHW tank, two hydraulic pressure units (MADG250), and several auxiliary components such as temperature sensors and insulation material.

The core part of the system, consisting of the Daikin heat pump connected to the latent energy storage tank, the sorption chiller, and the electric rack, was shipped by ITAE-CNR at the end of April 2021 after a complete and successful testing in their laboratory. The dry cooler was shipped by Fahrenheit and arrived to Almatret in June 2021. The size and weight of the dry cooler, combined with the space limitations mentioned above, led to the decision to locate it in a room next to the HYBUILD equipment room. For that, additional work was necessary to improve the conditions of the floor of the room to make it suitable for hosting the dry cooler.

After most of the key system components were already at the demo site, UDL contacted the installer company to start the installation and to make all hydraulic and electrical connections between components. Several meetings were held in April and May 2021 between UDL and the installer company to provide them all the information regarding the system components and to make a full inventory of all material and components of the system. Likewise, the details related to the operating conditions of the system were discussed as well as the schedule for the installation and commissioning of the system.

The installation of the system started with the placement of all the components in their location in the HYBUILD equipment room, according to the schematic shown in Figure 7, prepared by COMSA along with other 3D schematics. At the same time, the order of all the necessary material for the hydraulic and electrical connections was made.

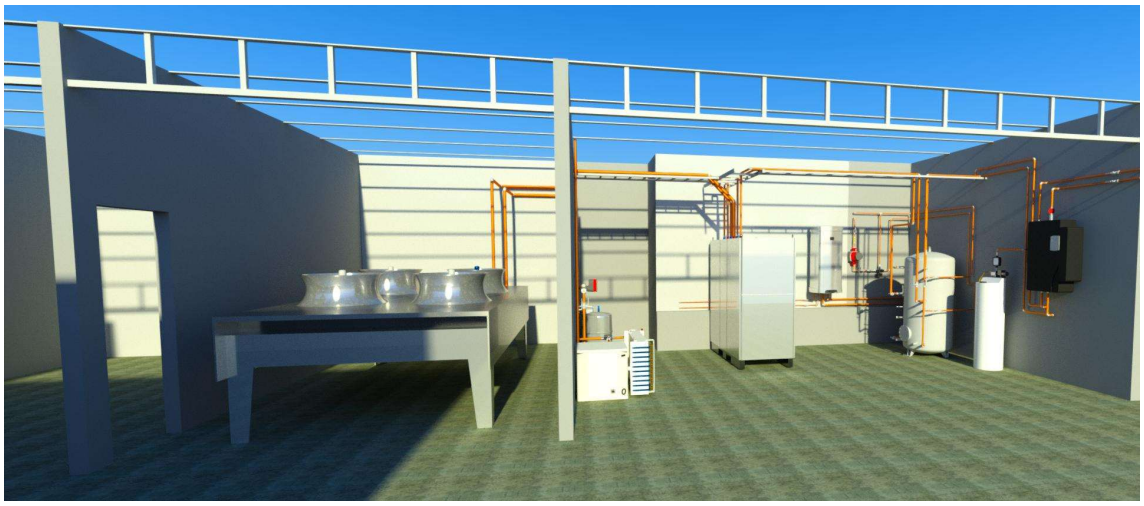

Figure 7. Drawing of the location of the different components in the HYUILD equipment room in Almatret

After all components were placed in their location, the following hydraulic connections between the main system components were realized:

- The solar pump station and the solar field of Fresnel collectors.
- The buffer tank and the sorption chiller, the DHW tank, the solar pump station, and the building heating system.
- The heat pump + latent storage and the building cooling system and the sorption chiller.
- The sorption chiller and the dry cooler.
- The DHW tank and the gas boiler.
- The filling unit and all hydraulic circuits.

Moreover, a dedicated connection between the HYBUILD system with the tap water was done to provide fresh water to the filling unit, as well as to an emergency shower that was also installed near the equipment room for safety reasons.

Since the HYBUILD equipment room is in direct contact with the outdoor air, a mixture of water and glycol was filled in the hydraulic circuits to avoid freezing of the water inside the pipes during the cold periods in winter, when the outdoor temperature can drop down to -5 ºC or even less. The circuits connected with the sorption chiller were also filled with a corrosion inhibitor material to protect the heat exchangers from corrosion. When all hydraulic connections were completed and it was checked that there is no leakage in the system, the pipes were insulated to avoid thermal losses to the ambient.

From the electric connection point of view, several electric connections of the components were also realized. A new PV system was installed by the local company Solenver, whose cost was paid by the Almatret municipality with own funding. The PV system consists of 12 panels of monocrystalline Jinko Solar Cheetah type having a power of 410 Wp each panel. The panels were connected in two strings and connected to the string optimizer Ampt String Optimizer V600 Series. Moreover, electric connections between the electric rack, the string optimizer, the heat pump, and the power grid were performed.

Different electric panels were installed, for individual components or subsystems, and also one for the main distribution circuit and one corresponding to the main protection circuit. A lighting system was also installed in the equipment room.

Furthermore, several devices that will be used for system monitoring and control were also installed. For the monitoring of the system, five thermal energy meters, three power meters, temperature sensors to measure the temperature in the different parts of the system as well as the indoor and ambient temperature, one flow meter in the primary circuit of the solar field,

pressure sensors, and one pyranometer were installed. Most of these sensors were provided by UDL from own funding.

The above-mentioned components, along with the sensors and auxiliary elements such as motorized valves, pumps, temperature and pressure sensors, etc. already installed in the different components, were also used for control purposes of the thermal part of the system. Therefore, these components were connected to the auxiliary PLC built and programmed by UDL, and installed in the control room next to the main distribution circuit panel.

2.2.2 Commissioning process of the demo-system

The installer company that won the tender launched by UDL performed most of the hydraulic and electric connections of the system. According to their estimations, it would take around six weeks to complete the installation of the system. Since the installation started on 20 May 2021, the initial date for the commissioning of the system was the week of 5 July 2021.

Therefore, relevant partners for the commissioning were informed and invited to travel to Almatret to assist in the commissioning of the system. Those partners that couldn't participate on-site, were asked to be full-time available online in case their support was needed. However, due to delays in the installation because of material shortage, the commissioning had to be delayed and rescheduled for 23 July 2021.

Other than the installer company, the following HYBUILD partners were present in Almatret for the commissioning: UDL, ALM, ITAE-CNR, FAHR, ENG, COMSA. Other partners such as NTUA, CSEM, PINK, and AKG confirmed their availability online, either in July or September 2021. Moreover, the installer who did the installation of the fan-coil system inside the house also participated to finalise the connections with the HYBUILD system and to fill the hydraulic circuit. Although Fresnex was not a project partner at the time of the installation and commissioning, Antoni Castells, who worked at Fresnex during the time when they were a project partner, also provided support on-site several times.

During the installation and commissioning of the system, UDL provided the required support to the installer and acted as the link between project partners and the installer company. Moreover, UDL supervised the correct connections of the components with the auxiliary PLC and checked that the low-level control worked properly. ALM assisted in providing logistical support and did a great effort to respond to any need of the installer company or any other project partner. Due to the fact that ITAE-CNR were very familiarized with the core part of the system that was tested in their laboratory, their presence in Almatret was very helpful in providing support to the commissioning of the heat pump and sorption chiller, as well as to solve possible issues related to these components. The presence of one representative from FAHR on 22 and 23 July helped in completing the electric connections between the dry cooler and the sorption chiller, as well as to fill the corrosion inhibitor in the hydraulic circuits connected with the sorption chiller. From the control point of view, ENG provided the computer that contained the Master controller and helped in the realization of communication between the high-level and the low-level control. COMSA was present in Almatret on 23 July to supervise the installation and to check the current status and issues encountered before the commissioning. Antoni Castells went to Almatret to check that the main components of the solar collectors were still working after almost two years in Almatret without being used.

Prior to the commissioning, the key components and actions required for the different subsystems or components were checked. For that, a check-list was prepared by UDL as shown in Table 2.

Table 2. Check-list for supervision of the installation in Almatret

Component or item	No.	Description	Responsible partner	Current state				Depends on	Comments
				Date 1	Date 2	Date 3	Date 4		
1	1.1								
	...								
	1.n								
2	2.1								
	...								
	2.x								
⋮									
n	n.1								
	...								
	n.x								

For the solar field of Fresnel collectors, the correct installation of the sensors and connections to the controller was checked, as well as the installation of a safety valve of 1.5 bar needed for safety reasons. A test was done in June 2021 to check engines performance, which were operating satisfactorily. During July 2021, the mirrors were cleaned, and another test was done to check whether the controller was able to automatically concentrate the solar radiation on the receiver.

For the solar pump station, the correct connection operation was checked to confirm that the pumps work properly and that there is no air in the system. The correct reading of all temperature sensors connected to the controller of the pump station was also checked.

For the buffer tank, the correct installation of all temperature sensors and insulation material was checked, as well as all valves and other sensors in the connections with the other equipment.

For the DHW, the correct installation of sensors, as well as the correct control of the circulation pumps, mixing valve, and gas boiler from the auxiliary PLC was checked.

For the heating system, the correct operation of the circulation pumps and of the gas boiler in the heating mode was checked. The control of the pumps and building thermostat from the auxiliary PLC was checked.

For the sorption module, the correct installation of auxiliary components such as vent valves and of the ethernet cable for the connection with the Master controller was checked. The vacuum in the adsorber circuit was also checked. Moreover, the hydraulic and electric connection of the dry cooler with the sorption module was checked, as well as the installation of the expansion vessel in that circuit.

For the heat pump, an additional amount of refrigerant was filled in the system to reach the correct charge level. The correct connection of all sensors and auxiliary equipment installed in the heat pump and the latent storage with the auxiliary PLC was checked.

For the cooling system connected with the heat pump, the correct operation of the circulation pumps and of the fan-coils was checked, as well as the correct control of this subsystem from the auxiliary PLC.

For the electric rack, a firmware update was necessary, which was done according to indications received from CSEM.

The Master controller was installed in the control room and connected with the system through a local network.

2.2.3 Installation issues / adjustments

This section presents the different problems that were encountered during the installation and commissioning of the system and how they were tackled.

The first problem that affected the entire installation and led to a long delay in the installation of the system was the shortage of material necessary for the installation, as an indirect consequence of the COVID-19 crisis. While some materials such as expansion vessels, pipes, or insulation could be purchased on time, other materials or equipment such as pumps, heat exchangers, filling unit, or electric wires were much more difficult to get than expected.

The second problem that arose before system commissioning was a leakage found in the Fresnel solar collectors after the primary circuit was filled with water and pressurized, and the receiver was heated up to the maximum operating temperature. The leakage occurred at one of the junctions between two modules of the central receiver, and especially when the temperature of the receiver was variating. Antoni Castells (former Fresnex partner) was contacted several times to determine the possible cause of and solution for the leakage in the solar field. Initially, the original gaskets were replaced by new ones provided by Antoni Castells, but the problem was not solved. After that, the original nuts were replaced by self-locking nuts and the problem with that junction was solved. In spite of it, other leakages occurred in two other junctions, so that the original nuts were replaced by self-locking nuts in all the junctions, and the leakage problem seemed to be solved.

Also related to the solar field, some issues were encountered with the controller of this component. Specifically, the controller of the solar field was not able to prevent the temperature of the water inside the receiver from exceeding the boiling point. Likewise, the controller was not able to make the mirrors correctly concentrate solar radiation on the receiver. Therefore, the required changes were implemented in the controller of the solar field with the on-site support of Antoni Castells and remotely by an Austrian control company linked to the current company of Antoni Castells (Ecotherm).

In addition, in February 2022, two of the three motors acting on the solar field mirrors stopped working. Antoni Castells was contacted once again and told us that the motors had to be replaced as they were out of order and the technology was obsolete. Replacement is scheduled for the end of March 2022.

Another issue faced during the commissioning was the fact that the electric system was not working properly, which made it impossible to test the correct operation of the heat pump and sorption system. Despite the presence on-site of one representative from ITAE-CNR, who was familiar with the electric rack that had already been used for testing of the system in their laboratory prior to the shipment to Almatret, it was not possible to realize the full system commissioning at the planned date.

After consulting it with CSEM, different possible explanation for the incorrect operation of the electric system were explored. In a first step, CSEM solved the issue with the remote connection

to the PLC of the DC bus. After that, it was detected that the string optimizer didn't reach the voltage required by the DC bus and a reverse current was even observed. Following CSEM suggestion, the connection between the PV system and the string optimizer was double-checked, and it was found that the type of connectors used was not the one specified by the manufacturer. Moreover, the required blocking diode needed to prevent reverse current was not installed. Therefore, the connectors were replaced with the correct ones and the blocking diode was installed at the correct location.

Subsequently, it was detected that the string optimizer could not reach the 520 V established to operate correctly on the DC-Bus. After a thorough analysis with CSEM, it was decided to add one PV panel to each string in the solar field. Therefore, leaving a total of 7 PVs per string as the final installation.

During the presence in Almatret of the technician from FAHR, he realized that the location of the sorption chiller was not correct because there was not enough space between the back part of the sorption chiller and the wall next to which it was located. Therefore, since all hydraulic connections were already completed, the installer company was contacted again to move the sorption chiller 1 m away from the wall.

After the calibration of the flow meter in the primary circuit of the solar field, it could be noticed that the value of the flow rate in that circuit was far below the expected value. A value of the flow rate much lower than the nominal one makes it difficult or even impossible to properly charge the buffer tank. UDL and PINK worked then together during several weeks to solve the problem.

Following several purges of the solar field to verify that the low flow rate in the solar field circuit could not be attributed to air accumulation in the system, isolation valves and pressure sensors were installed on both the forward and return lines of the solar field to section off the field and measure the pressure drop. After verifying that the pressure drop of the solar field was working as estimated, the piping connections were modified eliminating high pressure drop points, achieving the previously estimated flow values.

During the Spring of 2022, the three motors acting on the solar field mirrors were replaced along with the mechanisms that connect the motors with the mirrors, following the suggestion made by Antoni Castells to improve the reliability of this component of the system. Moreover, additional work on updating and improving the control of the solar field was also performed after the replacement of the motors was done.

After all pending issues were finally solved, a few tests were carried out to check the correct operation of the system in different operation modes. These tests made it possible to identify additional minor issues that required some further adjustments in the low-level system control or in some metering devices.

2.2.4 Pictures and schemes

Figure 8. Outdoor installation in Almatret

Figure 9. HYBUILD system components in Almatret

Figure 10. Hydraulic connections and PLC components in Almatret

Figure 11. Hydraulic installation parts in Almatret

Figure 12. Control visual interface in Almatret

2.3 Commissioning of the demonstrator in Aglantzia

- Aglantzia, Cyprus

Figure 13. Aglantzia demo site building

- **Climate:** Mediterranean – subtropical
- **Site description**: Kiriacou Karaoli Square (Aglantzia)
- **Date of construction**: 2005
- **Current use of the building**: Multifunctional center
- **Area**: 140 m^2

The Aglantzia case study is a listed building located in the city centre square. This pilot aims at converting the current building as a cornerstone of social interaction and creative activities. The building will become a benchmark for a permanent digital exhibition of renewable energy technologies and supportive equipment to serve as a space for informing the society about the use of smart technologies in our homes capable of offering the transition to a low carbon economy and high levels of energy savings. The hybrid compact storage system for Mediterranean climate is installed in this pilot site.

The installation of the HYBUILD system has been carried out during summer 2021, and the commissioning of the system was finalized by the third week of March 2022. The whole commissioning process as well as all the problems that arose, are described in detail in the following sections.

2.3.1 Description of the installation works

The case study is a listed building located in the city centre square of Aglantzia. This pilot aims at converting the current building as a destination that will be a cornerstone of social interaction and creative activities.

The building will become a benchmark for a permanent digital exhibition of renewable energy technologies and supportive equipment to serve as a space for informing the society about the use of smart technologies in our homes capable of offering the transition to a low carbon economy and high levels of energy savings.

In this context, the proposal aims at creating a multifunctional space which, apart from the promotion of smart technologies, will have the possibility of hosting events, seminars, artistic performances, etc. and at the same time it will function as a reading hall with a digital library for young citizens and students.

The area of building including external walls is 141 m^2 and excluding external walls is 114 m^2.

For the energy performance classification of the selected building, An Energy Performance Certificate (EPC) has been carried out, in alignment with the 2002/91/EC European Union Directive. Additionally, an Energy Efficiency Study, which includes more details in terms of use,

systems and construction characteristics, has been performed to collect more accurate results in order to facilitate the sizing of the new system.

The building is connected to the distribution grid of the Electricity Authority of Cyprus. The electrical installation of the building has been upgraded from single phase (230 V) to three phase system (400 V line - line).

A photovoltaic system with 5 kWp capacity (16 panel of 310 Wp each) has been installed and connected on the DC bus of the electric rack provided by CSEM. The cost for the purchase and the installation of the photovoltaic system was covered by the Municipality.

In addition, a battery energy storage unit is connected to the DC bus through a DC/DC bidirectional charge controller, and a bidirectional DC/AC converter has been installed for the connection with the main distribution grid. Furthermore, the DC driven Heat Pump is connected directly to the DC busbar and provides heating and cooling to cover the building demands. The AC loads will be supplied from the AC side of the DC/AC inverter.

There is no district heating system in the area. The domestic hot water is provided from the electric water heater. A 1.5 kW AC electric water heater is already installed in the building in order to cover the needs for domestic hot water.

Hereafter, a brief description of the installation and commissioning works is provided related to the demo site of Aglantzia, Cyprus.

Although in the case of the Cyprus demo site the Mediterranean system was installed as in the case of Almatret, the system of Aglantzia presents several modifications to cover the needs of the building always in accordance with local laws and regulations.

More specifically, the Aglantzia system does not include solar thermal in contrast to the Almatret system. The building of Aglantzia due to its use as a multifunctional centre and exhibition centre, does not have high demands on domestic hot water, so the system was adapted according to the real needs of the building.

The existing cooling-heating system of the building was replaced with a new system with fan coil units which have been connected to the Heat Pump and the Dry cooler and the rest of the system components to provide cooling-heating to the building. The detailed P&ID diagram of the Mediterranean system adaptation to Aglantzia demo is shown in Figure 14.

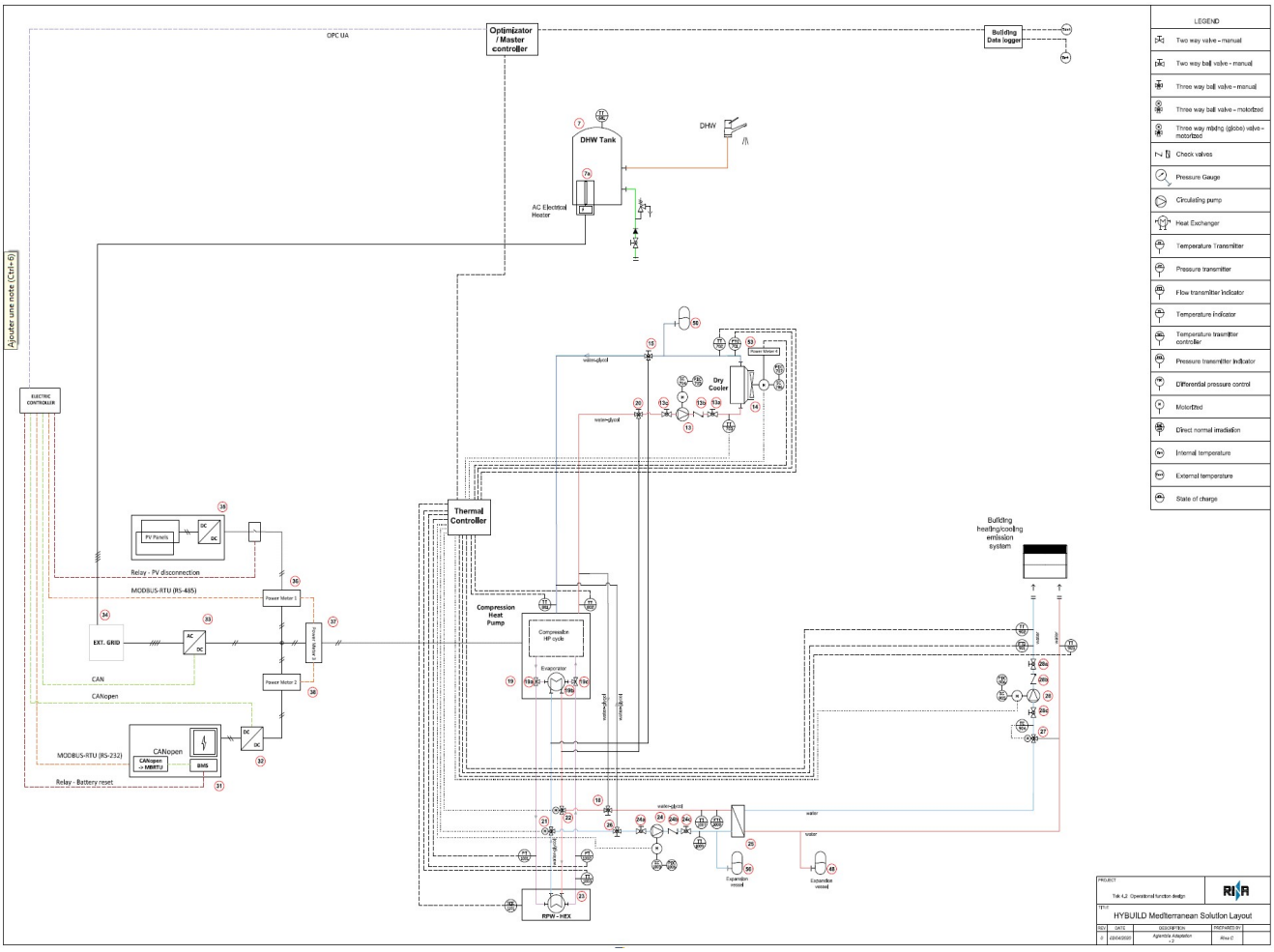

Figure 14. P&ID diagram for the HYBUILD system of Aglantzia demo site

Initially, the building was renovated by increasing the insulation of the roof (i.e. 12 cm of extruded polystyrene) to save energy by reducing losses. The cost for the purchase and the installation of the roof insulation was covered by the Municipality. In addition, some interior renovations were made to better serve the public that will use the building. Figure 15 and Figure 16 show an overview of the renovation process.

Figure 15. Photo from the installation of roof insulation

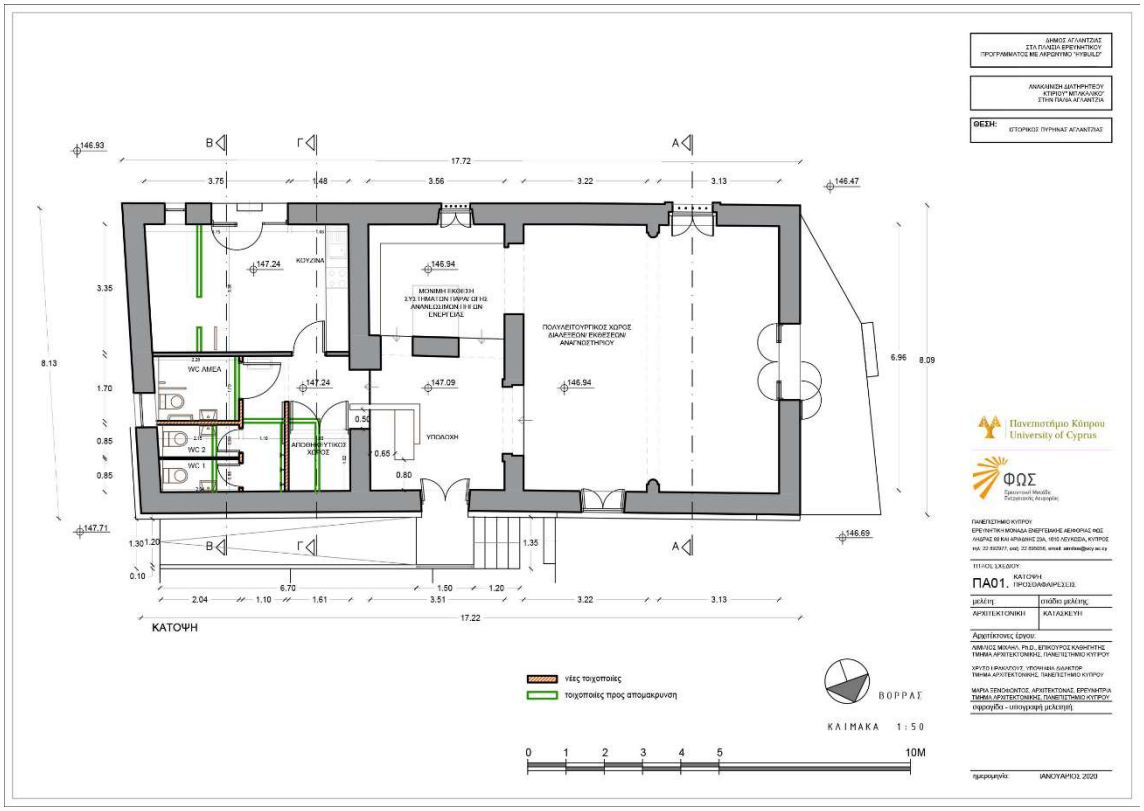

Figure 16. Layout plan of the building with the interior renovations

The electrical installation of the building was then modified according to the requirements of the project and the electrical distribution system of the building upgraded from single phase to three phase.

Then we proceeded to the study and installation of the photovoltaic system on the roof. Initially the installed capacity of the photovoltaic was 3 kWp but then another 2 kW were added to the already installed system increasing the installed power capacity of the system to 5 kWp to meet the requirements of the DC / DC string optimizer. The 16 photovoltaic panels are connected in 2 strings of 8 panels each. The two strings end in the AMPT string optimizer where they become one which ends in the DC bus of the electric rack.

At the same time, the Municipality of Aglantzia announced a tender to select the companies that would proceed with the installation of HYBUILD systems (electrical and mechanical installation). After receiving the various systems from the technology providers, the companies that won the tender were invited to proceed with the installation of the components. Figure 17 and Figure 18 show the floor plan of the building with the placement of the various machines and some details of the installation components and pipelines.

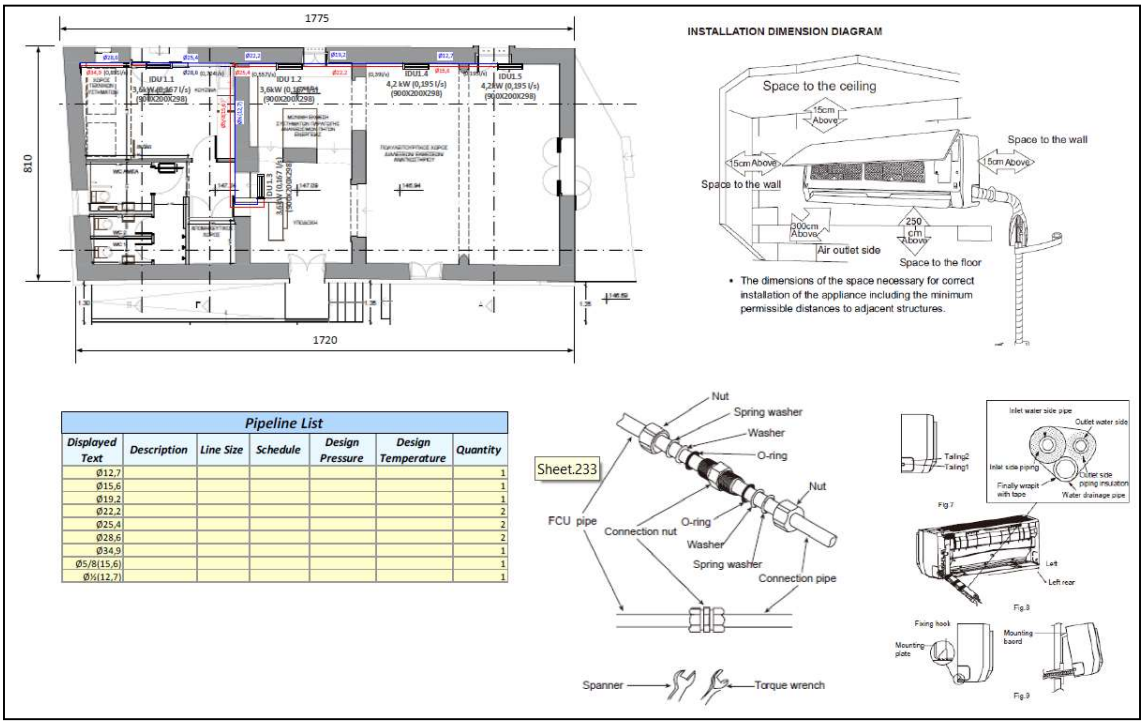

Figure 17. Plan of the building with heating / cooling distribution system

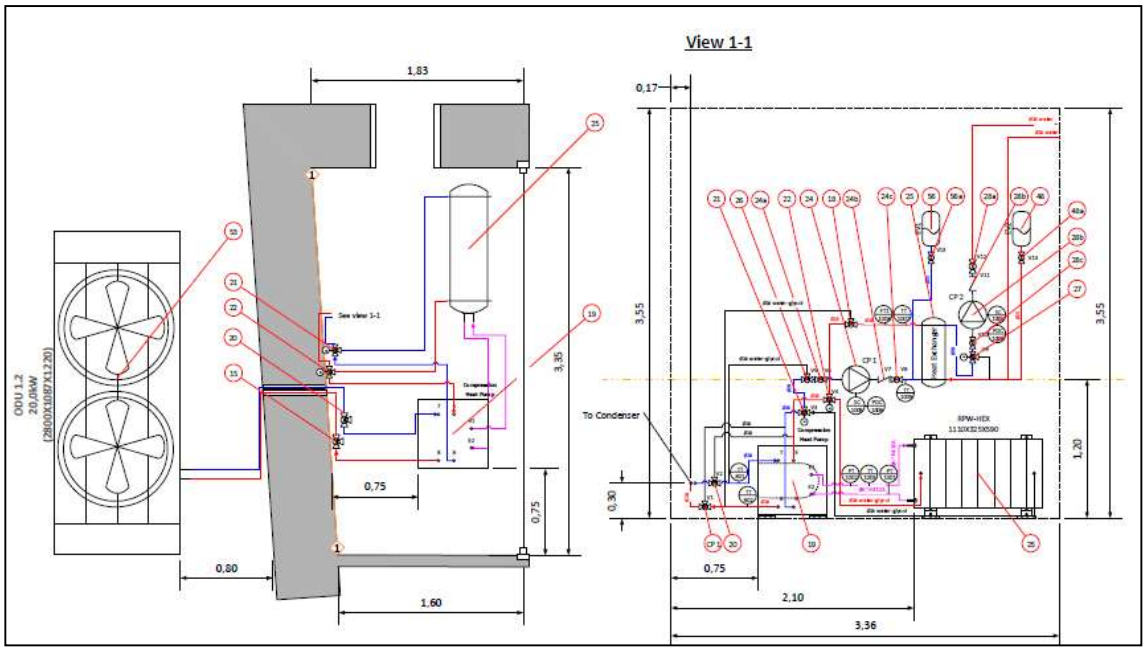

Figure 18. Plan of the mechanical room where indoor and outdoor components are placed

In the meantime, the companies that won the tender proceeded to order all the necessary equipment for the interconnection of the systems.

Separate electrical panels were installed to power the systems. A central panel for the distribution of electricity in the building was installed, followed by a separate panel for the supply of mechanical systems and a separate panel for the PLC.

Several devices that will be used for system monitoring and control were also installed. For the monitoring of the system, power meters, temperature sensors to measure the temperature in the different parts of the system, pressure transmitters, flow meters as well as a complete weather station including indoor and outdoor temperature sensors, wind velocity and direction sensor, and rain gauge were installed. Most of these sensors were provided by UCY.

The above-mentioned components, along with the sensors and auxiliary elements such as motorized valves, pumps, temperature and pressure sensors, etc. already installed in the different components, were also used for control purposes of the thermal part of the system. Therefore, these components were connected to the auxiliary PLC built and programmed by UCY, and installed in the control room next to the mechanical panel.

2.3.2 Commissioning process of the demo-system

Before the commissioning of the system, all the connections between the different components of the system were performed by the electrical and mechanical installers. According to the terms of the tender, the installation companies that won the tender had 2 months to complete the installation from the day of receipt of all the components. Despite the long delay that occurred in the shipment of the HYBUILD systems, the installation companies behaved with impeccable professionalism and completed the installation in a very short time. The coordination and the supervision of the installation of the system of HYBUILD was carried out by the Municipality of Aglantzia with the Technical support of the design consultants of the Municipality and the cooperation of the UCY.

The University of Cyprus, throughout the design and installation of the systems, coordinated the work for the proper installation of the system and was the connecting link between the installers and the partners of the project.

In addition, the University of Cyprus has a very good cooperation with the Municipality of Aglantzia for the purchase of equipment that will be installed in the building (furniture, computers, projectors, etc.) as well as for the access of the users and citizens to platforms of the University of Cyprus (library, some courses, etc.).

In parallel with the work in the field, the University of Cyprus collaborated perfectly with ENG and CSEM for the installation of the control and monitoring software on the local pc and for the connection of the software with appropriate sensors and actuators.

After all the systems were installed, we programmed and installed the auxiliary PLC according to the specifications and functions of the system. After its installation and connection with all the sensors and the various components of the system was completed, an on-site inspection was performed and the proper operation of the PLC confirmed.

After all the installations and the controls of the system were completed, the commissioning was set on 16/11/2021.

The following emerged during the commissioning:

a) The electric rack works normally. It receives the production from the photovoltaics, the battery is charged and discharged accordingly, while energy is exchanged with the main distribution network of Electricity Authority of Cyprus.
b) The master controller operates normally, communicating with the electric rack and with the auxiliary PLC. Data are successfully acquired from Netatmo, Shelly, electrical rack and auxiliary PLC, and stored in influx DB and visualized in draft Grafana dashboard.

Main issue:

After the completion of the works that were completed in accordance with the provided drawings and diagrams, during the procedure of commissioning we diagnosed that the system had no R410A gas in refrigerant circuit. More details of this issue are presented in section 2.3.3.

Despite the issue that arose, the commissioning was successfully completed in the third week of March 2022.

2.3.3 Installation problems / adjustments

From the initial stages of the project, some problems arose, mainly with securing the necessary approvals from the competent state departments. Because the building chosen for the installation of the HYBUILD systems is a listed building, obtaining a permit to install the photovoltaic system on the roof of the building was quite difficult. Eventually, however, we managed to obtain the necessary installation permits and proceeded with the installation of the photovoltaic system.

The initial design of the system for the demo site of Aglantzia included solar thermal which would be supplied by the company FRESNEX which was also a partner in the project. Eventually, however, due to the lack of space, the difficulty of securing approval from the local authorities, but also due to the departure of the company FRESNEX from the project, it was decided to modify the system to operate without the need to install solar thermal. This decision was discussed with the entire consortium of the project and the new design of the system was approved by the project officer.

As mentioned earlier in the previous section, during the final check and the commissioning of the HYBUILD system, we diagnosed that the system had no R410A gas in refrigerant circuit. In order to find the reason of this issue, we followed a specific procedure and several actions have been taken as described below:

a. Filling the refrigerant circuit with nitrogen 30 bar pressure for 48hours.
b. After 48hours, a re-check has been made and the system had 12 bar pressure, indicating that there was loss in the circuit system.
c. Following that, we Refilled the system again with nitrogen 30 bar pressure. We conducted a diligent check for loss in every piping's fittings and connections in the refrigerant circuit system. During the check for gas loss, we found a valve broken and one nut at the heat exchanger output.
d. Immediately we found in the market a new valve and replaced the broken one. As for the nut, we couldn't find in the market and we proceeded with a manufacturing process using a lathe machine. Also we manufactured a plastic fiber for the nut.
e. After the replacement of the faulted fittings and accessories we proceeded with a new test with nitrogen 30 bar pressure for 48 hours.
f. After the pressure was re-checked the refrigerant circuit pressure was 15 bar, stating that there was again a loss in the refrigerant circuit system.
g. In order to proceed with a further diagnose and identify in which part of the system was the loss (heat pump or heat exchanger), we separated the 2 circuits and we inserted in both of the systems nitrogen 30bar pressure.
h. After 48 hours we checked the pressures of each circuit and the heat exchanger circuit was 12 bar pressure and the heat pump circuit remained at 30 bar pressure.

Based on these recordings, we deduced that there is loss inside the heat exchanger.

After consultation with the partners and the project coordinator, it was decided to bypass the RPW-HEX at this stage due to the long time required to repair it, as well as the high cost of repair or replacement in case it is not possible to repair.

2.3.4 Pictures and schemes

Figure 19. PV panels in Aglantzia

Figure 20. HYBUILD system components in Aglantzia

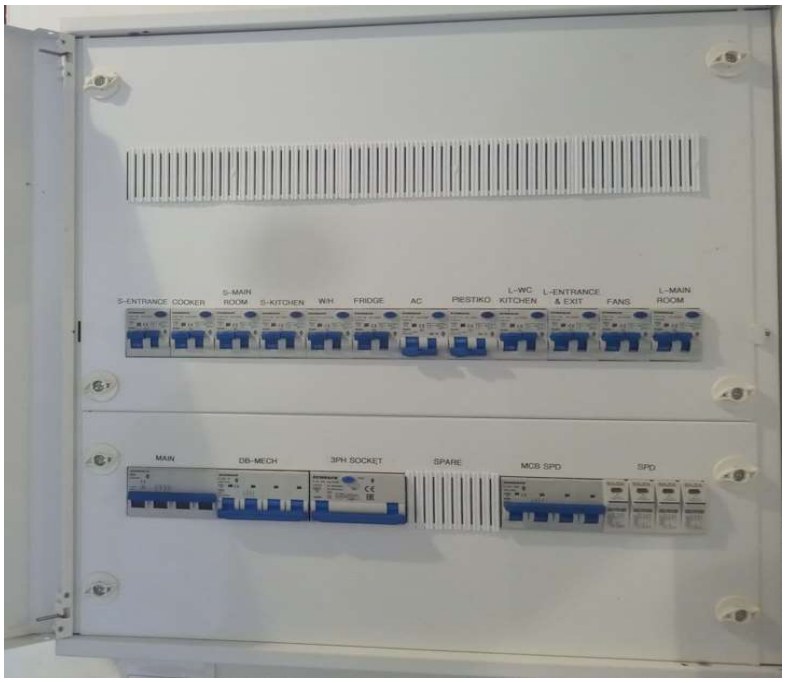

Figure 21. Logic control box with PLC in Aglantzia

2.4 Commissioning of the demonstrator in Langenwang

- Langenwang, Austria

Figure 22. Langenwang demo site building

- **Climate:** Continental
- **Site description**: Office section of the Pink main building in Langenwang
- **Date of construction**: 1960s
- **Current use of the building**: Office with social room and toilets
- **Area**: 180 m^2

HYBUILD Austrian pilot site had a retrofit realized in 2020 to improve the comfort and to decrease the energy consumption. The office is split into four areas: Single offices, plan office, meeting room and social room. The hybrid compact storage system for continental climate will be installed at this pilot site. The maximum heating power consumption expected after the foreseen retrofitting operations is 10 kW. The following technologies have been applied in the building: PV, PCM thermal latent storage, Heat pump.

The installation and commissioning occurred during late 2020. Fine tuning of the installation has been carried out during the first semester of 2021, leading to a fully operative demo by summer 2021.

2.4.1 Description of the installation works

The technical room to take all the continental system components has been prepared in the basement of the company Pink GmbH in Langenwang, Austria.

The real heating and cooling load are provided by the office section of the company in the eastern part of the building (marked in orange).

Figure 23. Plan of the installation area

The offices area has both heating and cooling systems. A low-temperature heating system has been installed to be connected to the HYBUILD system.

The hot water demand is basically at the shower rooms, as there was a risk not to cover all the DHW production, an artificial load has been applied.

The load profile has been defined by EURAC and implemented into the control system. More specifically, three different draw-off profiles are implemented for the three enerboxxes present at the demo. These three profiles are obtained from the profiles used in the HYBUILD Continental reference building, where 10 dwellings with a net area of 50 m² each are considered. These profiles are obtained with a specific software (DHWCalc) that allows to set the higher/lower probability to have DHW user demand in certain hours during the day and in different days of the week. Last, they present a daily DHW demand of around 100 l/day. This can be considered representative of the demand of around 2 persons (considering a medium demand of 50 l/pers/day).

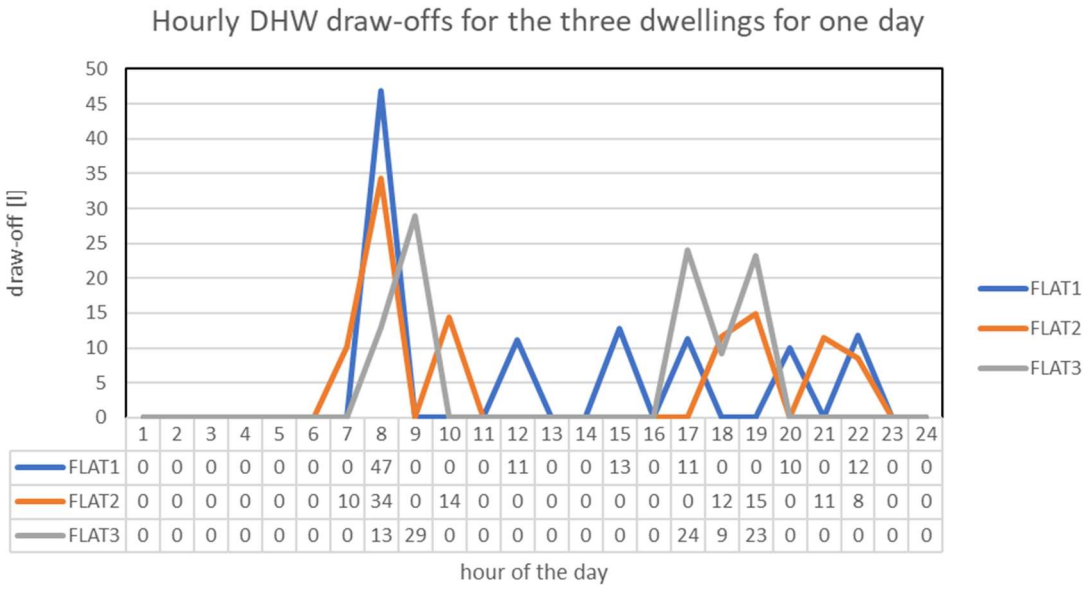

	1	2	3	4	5	6	7	8	9	10	11	12	13	14	15	16	17	18	19	20	21	22	23	24
FLAT1	0	0	0	0	0	0	0	47	0	0	0	11	0	0	13	0	11	0	0	10	0	12	0	0
FLAT2	0	0	0	0	0	0	10	34	0	14	0	0	0	0	0	0	0	12	15	0	11	8	0	0
FLAT3	0	0	0	0	0	0	0	13	29	0	0	0	0	0	0	0	24	9	23	0	0	0	0	0

Figure 24. DHW draw-offs on a one-day basis

The whole installation is described on the next figures (first a general figure, then a more detailed vision of each group of components).

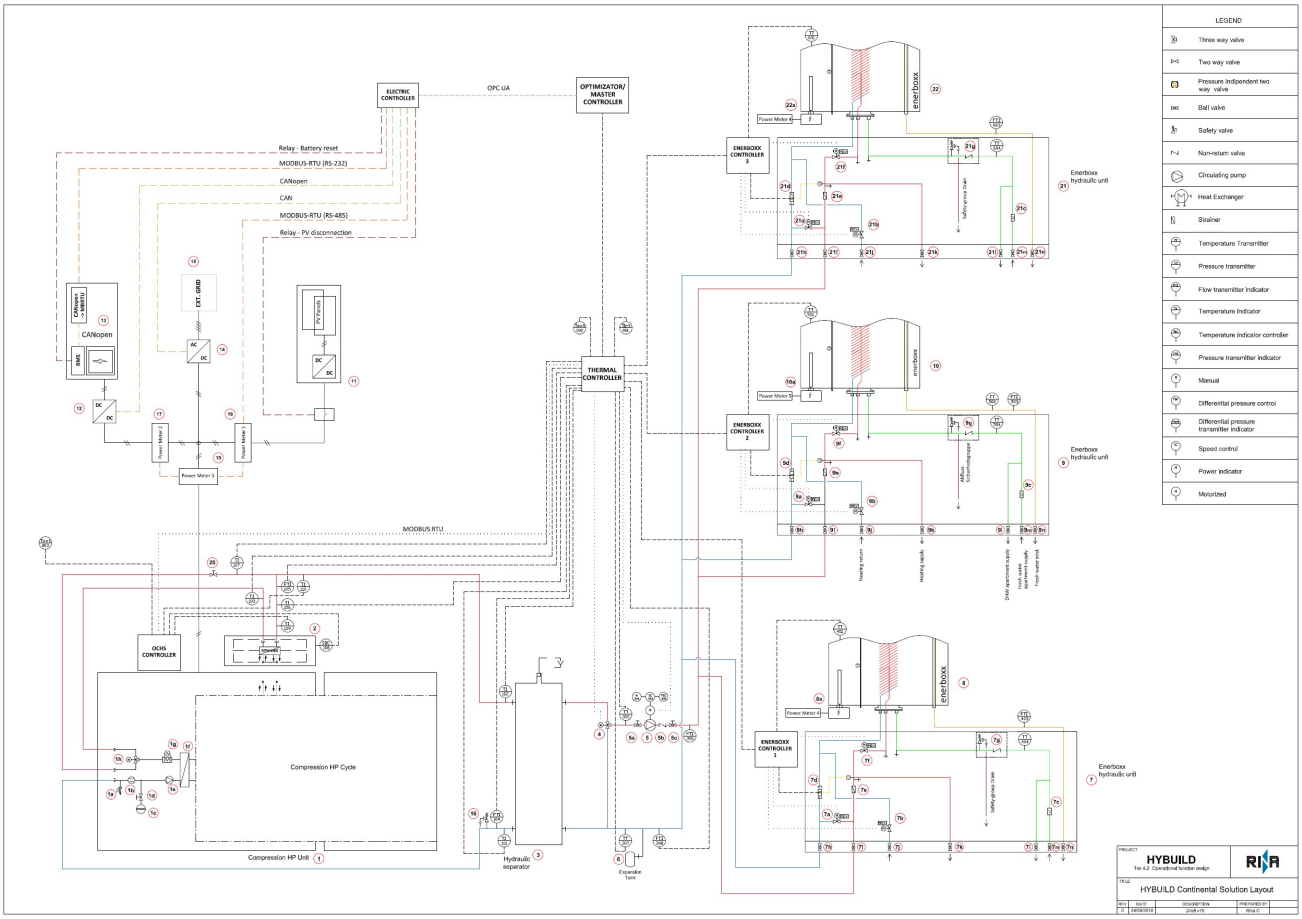

Figure 25. General scheme of installation in Langenwang

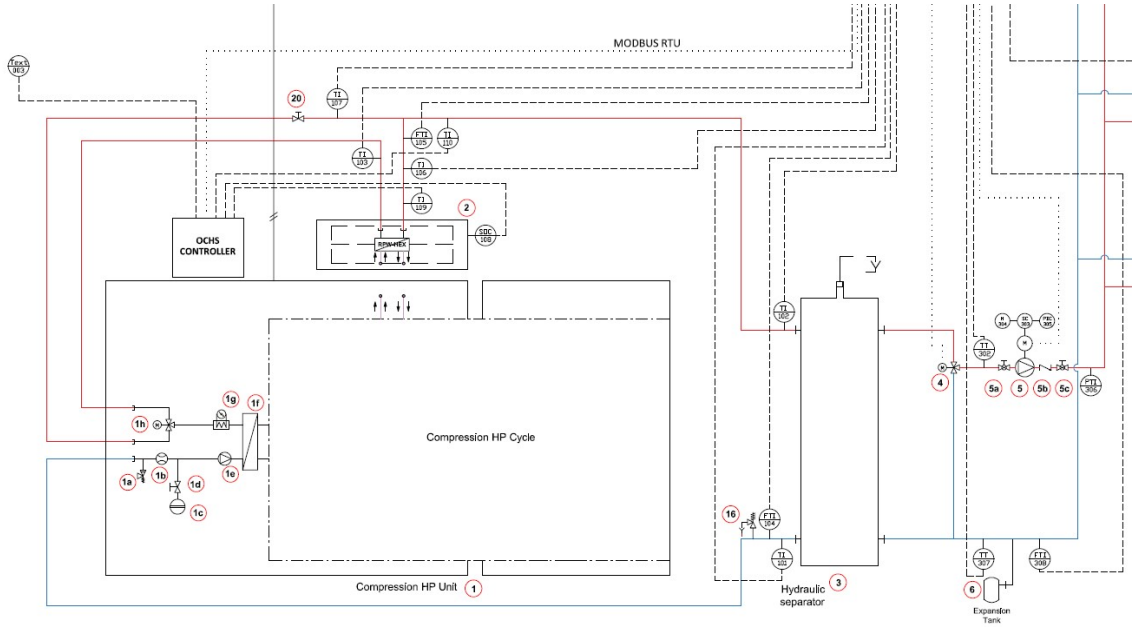

Figure 26. Thermodynamic components (linked to thermal controller)

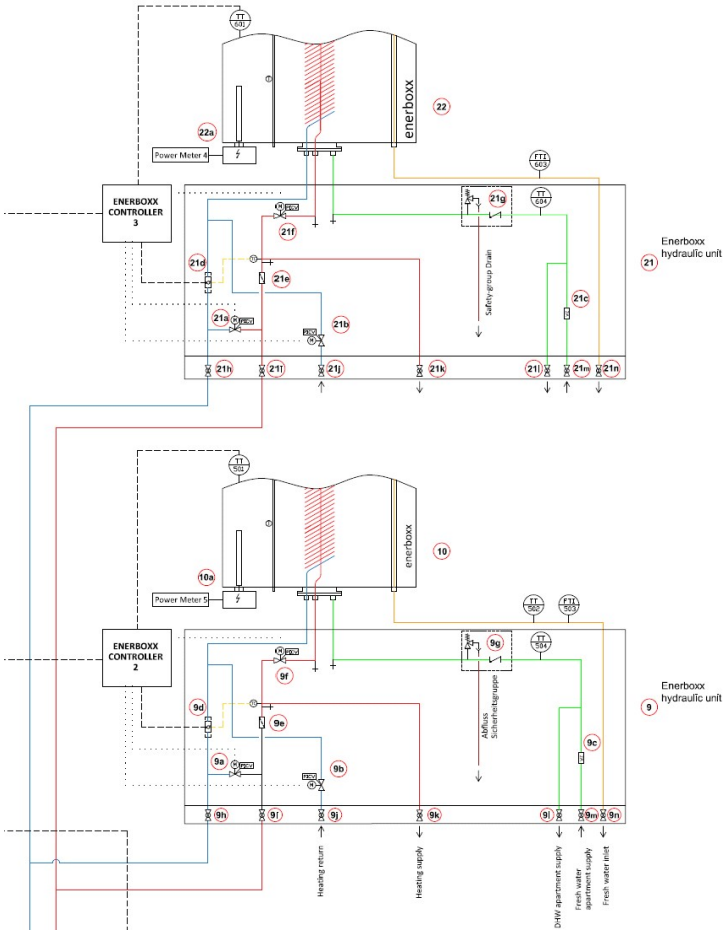

Figure 27. Enerboxx components (linked to thermal controller)

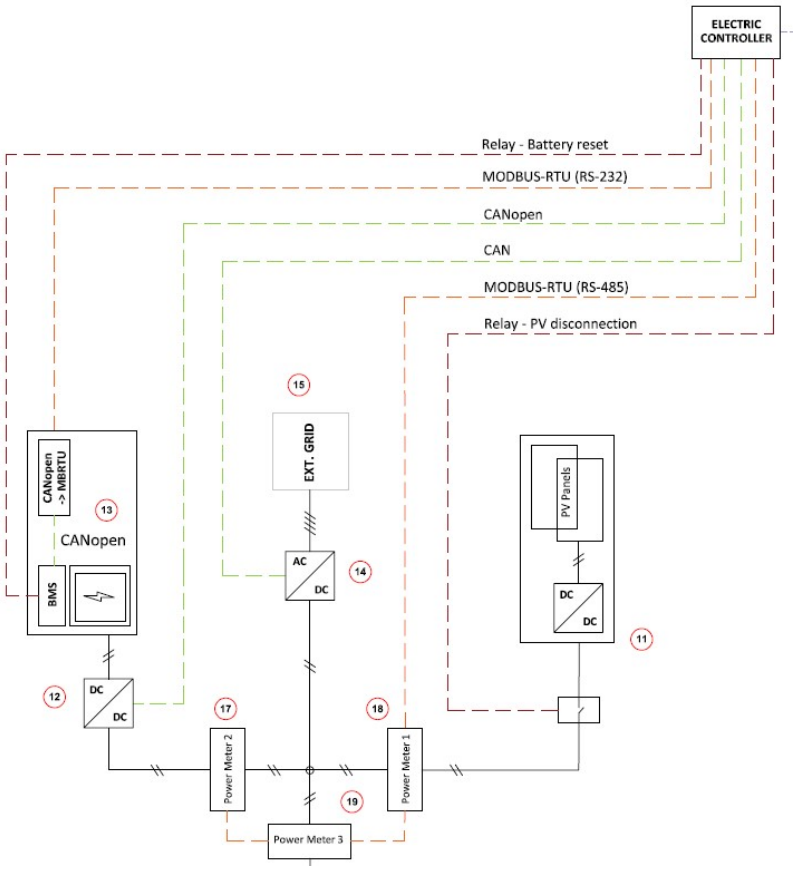

Figure 28. Electric components

2.4.2 *Commissioning process of the demo-system*

Works in the new demo started during November 2019 (M26). Within the period M26 to M36 (November 2019 to November 2020), the preparations and main works to install the continental demo at the new location in Langenwang (Austria) have been performed:

1- Preparation of the technical room for the installation.
2- Installation and connection of a cooling/heating ceiling at the plan office.
3- Installation of a 6.2 kWp PV-plant.
4- Proper wiring to integrate the DC-Rack and battery.
5- Placement and hydraulic installation of the RPW-HEX.
6- Positioning of the heat-pump outdoor unit.
7- Hydraulic installation of the decentralized sensible domestic hot water tanks with integrated hydraulic modules.
8- Hydraulic installation of the hydraulic switch and the district heating backup connection.

The installation has been performed by personnel of PINK and external local companies for special tasks.

The post-intervention strategy has been discussed with the help of all partners involved in HYBUILD demonstration work package. The installation of the heat pump and the commissioning of the new HYBUILD system was scheduled for November-December 2020. Therefore, a full year of post-intervention monitoring has been guaranteed in the continental demonstration.

Eurac is the responsible for the data collection and data quality control for the continental demonstrator, which has been collected from the installation until now.

2.4.3 Installation problems / adjustments

By end of December 2020 the HYBUILD system is running in Langenwang. At that time some adjustments were still to be made.

During the following months several issues have been observed, analyzed and solved continuously. In this section, we provide several examples of these issues to illustrate how the commissioning activity has been tackled over the months following the installation.

In January, these problems have been observed then solved:

- Data from the thermal controller is collected, but there is no access locally to the real-time electrical consumption. However, the electrical consumption data is fully registered from that moment to the end of the project.
- EURAC-CSEM-PINK-ENG discussed and confirmed the PV/battery charging management strategy. An issue is still to be solved with the string optimizer, there is an issue with the electrical storage data. involved partners discussed this problem to solve it.
- ENG provides data access of Pink demo to PINK, NBK, OSCHNER, AIT and CSEM via GRAFANA.

In February 2021, some problems have been observed with different components:

- A pressure sensor in the HP is not working, thus impacting the performance of the heat pump. Ochsner is aiming at solving this problem.
- As a consequence, it is not possible to run an automatic mode.
- A DC rack is always shutting down after a few hours of operation, thus having issues to provide the energy to the HP. CSEM worked on a solution.
- Further data checking is necessary in order to ensure they are collected correctly.

In March 2021:

- Errors appeared on the DC/DC converter, during the battery charging phase. ITAE, CSEM, ENG, and PINK worked to solve the problem.
- An optimization of the hydraulic charging of the DHW-tanks (Enerboxxes) has been decided.

In April 2021:

- The external insulation of the RPW-HEX has been done, in addition to the already existing one coming from AIT or AKG.
- From the hardware point of view, everything is completely finished.

In February/March 2022:

- After analysing monitored data, it has been found that the system was not working as expected. In particular, the management of the RPW-HEX discharge was not the one foreseen and the RPW-HEX was basically never fully discharged. After some different tests, some measurement errors have been detected and solved and the control logic has been revised thanks to the contribution of PINK,

AIT, OCHSNER, EURAC, NBK, UDL, COMSA. From March 9th the system is operating with the RPW-HEX that is fully discharged.

2.4.4 Pictures and schemes

Figure 29. Langenwang demo building

Figure 30. Preparation of the technical room for installation

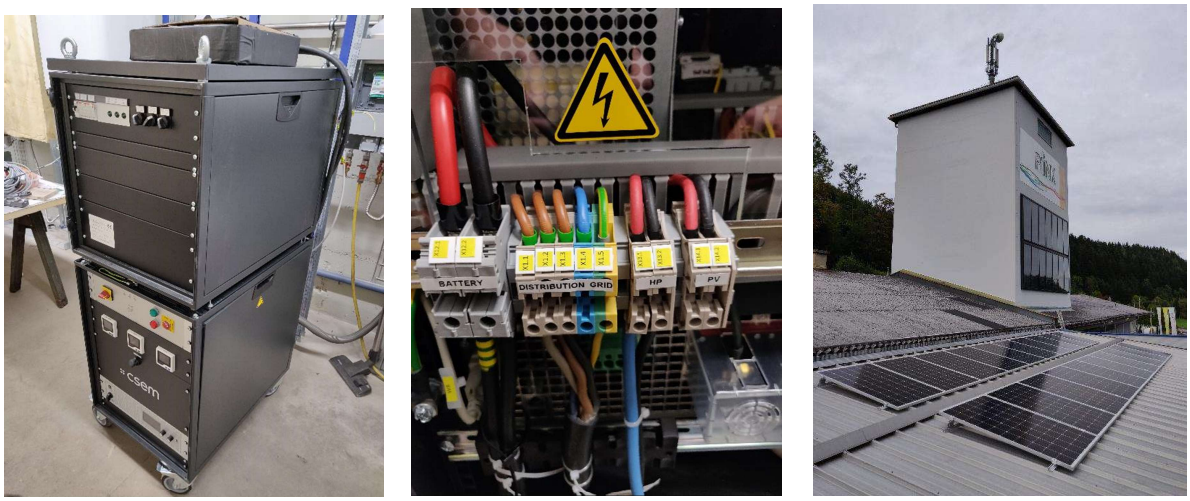

Figure 31. DC-Rack and battery are ready for implementation

Figure 32. PINK storage, hydraulic network and, Ochsner outdoor unit installation

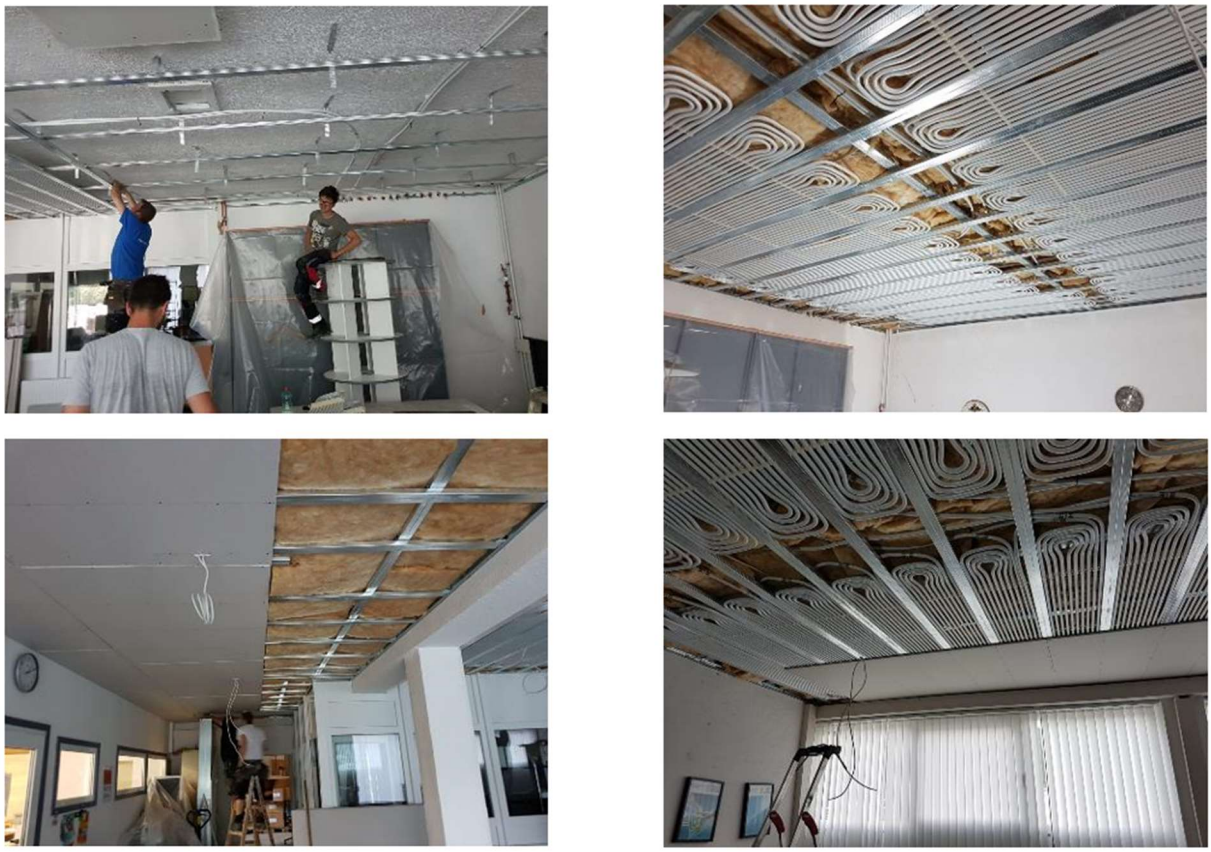

Figure 33. Cooling/heating ceiling installation

3 Data and component analysis

3.1 Almatret demo site

3.1.1 General scheme and sensors

Figure 4 shows the general connection diagram of the Almatret demo. Each component, with its respective sensors, are detailed below.

Figure 34 shows the sensors connected to the solar field. They consist of an energy meter that provides send and return temperatures, flow rate, volume and power. They monitor the energy delivered from the solar field to the buffer tank. A temperature and humidity sensor and a pyranometer.

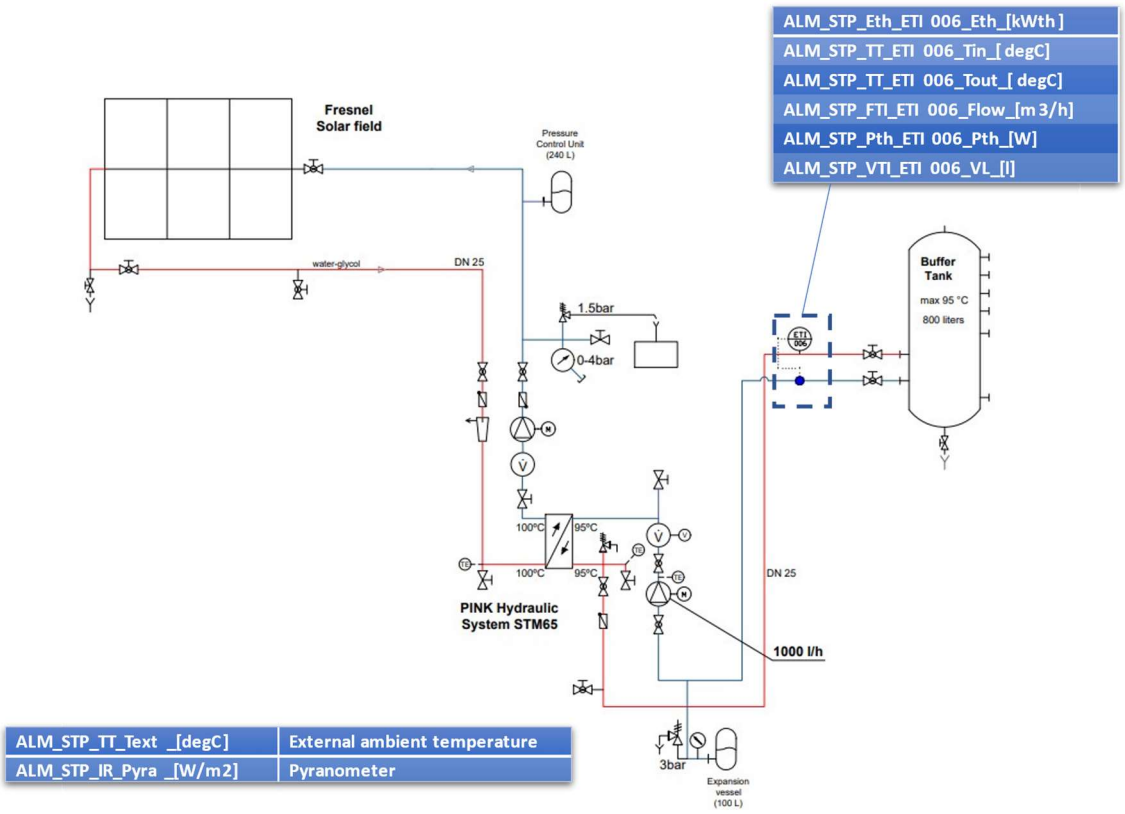

Figure 34. Sensor variables on the solar thermal components

Figure 35 shows the sensors connected to the system for hot water delivery. These consist of three energy meters that provides send and return temperatures, flow rate, volume and power. They monitor the energy delivered from the buffer tank to the DHW tank, from the DHW tank to the boiler, and from the boiler to the DHW delivery. Additionally, there is a temperature sensor in the buffer tank and a temperature sensor in the DHW tank.

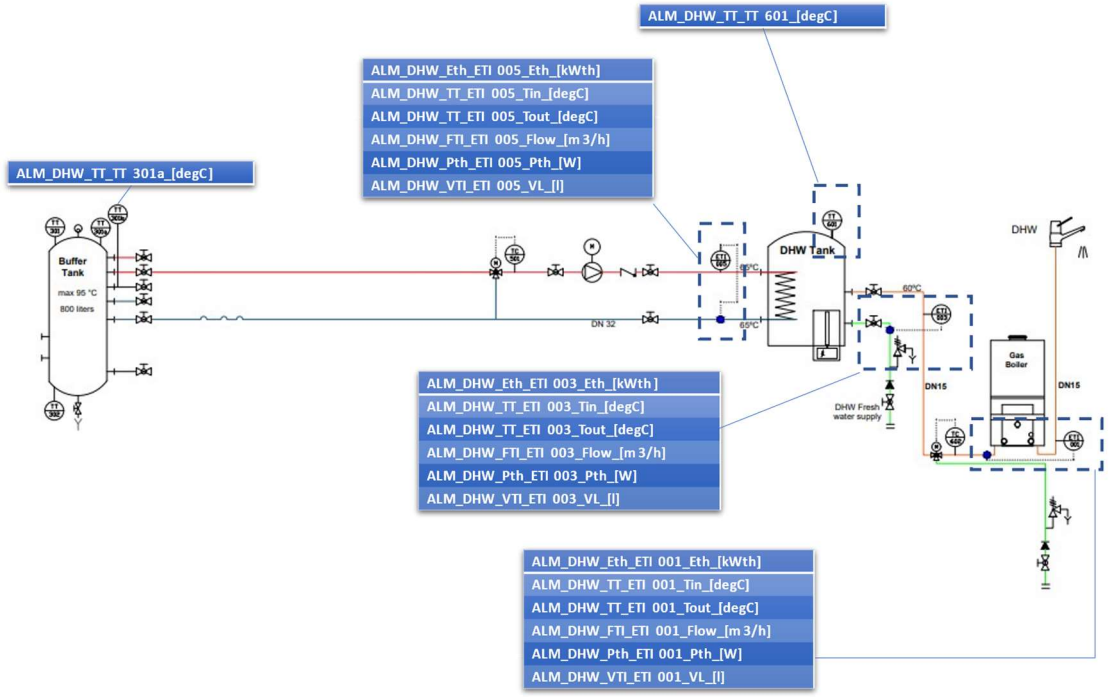

Figure 35. Sensor variables on the DHW components

Figure 36 shows the sensors connected to the system for space heating delivery. These consist of two energy counters that provides the send and return temperatures, flow rate, volume and power. They monitor the energy delivered from the buffer tank to the gas boiler and the space heating distribution system, and the energy input from the gas boiler to the space heating system. Additionally, there is a temperature sensor in the buffer tank.

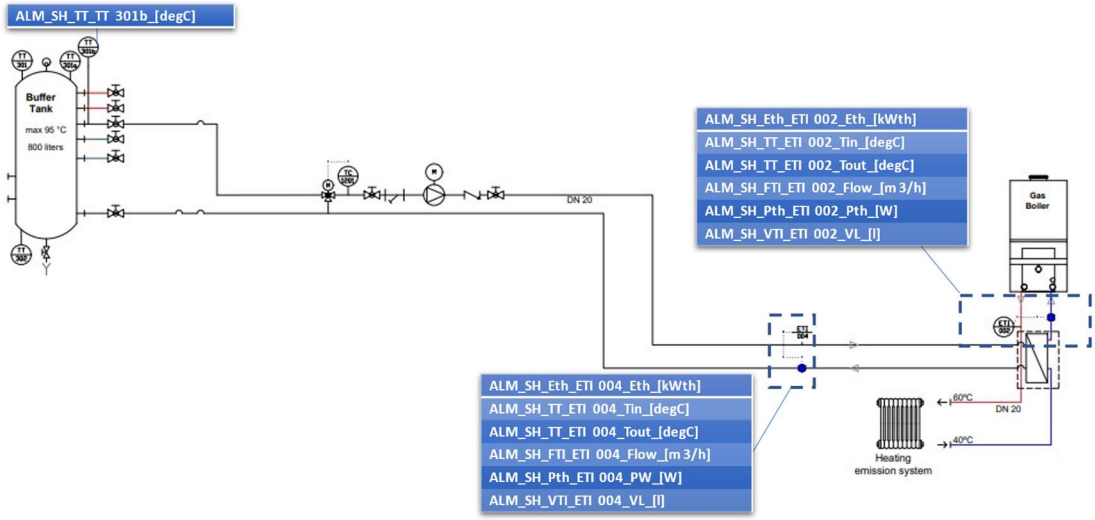

Figure 36. Sensor variables on the Spate heating components

Figure 37 shows the sensors connected to the heat pump module. These consist of an energy meter that provides send and return temperatures, flow rate, volume and power. They monitor the energy delivered from the HP to the distribution system of the house. In addition, we have temperature sensors at the evaporator and condenser send and return, and pressure sensors at the condenser and evaporator send and return.

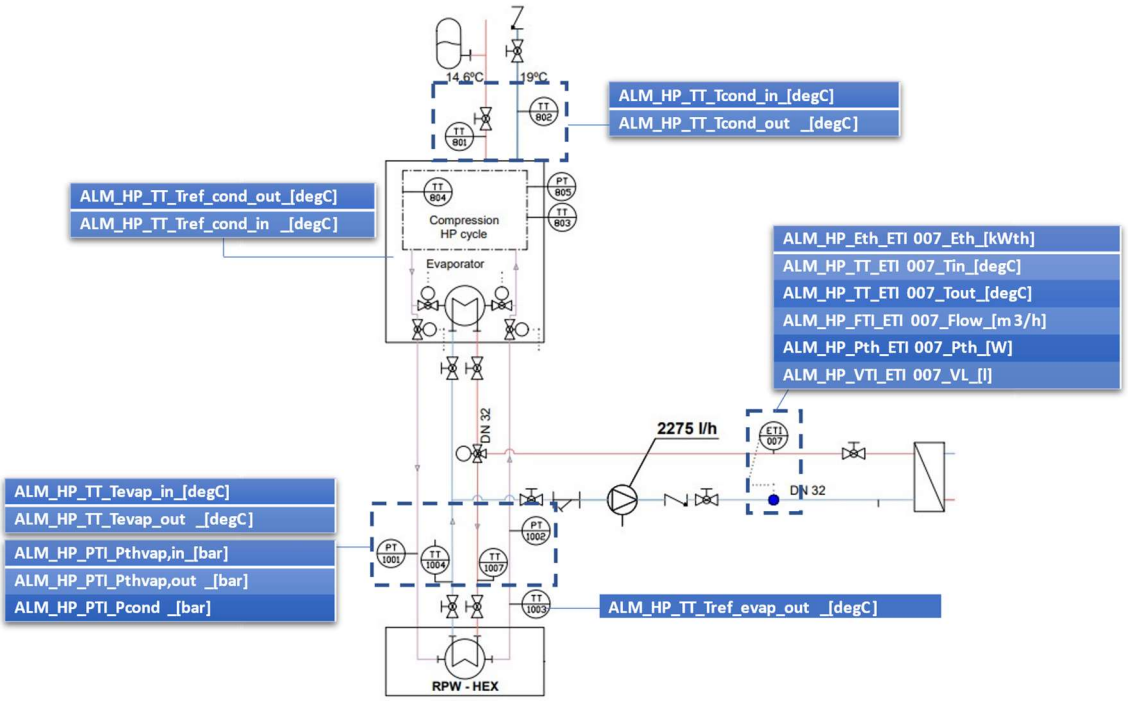

Figure 37. Sensors on the HP

Figure 38 shows the nine temperature sensors connected to the PCM storage tank.

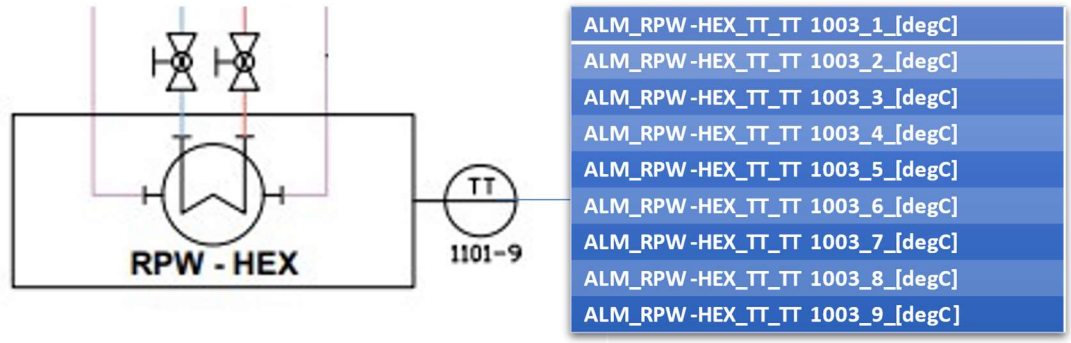

Figure 38. Temperature sensors on the PCM storage

Figure 39 shows the two temperature sensors connected to the fan coils inside the house.

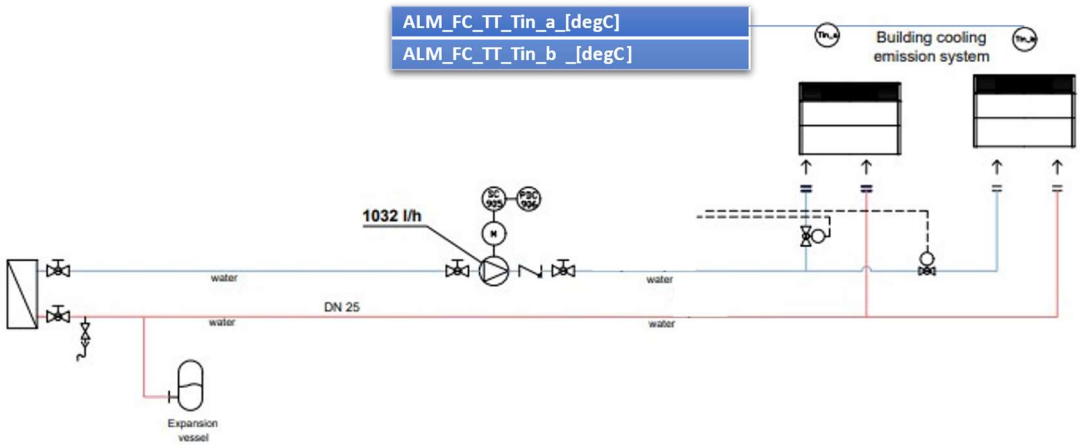

Figure 39. Sensors on the fan-coil distribution system

Figure 40 shows the temperature and flow sensors installed in the high, medium and low temperature circuits of the sorption system. As well as a temperature sensor for each of the two adsorber /desorber and evaporator/condenser module.

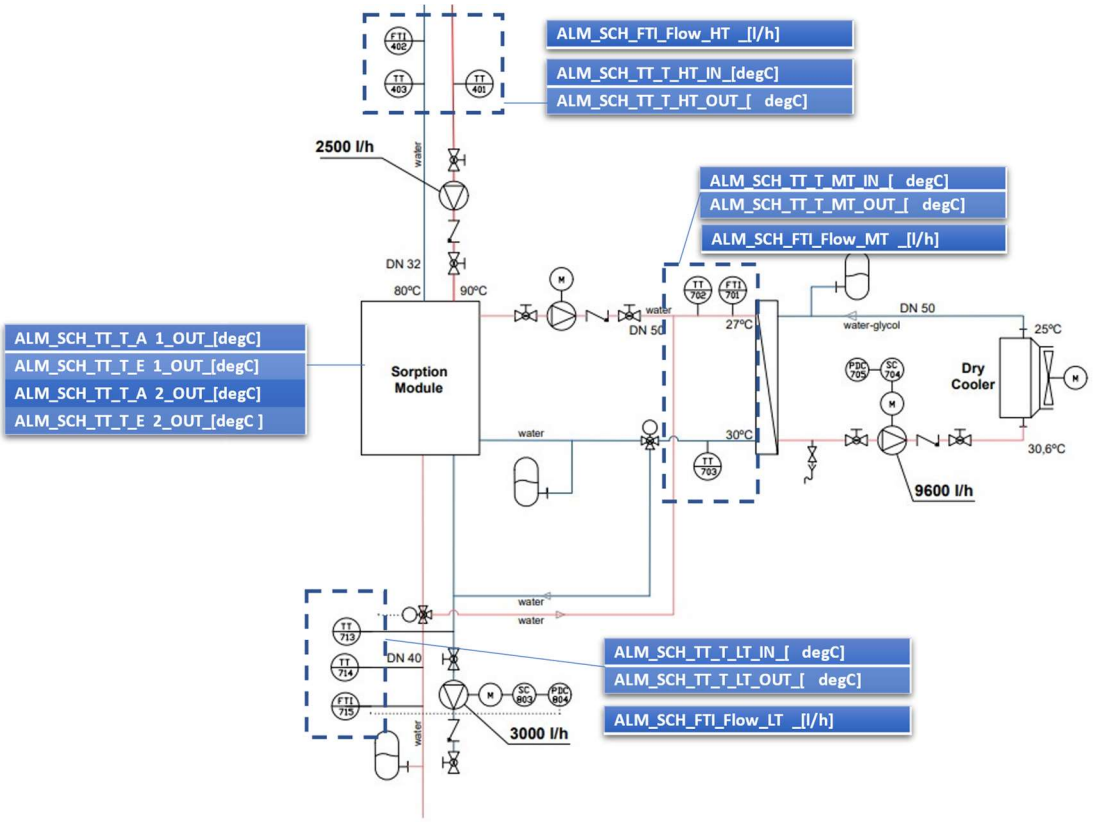

Figure 40. Variables on the sorption system

Figure 41 shows the voltage and power sensors installed in the DC-bus rack.

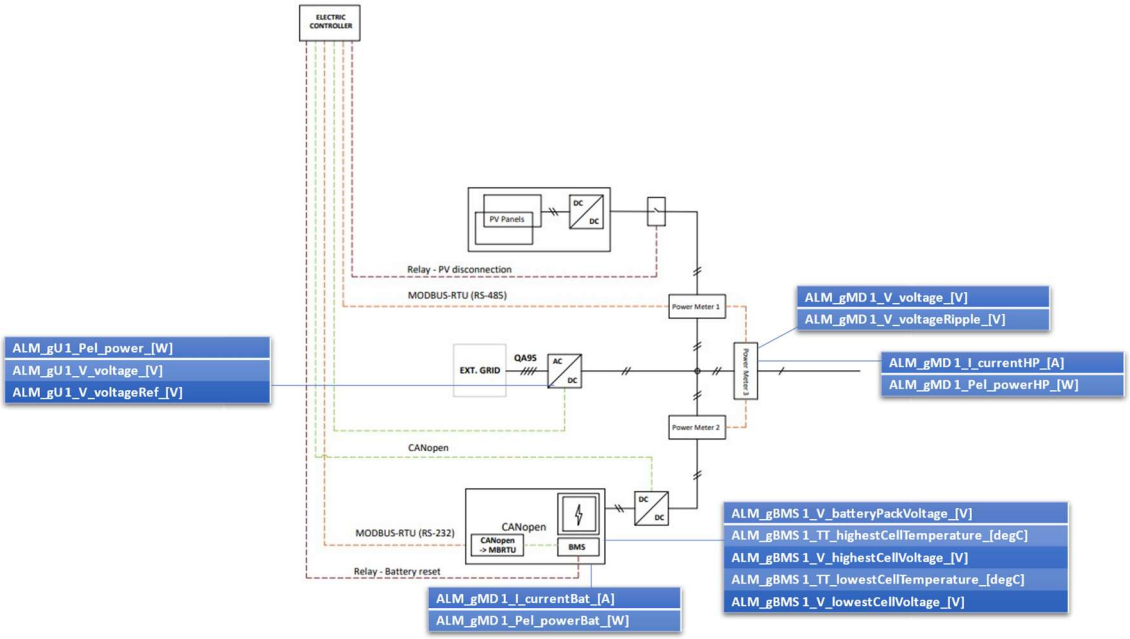

Figure 41. Variables on the DC-bus system

A summary table with all sensors, valves and signals used by the system controller and their unique identification code is shown in Table 3.

Table 3. List of all sensors and actuators of the Almatret demo system

Component	Variable name	Description
Solar thermal	ALM_STP_Eth_ETI006_Eth_[kWth]	Energy meter
Solar thermal	ALM_STP_TT_ETI006_Tin_[degC]	Energy meter
Solar thermal	ALM_STP_TT_ETI006_Tout_[degC]	Energy meter
Solar thermal	ALM_STP_FTI_ETI006_Flow_[m3/h]	Energy meter
Solar thermal	ALM_STP_Pth_ETI006_Pth_[W]	Energy meter
Solar thermal	ALM_STP_VTI_ETI006_VL_[l]	Energy meter
Solar thermal	ALM_STP_TT_Text_[degC]	External ambient temperature
Solar thermal	ALM_STP_IR_Pyra_[W/m2]	Pyranometer
DHW	ALM_DHW_Eth_ETI005_Eth_[kWth]	Energy meter
DHW	ALM_DHW_TT_ETI005_Tin_[degC]	Energy meter
DHW	ALM_DHW_TT_ETI005_Tout_[degC]	Energy meter
DHW	ALM_DHW_FTI_ETI005_Flow_[m3/h]	Energy meter

DHW	ALM_DHW_Pth_ETI005_Pth_[W]	Energy meter
DHW	ALM_DHW_VTI_ETI005_VL_[l]	Energy meter
DHW	ALM_DHW_Eth_ETI003_Eth_[kWth]	Energy meter
DHW	ALM_DHW_TT_ETI003_Tin_[degC]	Energy meter
DHW	ALM_DHW_TT_ETI003_Tout_[degC]	Energy meter
DHW	ALM_DHW_FTI_ETI003_Flow_[m3/h]	Energy meter
DHW	ALM_DHW_Pth_ETI003_Pth_[W]	Energy meter
DHW	ALM_DHW_VTI_ETI003_VL_[l]	Energy meter
DHW	ALM_DHW_Eth_ETI001_Eth_[kWth]	Energy meter
DHW	ALM_DHW_TT_ETI001_Tin_[degC]	Energy meter
DHW	ALM_DHW_TT_ETI001_Tout_[degC]	Energy meter
DHW	ALM_DHW_FTI_ETI001_Flow_[m3/h]	Energy meter
DHW	ALM_DHW_Pth_ETI001_Pth_[W]	Energy meter
DHW	ALM_DHW_VTI_ETI001_VL_[l]	Energy meter
DHW	ALM_DHW_SS_OM_DHW_[-]	DHW operation mode
DHW	ALM_DHW_TT_TT301a_[degC]	Top buffer tank temperature
DHW	ALM_DHW_TT_TT601_[degC]	Temperature DHW tank
Space heating	ALM_SH_Eth_ETI004_Eth_[kWth]	Energy meter
Space heating	ALM_SH_TT_ETI004_Tin_[degC]	Energy meter
Space heating	ALM_SH_TT_ETI004_Tout_[degC]	Energy meter
Space heating	ALM_SH_FTI_ETI004_Flow_[m3/h]	Energy meter
Space heating	ALM_SH_Pth_ETI004_PW_[W]	Energy meter
Space heating	ALM_SH_VTI_ETI004_VL_[l]	Energy meter
Space heating	ALM_SH_Eth_ETI002_Eth_[kWth]	Energy meter
Space heating	ALM_SH_TT_ETI002_Tin_[degC]	Energy meter
Space heating	ALM_SH_TT_ETI002_Tout_[degC]	Energy meter
Space heating	ALM_SH_FTI_ETI002_Flow_[m3/h]	Energy meter
Space heating	ALM_SH_Pth_ETI002_Pth_[W]	Energy meter

Space heating	ALM_SH_VTI_ETI002_VL_[l]	Energy meter
Space heating	ALM_SH_TT_TT301b_[degC]	Middle buffer tank temperature
Heat pump	ALM_HP_PTI_Pthvap,in_[bar]	Pressure transmitter
Heat pump	ALM_HP_PTI_Pthvap,out_[bar]	Pressure transmitter
Heat pump	ALM_HP_PTI_Pcond_[bar]	Pressure transmitter
Heat pump	ALM_HP_TT_Tevap_in_[degC]	Temperature transmitter
Heat pump	ALM_HP_TT_Tevap_out_[degC]	Temperature transmitter
Heat pump	ALM_HP_TT_Tcond_in_[degC]	Temperature transmitter
Heat pump	ALM_HP_TT_Tcond_out_[degC]	Temperature transmitter
Heat pump	ALM_HP_TT_Tref_evap_out_[degC]	Temperature transmitter
Heat pump	ALM_HP_TT_Tref_cond_out_[degC]	Temperature transmitter
Heat pump	ALM_HP_TT_Tref_cond_in_[degC]	Temperature transmitter
PCM storage (RPW-HEX)	ALM_RPW-HEX_TT_TT1003_1_[degC]	Temperature transmitter
RPW-HEX	ALM_RPW-HEX_TT_TT1003_2_[degC]	Temperature transmitter
RPW-HEX	ALM_RPW-HEX_TT_TT1003_3_[degC]	Temperature transmitter
RPW-HEX	ALM_RPW-HEX_TT_TT1003_4_[degC]	Temperature transmitter
RPW-HEX	ALM_RPW-HEX_TT_TT1003_5_[degC]	Temperature transmitter
RPW-HEX	ALM_RPW-HEX_TT_TT1003_6_[degC]	Temperature transmitter
RPW-HEX	ALM_RPW-HEX_TT_TT1003_7_[degC]	Temperature transmitter
RPW-HEX	ALM_RPW-HEX_TT_TT1003_8_[degC]	Temperature transmitter
RPW-HEX	ALM_RPW-HEX_TT_TT1003_9_[degC]	Temperature transmitter
Heat pump	ALM_HP_Eth_ETI007_Eth_[kWth]	Energy meter
Heat pump	ALM_HP_TT_ETI007_Tin_[degC]	Energy meter
Heat pump	ALM_HP_TT_ETI007_Tout_[degC]	Energy meter
Heat pump	ALM_HP_FTI_ETI007_Flow_[m3/h]	Energy meter
Heat pump	ALM_HP_Pth_ETI007_Pth_[W]	Energy meter
Heat pump	ALM_HP_VTI_ETI007_VL_[l]	Energy meter

Fan-coils	ALM_FC_TT_Tin_a_[degC]	Temperature transmitter
Fan-coils	ALM_FC_TT_Tin_b_[degC]	Temperature transmitter
Solar thermal	ALM_STP_Pel_Pel_solar_[W]	Electric power meter
Sorption	ALM_HP_Pel_Pel_sorption_[W]	Electric power meter
Auxiliary	ALM_aux-controller_Pel_Pel_aux_[W]	Electric power meter
Sorption	ALM_SCH_TT_T_HT_IN_[degC]	Inlet high temperature circuit
Sorption	ALM_SCH_TT_T_HT_OUT_[degC]	Outlet high temperature circuit
Sorption	ALM_SCH_TT_T_MT_IN_[degC]	Inlet medium temperature circuit
Sorption	ALM_SCH_TT_T_MT_OUT_[degC]	Outlet medium temperature circuit
Sorption	ALM_SCH_TT_T_LT_IN_[degC]	Inlet low temperature circuit
Sorption	ALM_SCH_TT_T_LT_OUT_[degC]	Outlet low temperature circuit
Sorption	ALM_SCH_TT_T_A1_OUT_[degC]	Adsorber 1/Desorber 1 outlet temperature
Sorption	ALM_SCH_TT_T_E1_OUT_[degC]	Evaporator 1/Condenser 1 outlet temperature
Sorption	ALM_SCH_TT_T_A2_OUT_[degC]	Adsorber 2/Desorber 2 outlet temperature
Sorption	ALM_SCH_TT_T_E2_OUT_[degC]	Evaporator 2/Condenser 2 outlet temperature
Sorption	ALM_SCH_FTI_Flow_HT_[l/h]	Volume flow HT circuit
Sorption	ALM_SCH_FTI_Flow_MT_[l/h]	Volume flow MT circuit
Sorption	ALM_SCH_FTI_Flow_LT_[l/h]	Volume flow LT circuit
Sorption	ALM_SCH_PERCENT_Pump_Speed_HT_[%]	Actual value of the pump in the high temperature circuit
Sorption	ALM_SCH_PERCENT_Pump_Speed_MT_[%]	Actual value of the pump in the medium temperature circuit
Sorption	ALM_SCH_PERCENT_Pump_Speed_LT_[%]	Actual value of the pump in the low temperature circuit
Electric rack	ALM_gBMS1_V_batteryPackVoltage_[V]	Measured battery pack voltage
Electric rack	ALM_gBMS1_TT_highestCellTemperature_[degC]	Highest cell temperature in battery pack
Electric rack	ALM_gBMS1_V_highestCellVoltage_[V]	Highest cell voltage in battery pack

Electric rack	ALM_gBMS1_TT_lowestCellTemperature_[degC]	Lowest cell temperature in battery pack
Electric rack	ALM_gBMS1_V_lowestCellVoltage_[V]	Lowest cell voltage in battery pack
Electric rack	ALM_gBMS1_BOOL_lowPowerMode_[-]	1 = CMU power on, 0 = CMU power off
Electric rack	ALM_gBMS1_BOOL_mainContactorState_[-]	1 = close, 0 = open
Electric rack	ALM_gBMS1_BOOL_mainContactorWaitStatus_[-]	1 = wait for close, 0 = no wait
Electric rack	ALM_gMD1_V_voltage_[V]	Measured DC bus voltage
Electric rack	ALM_gMD1_V_voltageRipple_[V]	Measured DC bus voltage ripple
Electric rack	ALM_gMD1_I_currentBat_[A]	Measured battery current (+ : charging / - : discharging)
Electric rack	ALM_gMD1_Pel_powerBat_[W]	Measured battery power (+ : charging / - : discharging)
Electric rack	ALM_gMD1_I_currentHP_[A]	Measured heat pump current
Electric rack	ALM_gMD1_Pel_powerHP_[W]	Measured heat pump power
Electric rack	ALM_gMD1_I_currentPV_[A]	Measured PV current
Electric rack	ALM_gMD1_Pel_powerPV_[W]	Measured PV power
Electric rack	ALM_gU1_Pel_power_[W]	Measured power of the DC output
Electric rack	ALM_gU1_V_voltage_[V]	Measured voltage of the DC output
Electric rack	ALM_gU1_V_voltageRef_[V]	Voltage reference of the DC output

3.1.2 Operational modes

According to deliverable D4.2, the system installed at the Almatret demo site can operate in different modes: cooling, heating, charging, DHW, and solar field. These modes are summarized in Table 4 and according to Figure 4 and Figure 34-Figure 41.

Table 4. Operating modes of the Almatret demo system

Operation mode	Main components operations	Actuators mode
Solar field mode	• Fresnel solar field (1) feeding the buffer tank (4)	• Pumps (2g) and (2s) in mode ON
DHW mode	• DHW tank (7) fed by the buffer tank (4)	• Pump (6) in mode ON

Charging Mode 1	• RPW-HEX (21) charging • Heat pump (19) in mode ON • Adsorption module (9) in mode OFF • Electricity provided by the electric sub-system	• Valve (21) open 'RPW-HEX - User' circuit • Valves (12) and (16) open 'Dry cooler - HP' circuit • Valves (19a) and (19b) closed • Valves (19c) and (19d) open • Pumps (24) and (28) in mode OFF • Pumps (13) and (17) in mode ON • Pumps (8) and (10) in mode OFF • Electric controller open external grid circuit (34) or electric battery circuit (31) or PV panel circuit (35)
Charging Mode 2	• RPW-HEX (21) charging • Heat pump (19) in mode ON • Adsorption module (9) in mode ON exploiting the buffer tank (4) energy • Electricity provided by the electric sub-system	• Valve (21) open 'RPW-HEX - User' circuit • Valve (16) open 'Dry cooler - Adsorption module' circuit • Valve (12) open 'Adsorption module - HP' circuit • Valves (19a) and (19b) closed • Valves (19c) and (19d) open • Pumps (24) and (28) in mode OFF • Pumps (8), (10), (13), and (17) in mode ON • Electric controller open external grid circuit (34) or electric battery circuit (31) or PV panel circuit (35)
Cooling Mode 1	• Cooling provided by the RPW-HEX (23) • Heat pump (19) in mode OFF • Adsorption module (9) in mode OFF	• Valve (21) open 'RPW-HEX - User' circuit • Pumps (24) and (28) in mode ON • Pumps (8), (10), (13), and (17) in mode OFF
Cooling Mode 2	• Cooling provided by the heat pump (19) using the standard evaporator (19b) • RPW-HEX (23) bypassed • Adsorption module (9) in mode OFF • Electricity to the heat pump (19) provided by the electric sub-system	• Valve (21) open 'HP - User' circuit • Valves (12) and (16) open 'Dry cooler - HP' circuit • Valves (19a) and (19b) open • Valves (19c) and (19d) closed • Pumps (24) and (28) in mode ON • Pumps (13) and (17) in mode ON • Pumps (8) and (10) in mode OFF • Electric controller open external grid circuit (34) or electric battery circuit (31) or PV panel circuit (35)

Cooling Mode 3	• Cooling provided by the heat pump (19) • RPW-HEX (23) charged/discharged simultaneously • Adsorption module (9) in mode OFF • Electricity to the heat pump (19) provided by the electric sub-system	• Valve (21) open 'RPW-HEX - User' circuit • Valves (12) and (16) open 'Dry cooler - HP' circuit • Valves (19a) and (19b) closed • Valves (19c) and (19d) open • Pumps (24) and (28) in mode ON • Pumps (13) and (17) in mode ON • Pumps (8) and (10) in mode OFF • Electric controller open external grid circuit (34) or electric battery circuit (31) or PV panel circuit (35)
Cooling Mode 4	• Cooling provided by the heat pump (19) using the standard evaporator (19b) • RPW-HEX (23) bypassed • Adsorption module (9) in mode ON, exploiting the buffer tank (4) energy • Electricity to the heat pump (19) provided by the electric sub-system	• Valve (21) open HP - User' circuit • Valve (16) open 'Dry cooler - Adsorption module' circuit • Valve (12) open 'Adsorption module - HP' circuit • Valves (19a) and (19b) open • Valves (19c) and (19d) closed • Pumps (24) and (28) in mode ON • Pumps (8), (10), (13), and (17) in mode ON • Electric controller open external grid circuit (34) or electric battery circuit (31) or PV panel circuit (35)
Cooling Mode 5	• Cooling provided by the heat pump (19) • RPW-HEX (23) charged/discharged simultaneously • Adsorption module (9) in mode ON, exploiting the buffer tank (4) energy • Electricity to the heat pump (19) provided by the electric sub-system	• Valve (21) open 'RPW-HEX - User' circuit • Valve (16) open 'Dry cooler - Adsorption module' circuit • Valve (12) open 'Adsorption module - HP' circuit • Valves (19a) and (19b) closed • Valves (19c) and (19d) open • Pumps (24) and (28) in mode ON • Pumps (8), (10), (13), and (17) in mode ON • Electric controller open external grid circuit (34) or electric battery circuit (31) or PV panel circuit (35)

Heating Mode 1	• Heating only provided by the gas boiler (39) • Heat pump (19) in mode OFF • Adsorption module (9) in mode OFF	• Pump (41) in mode OFF • Pumps (24) and (28) in mode OF • Pumps (8), (10), (13), and (17) in mode OFF
Heating Mode 2	• Heating provided by the buffer tank (4) with reheating provided by the gas boiler (39) if needed • Heat pump (19) in mode OFF • Adsorption module (9) in mode OFF	• Pump (41) in mode ON • Pumps (24) and (28) in mode OF • Pumps (8), (10), (13), and (17) in mode OFF

3.1.3 Measurements collected and selection of reference periods (summer)

As seen in Figure 34 to Figure 41, there are many sensors used to monitor HYBUILD system operation. For the analysis of the thermal part of the system, the main parameters evaluated are:

- Temperatures (*T*)
- Solar thermal collectors efficiency (*η_ST*)
- Thermal seasonal energy efficiency ratio ($SEER_{th}$)
- Thermal seasonal performance factor (SPF_{th})
- Solar and auxiliary element energy contributions for DHW production (*SC_DHW*)

Regarding the electrical part, the main parameters evaluated are:

- PV system performance (*η_PV*)
- Electric seasonal energy efficiency ratio ($SEER_{el}$)
- Electric seasonal performance factor (SPF_{el})

Regarding the overall system, the main parameters evaluated are:

- Cooling mode daily hours of operation and daily operation share (*CM_share*)
- Self-consumption (SC_{el})
- Self-sufficiency (SS_{el})
- Share of renewables (SR_{el})

In order to analyse the behaviour of these KPIs in a quick and consistent way and to be able to make adjustments to the control, if necessary, the concept of representative week is established. The representative week corresponds to a week in which the weather conditions are representative for the season of the year to be studied at the selected location. Following this approach, the week of 18-24 July was selected as the representative week to analyse the HYBUYILD system for Mediterranean climate at the Almatret demo site.

3.1.3.1 Temperature measurements

The outdoor ambient temperature trend for the representative summer week of the HYBUILD system in Almatret can be seen in Figure 42. The figure shows that the ambient temperature

varies from 17.5 to 36.2 °C, this trend shows the need for the development of the HYBUILD system with more and more frequent heat waves in Europe and hotter summers.

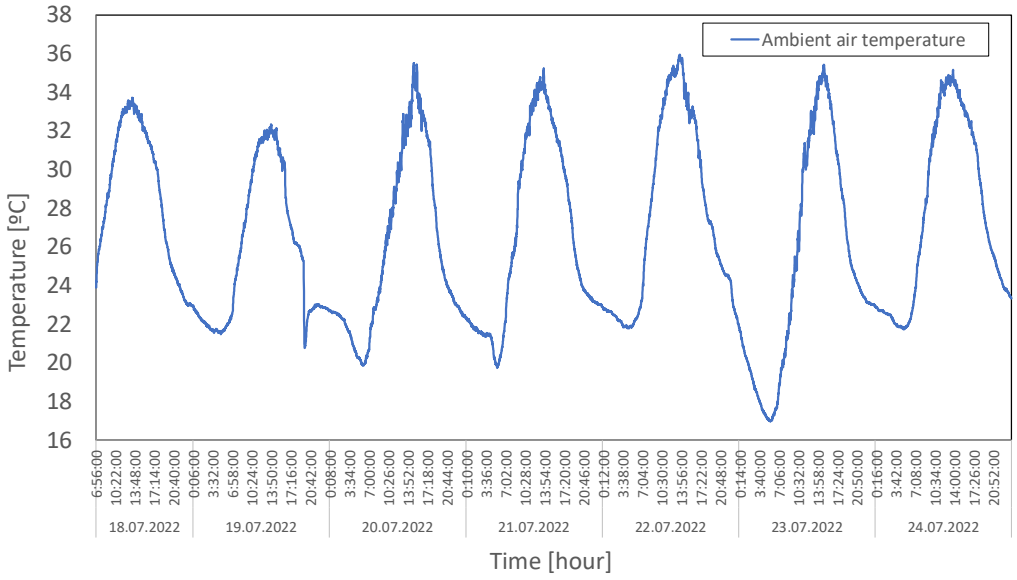

Figure 42. External ambient temperature trend during summer representative week

The internal temperature of the different zones connected to the HYBUILD system is reported in Figure 43. The temperature of all monitored zones is between 22 °C and 28 °C and most of the time in the range of 24 °C - 26 °C. The analysed values indicate that the HYBUILD system guarantees in extreme conditions the maximum indoor comfort temperature (considered in this context equal to 28 °C). Moreover, during 90% of the analysed period the indoor temperature is below 26 °C set-point of thermal comfort established in Spain. Figure 43 shows a similar trend between both zones inside the dwelling, largely due to the fact that the occupancy of both zones was similar in the analysed period. However, no direct correlation was found between the internal temperature of the different zones connected to the HYBUILD system and the external ambient temperature (this corroborates the correct functioning of the system).

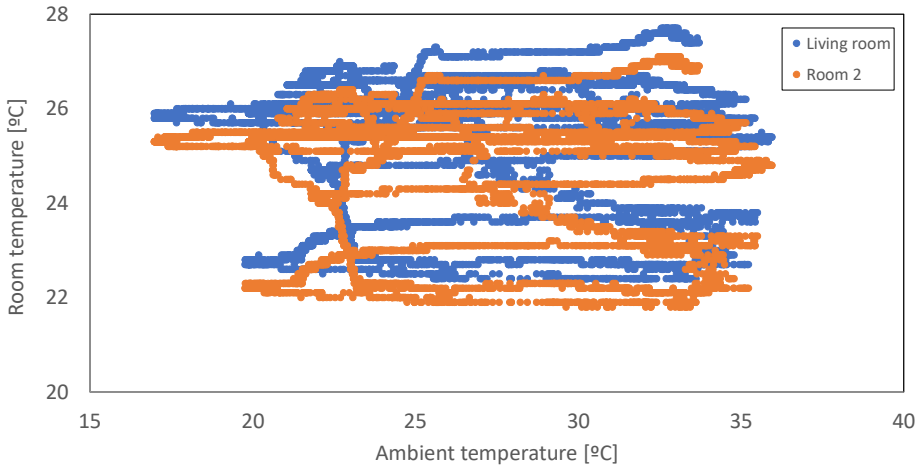

Figure 43. Internal temperature of the various zones connected to HYBUILD Mediterranean system during the representative summer week against external ambient temperature

The PCM temperature monitoring setup of the HYBUILD system is composed of 9 sensors distributed according to Figure 44. In order to analyse the temperature distribution inside the PCM tank during the operation of the heat pump, a representative hour of the system operation

was selected (Figure 45). The figure shows that the PCM acts as a buffer in the system maintaining a state of charge between 50% and 70% during system operation while maintain a suitable room temperature (Figure 43). Furthermore, it is observed that the upper part of the tank (T7, T8 and T9) was 4 °C above the average tank temperature during operation.

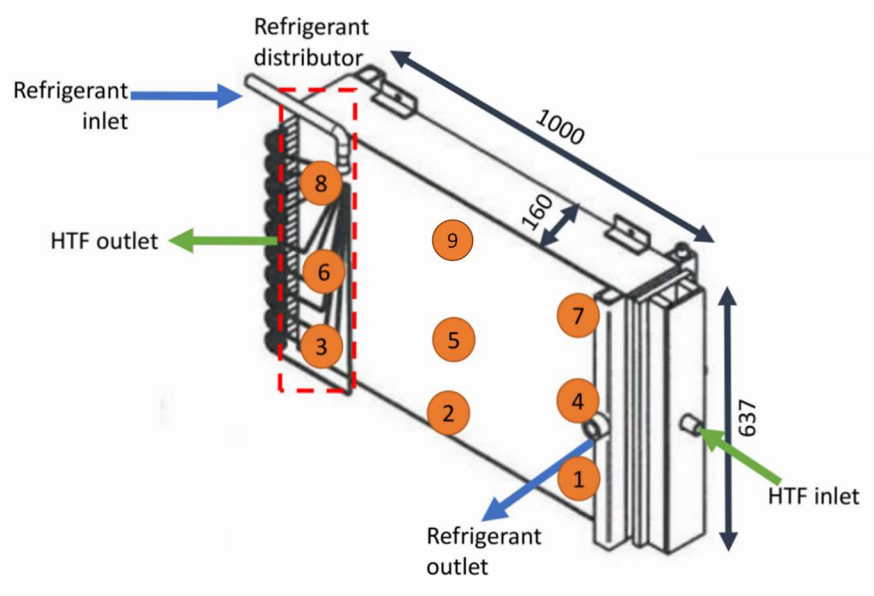

Figure 44. RPW-HEX temperature sensors distribution

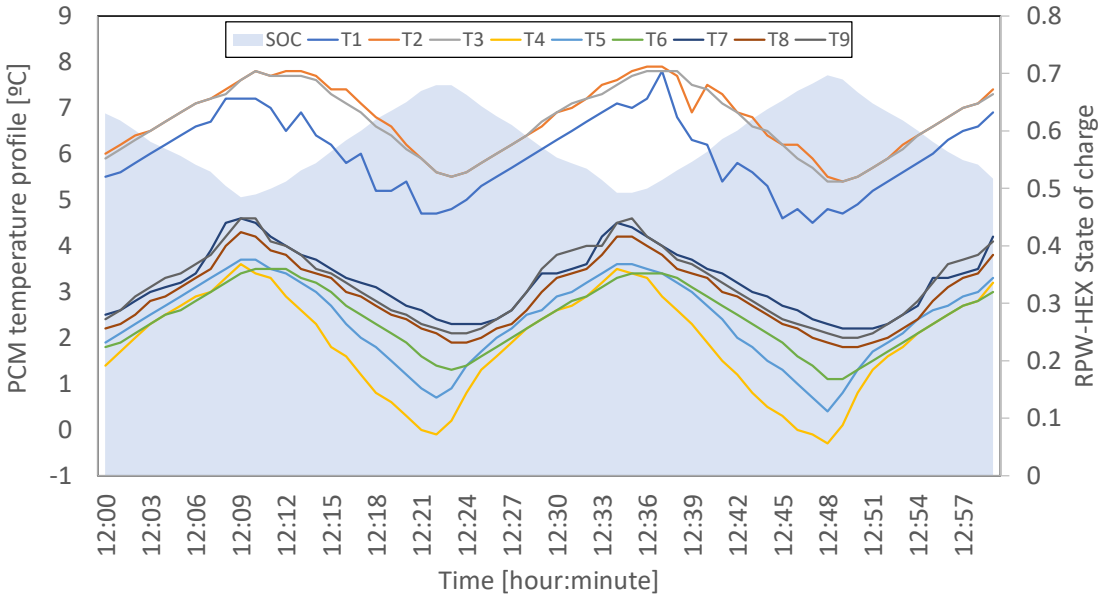

Figure 45. RPW-HEX PCM temperature and state of charge profile during an hour of cooling operation of the HYBUILD system

3.1.3.2 *Solar thermal collectors efficiency*

The solar thermal collectors efficiency (η_ST) refers to the amount of energy charged into the buffer tank in relation to the total amount of solar radiation incident on the collectors surface. Therefore, this parameter is calculated according to the following equation:

$$\eta_{ST} = \frac{Q_{buffer}}{Q_{solar}} = \frac{\Delta(ALM\_STP\_Eth\_ETI006\_Eth\_[kWth])}{ALM\_STP\_IR\_Pyra\_[W/m2] \cdot 60 \cdot \Delta t/1000} \quad (1)$$

where Q_buffer (in kWth) is the total energy charged into the buffer tank in a given time period Δt (in h), Q_solar (in kWth) is the total radiation incident on the collectors surface (global horizontal irradiance) during the same time period Δt. The factor 60 refers to the total surface area of solar collectors installed, 1000 is a conversion factor to express the solar radiation in kW, and Δt must be converted to hours. Figure 46 shows the daily average efficiency obtained from the solar collectors for the representative week of summer. The average efficiency for the week was 33.5%, a notable value when compared to the efficiencies for this system reported in the scientific literature.

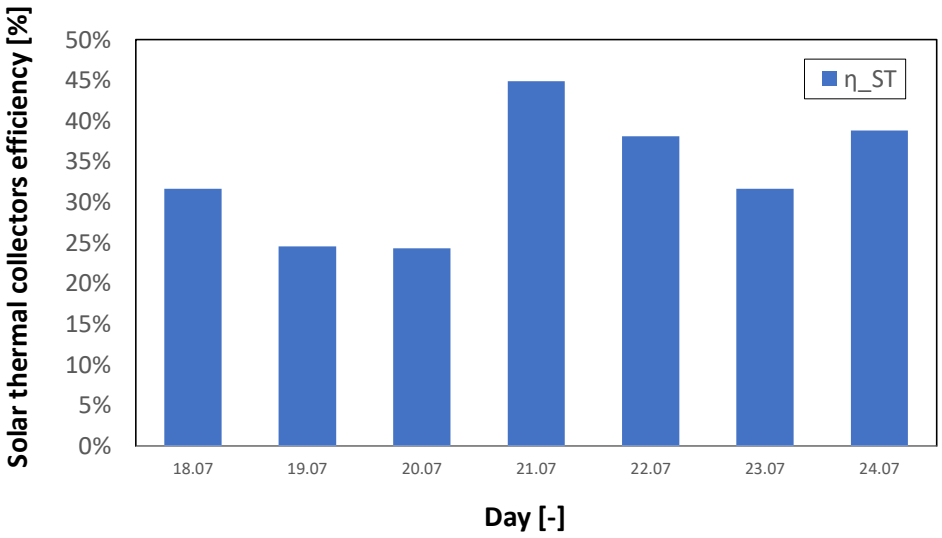

Figure 46. Almatret solar thermal collectors efficiency during summer representative week

3.1.3.3 *Thermal seasonal energy efficiency ratio*

This KPI refers to the adsorption module, which requires thermal energy at high temperature from the buffer tank to produce a cooling effect on the heat pump (HP) condenser (Figure 47).

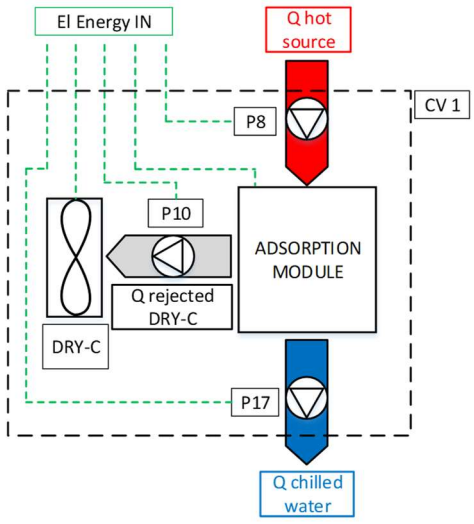

Figure 47. Scheme for the evaluation of adsorption module performance

Therefore, $SEER_{th}$ is calculated as in equation (2):

$$SEER_{th} = \frac{Q_{chilled\ water}}{Q_{hot\ source}} = \frac{\sum_{t=t_i}^{t=t_f}[ALM\_SCH\_FTI\_Flow\_LT\_[l/h] \cdot (ALM\_SCH\_TT\_T\_LT\_IN\_[degC] - ALM\_SCH\_TT\_T\_LT\_OUT\_[degC])]_t}{\sum_{t=t_i}^{t=t_f}[ALM\_SCH\_FTI\_Flow\_HT\_[l/h] \cdot (ALM\_SCH\_TT\_T\_HT\_IN\_[degC] - ALM\_SCH\_TT\_T\_HT\_OUT\_[degC])]_t} \quad (2)$$

where t_i and t_f refer to the initial and final time of the sorption system operation, respectively.

The control operated the sorption system whenever there was a demand for cooling and the buffer tank was kept above 80 °C. For the reference week, the equipment operated every day with the operating hours discussed in Section 3.1.3.9. During the representative week, the SEER of the sorption remained around 0.4.

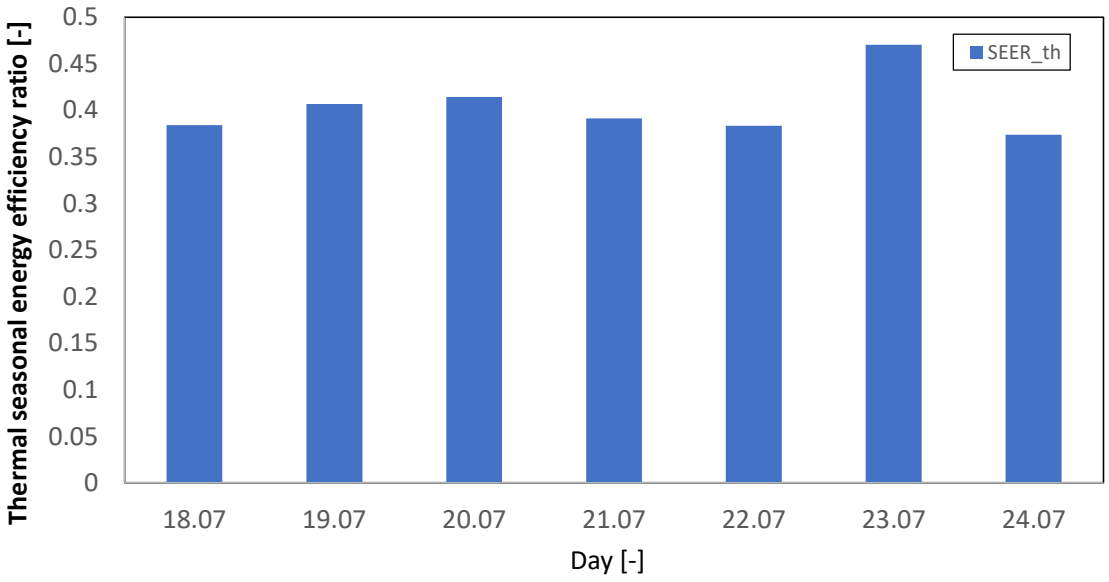

Figure 48. Almatret thermal seasonal energy efficiency ratio during summer representative week

3.1.3.4 Thermal seasonal performance factor

Thermal seasonal performance factor (SPF_{th}) is a KPI used to evaluate global system energy performance. It indicates the ratio between the cooling supplied to the building by the heat pump working in cascade with the sorption module ($Q_{cool\_supply\_BUI}$) and the energy supplied to the high-temperature circuit of the sorption module (Q_{hot_source}), as defined in equation (3) and shown in Figure 49**¡Error! No se encuentra el origen de la referencia.**:

$$SPF_{th} = \frac{Q_{cool\_supply\_BUI}}{Q_{hot\_source}} \quad (3)$$

In this case, the heat pump can work in different modes in the low-pressure side, such as PCM charging, RPW-HEX in 3-fluid mode, or using the standard evaporator. Therefore, an overall (global) performance SPF_{th} of the heat pump working in cascade with the sorption module can be calculated by combining the values obtained for each operating mode.

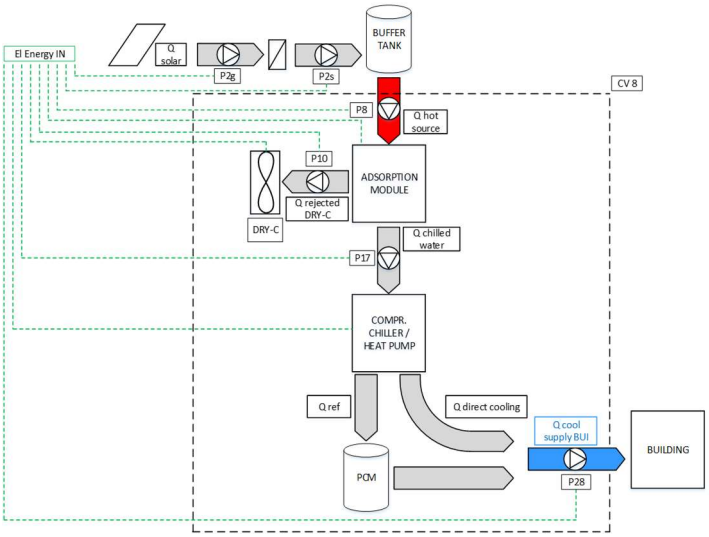

Figure 49. Mode of operation to calculate the thermal seasonal performance factor

The values obtained during the representative week of the thermal seasonal performance factor are shown in Figure 50. These show an average value of 0.48 demonstrating both the average value and the daily value that the cascade system achieved a 15%-20% improvement in operation compared to the individual sorption system operation (Figure 49).

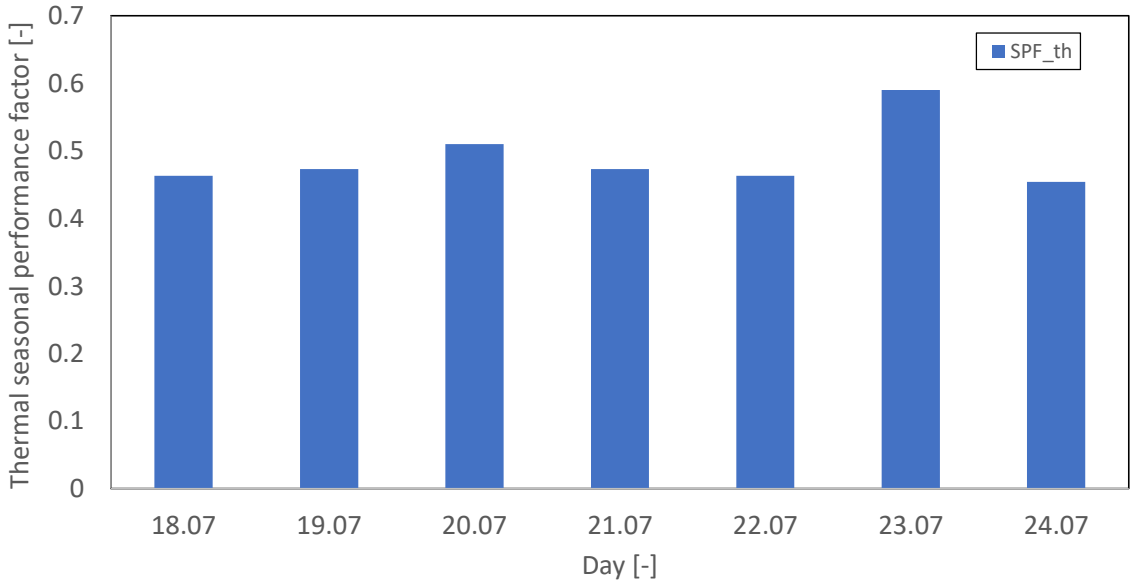

Figure 50. Almatret thermal seasonal performance factor during summer representative week

3.1.3.5 Solar and auxiliary element energy contributions for DHW production (SC_DHW)

The system installed at the Almatret demo site is able to cover part of the DHW demand of the building from thermal energy captured by the solar thermal system. Therefore, it is useful to evaluate the energy contribution from the solar system and from the auxiliary element (gas boiler).

The solar contribution to DHW demand (SC_{DHW}) is defined in equation (4):

$$SC_{DHW} = \frac{Q_{DHW\_tank}}{Q_{DHW\_tot}} = \frac{\Delta(ALM\_DHW\_Eth\_ETI003\_Eth\_[kWth])}{\Delta(ALM\_DHW\_Eth\_ETI001\_Eth\_[kWth]) + \Delta(ALM\_DHW\_Eth\_ETI003\_Eth\_[kWth])} \quad (4)$$

where Q_{DHW_tank} is the thermal energy supplied for DHW from the DHW tank and Q_{DHW_tot} is the total thermal energy supplied for DHW (both from the DHW tank and from the gas boiler).

Similarly, the auxiliary contribution to DHW (AC_{DHW}) is defined as in equation (5):

$$AC_{DHW} = \frac{Q_{DHW\_gas\_boiler}}{Q_{DHW\_tot}} = \frac{\Delta(ALM\_DHW\_Eth\_ETI001\_Eth\_[kWth])}{\Delta(ALM\_DHW\_Eth\_ETI001\_Eth\_[kWth]) + \Delta(ALM\_DHW\_Eth\_ETI003\_Eth\_[kWth])} \quad (5)$$

where $Q_{DHW\_gas\_boiler}$ is the thermal energy supplied for DHW from the gas boiler and Q_{DHW_tot} is the total thermal energy supplied for DHW (both from the DHW tank and from the gas boiler).

Figure 51 shows that 99% of the heat demand of the house, approximately 5 kWh per day, is supplied by the contribution of the solar collectors. The 1% contribution of the gas boiler is justified by the standby consumption of the boiler currently installed at Almatret.

(Figure 35).

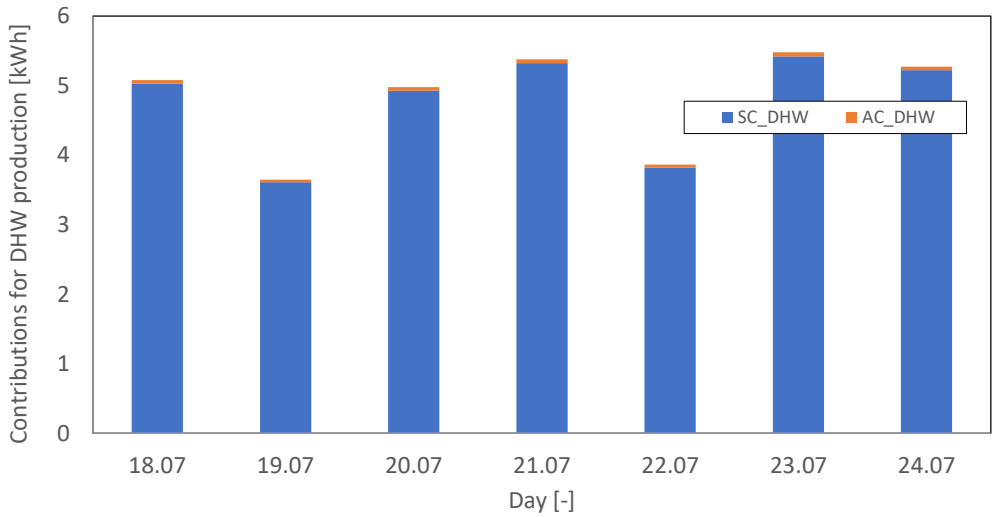

Figure 51. Almatret DHW production during summer representative week

3.1.3.6 PV system performance

The PV system performance (η_PV) refers to the amount of energy (electricity) supplied by the PV panels to the DC bus in relation to the total amount of solar radiation incident on a horizontal surface (global horizontal irradiance) having the same area as the total PV panels surface area. Since the surface of the PV panels is not horizontal, this variable is different from the standard PV efficiency and it should reflect the influence of the tilt angle of the PV panels on the electricity generation in different periods of the year. So, this KPI can be calculated according to equation (6):

$$\eta_{PV} = \frac{Q_{PV}}{Q_{solar}} = \frac{\sum_{t=t_i}^{t=t_f}(ALM\_gMD1\_Pel\_powerPV\_[W])_t}{\sum_{t=t_i}^{t=t_f}(ALM\_STP\_IR\_Pyra\_[W/m2])_t \cdot 28} \quad (6)$$

where Q_PV (in J) is the total electricity generated by the PV system during a given time period $\Delta t=t_f-t_i$ (in sec), where t_i and t_f refer to the initial and final time of the experiment, respectively, and Q_solar (in J) is the total amount of solar radiation incident on a horizontal surface having the same area as the total PV panels surface area. The factor 28 refers to the total surface area of PV panels installed.

For the representative week, the PVs delivered to the DC-bus was approximately 30 kWh per day with an average efficiency of 13.5%.

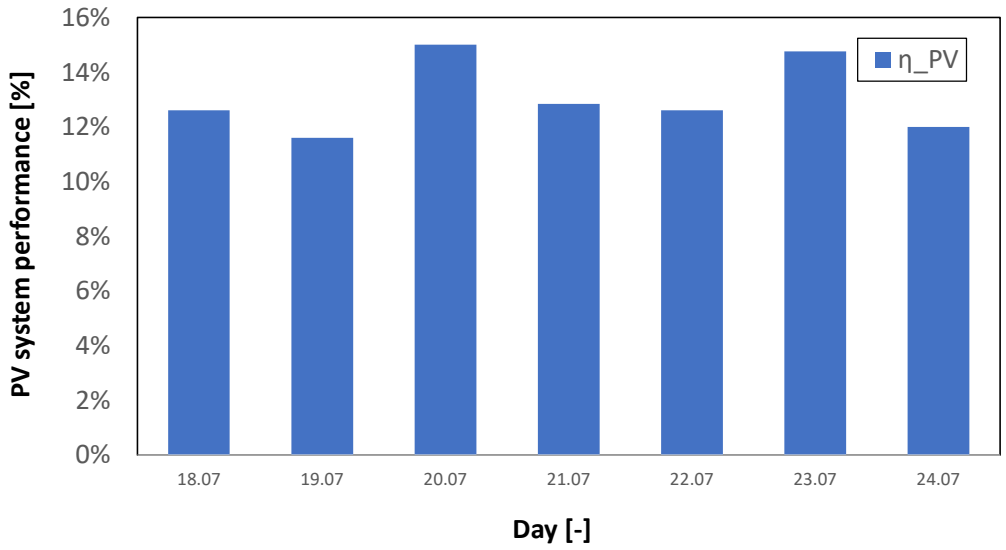

Figure 52. Almatret photovoltaic efficiency during summer representative week

3.1.3.7 Electric seasonal energy efficiency ratio ($SEER_{el}$)

This KPI applies to the heat pump, which requires electricity to produce a cooling effect on the building or on the PCM storage (RPW-HEX). $SEER_{el}$ is defined according to equation (7):

$$SEER_{el} = \frac{Q_{RPW-HEX} + Q_{standard}}{El\ Energy\ IN} \quad (7)$$

where $Q_{RPW-HEX}$ is the amount of cold supplied by the HP to the RPW-HEX, $Q_{standard}$ is the amount of cold supplied by the HP bypassing the PCM storage (i.e. using the standard evaporator), and $El\ Energy\ IN$ is the electricity consumption of the HP sub-system.

Since the cold supplied by the heat pump cannot be measured directly in the refrigerant circuit, it can still be estimated by means of the energy meter (ETI007) that measures the cold supplied to the building in any of the two possible ways (i.e., either through the RPW-HEX or through the standard evaporator). In this way, the term in the numerator of equation (7) ($Q_{RPW-HEX} + Q_{standard}$) consists of data measured by the energy meter ETI007.

Figure 53 shows that the electrical $SEER_{el}$ values of the HP ranged between 3.72 and 4, which is very similar to the values obtained in the laboratory tests at ITAE facility.

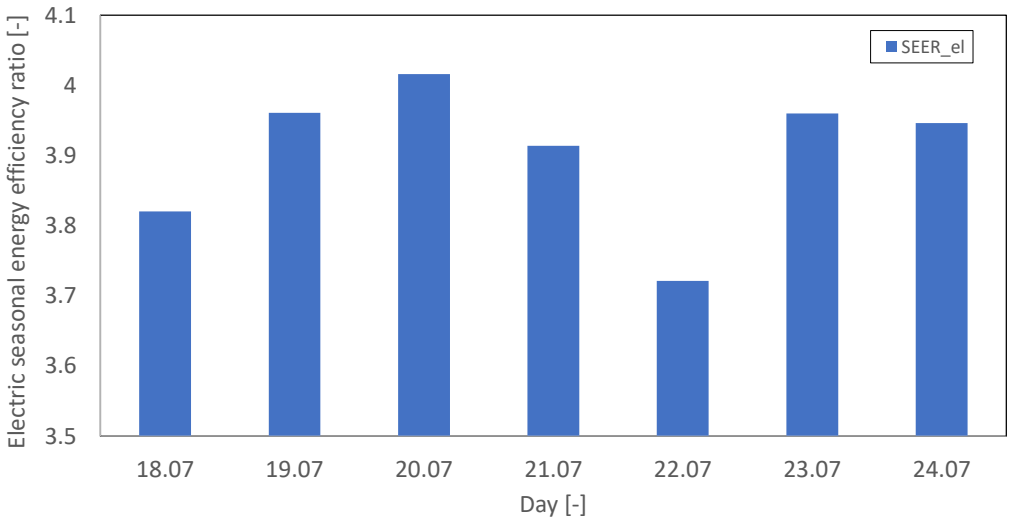

Figure 53. Almatret electric seasonal energy efficiency ratio during summer representative week

3.1.3.8 Electric seasonal performance factor (SPF_{el})

The definition of the electric seasonal performance factor (SPF_{el}) is similar to the thermal one, and it expresses the ratio between the cooling supplied to the building by the HP working in cascade with the sorption module ($Q_{cool\_supply\_BUI}$) and the total electricity consumption of the whole HYBUILD system (El_Energy_IN), as shown in Figure 54**¡Error! No se encuentra el origen de la referencia.** and defined in equation (8):

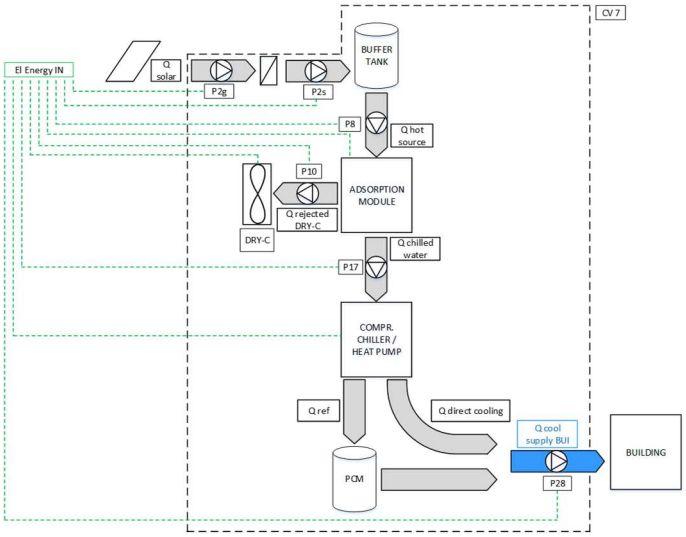

Figure 54. Mode of operation to calculate the electric seasonal performance factor

$$SPF_{el} = \frac{Q_{cool\_supply\_BUI}}{El\_Energy\_IN} \quad (8)$$

As seen in Figure 54**¡Error! No se encuentra el origen de la referencia.**, El_Energy_IN takes into account all electrical energy contributions: electricity consumed by the adsorption machine, by the dry cooler, by the HP compressor, and by all pumps connected in between the solar field, the sorption module, the dry cooler, the HP, and the cooling distribution circuit.

Similar to the SPF_{th} (Section 3.1.3.4), the SPF_{el} improved due to the cascade operation between the HP and the sorption system. In the representative week, the SPF_{el} ranged from 4.48 to 4.82,

which is between 15% and 20% daily improvement compared to the $SEER_{el}$ of the HP operating individually.

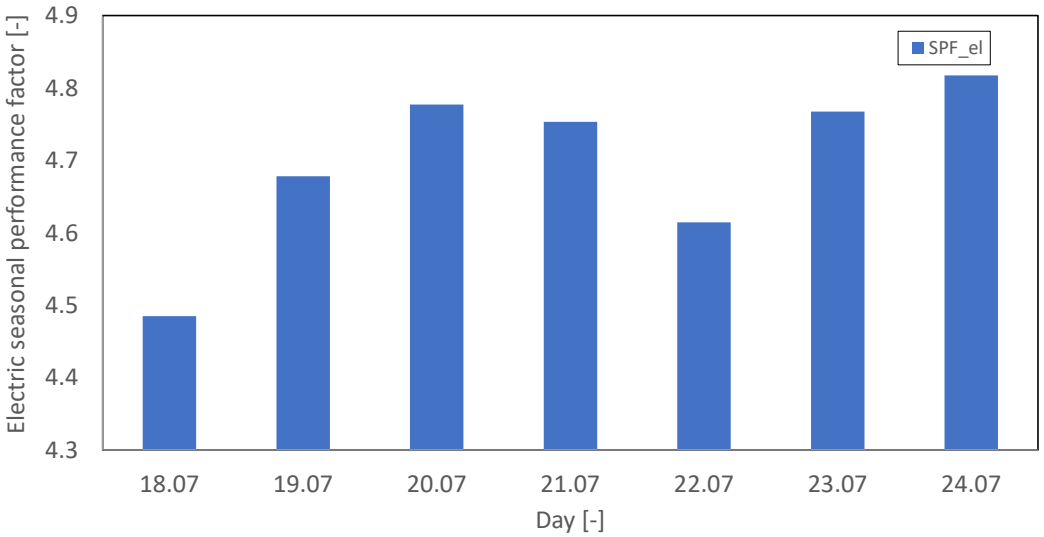

Figure 55. Almatret electric seasonal performance factor during summer representative week

3.1.3.9 Cooling mode daily hours of operation and daily operation share (CM_share)

The HYBUILD system operated providing cooling approximately 9.8 hours daily with a peak operation on Saturday 23.07 with 12.5 hours of operation and a minimum operation of 6.7 hours on Tuesday 19.07. The variations can be justified by the weather conditions, and the daily occupancy profile of the dwelling. Moreover, when analysing which operating modes contributed to the HYBUILD operation, Figure 56 shows that the system always operated using the RPW-HEX, using the PCM as a buffer between the cooling generation and energy demand of the house. The sorption assisted the operation of the HP mostly during the hours of peak solar radiation of the day (between 11 am and 4 pm), and during this period the solar field was able to maintain the water tank temperature at approximately 85 ºC.

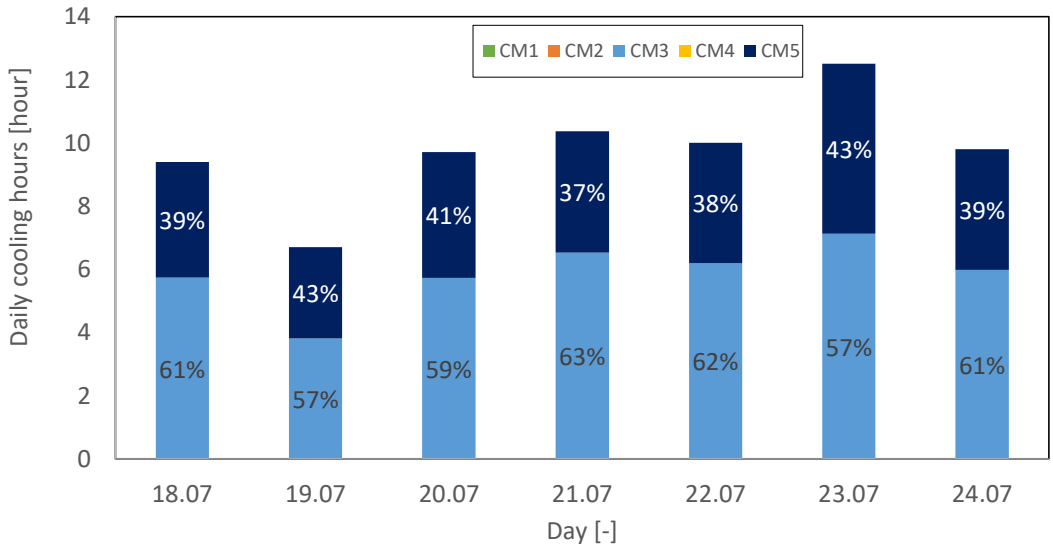

Figure 56. Almatret daily cooling hours and share of cooling operation modes during summer representative week

3.1.3.10 Self-consumption (SC_{el})

Self-consumption (SC_{el}) is a KPI that represents the fraction of energy produced by the PV system that is directly consumed by the load or stored into the battery, with respect to the total PV production, as shown in equation (9):

$$SC_{el} = \frac{\sum_{t=t_i}^{t=t_f}(E_{RES\_el})_t}{\sum_{t=t_i}^{t=t_f}(E_{RES-TOT\_el})_t} \quad (9)$$

where E_{RES_el} (in W) is the energy produced by PV that is directly consumed by the load or stored into the battery, while $E_{RES-TOT\_el}$ (in W) represents the total PV production at a given time t.

To determine E_{RES_el}, one should first calculate the power supplied from the grid (G, in W) as in equation (10):

$$G = HP + B - PV \quad (10)$$

where $HP = ALM\_gMD1\_Pel\_powerHP\_[W]$ is the power consumption of the heat pump, $B = ALM\_gMD1\_Pel\_powerBat\_[W]$ is the charging power of the battery, and $PV = ALM\_gMD1\_Pel\_powerPV\_[W]$ is the power generated by the PV system (in W).

The energy produced by PV and directly consumed by the load or stored into the battery at a given time t (E_{RES_el}, in W) can be calculated using equation (11):

$$E_{RES\_el} = \begin{cases} PV, & \text{if } (G \geq 0) \text{ or } (PV \leq HP) \\ HP + \delta_B \cdot B, & \text{otherwise} \end{cases} \quad (11)$$

where $\delta_B = 1$ if $B \geq 0$ and $\delta_B = 0$ if $B < 0$. As mentioned above, $E_{RES-TOT\_el} = PV$.

The Figure 57 shows that the HYBUILD system has a high level of self-consumption by using a high share of the electric energy produced by the PVs. Figure 57 shows an average value of 0.82 during the representative week and a maximum value of 0.92 on Friday 22.07.

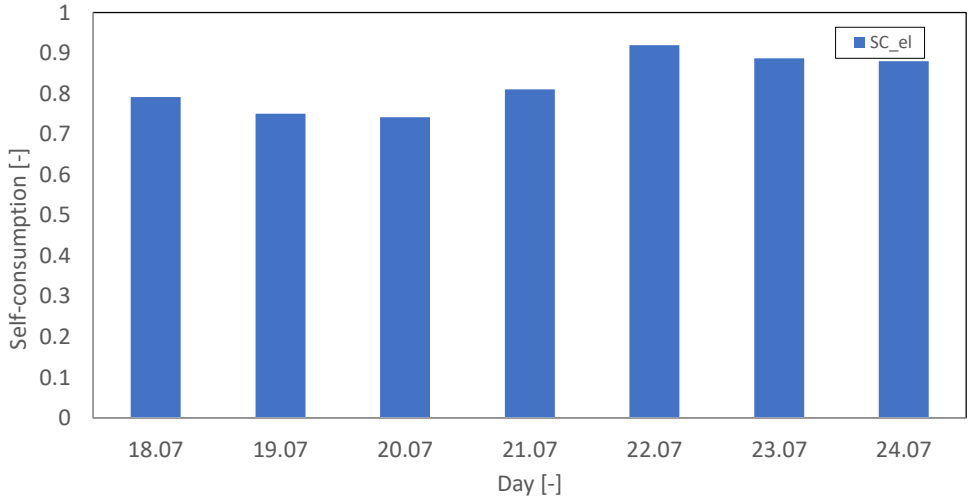

Figure 57. Almatret electric self-consumption during summer representative week

3.1.3.11 Self-sufficiency (SS_{el})

Self-sufficiency (SS_{el}) is a KPI that represents the fraction of energy produced by PV and directly consumed by the load or stored into the battery, with respect to the total load demand, as shown in equation (12):

$$SS_{el} = \frac{\sum_{t=t_i}^{t=t_f}(E_{RES\_el})_t}{\sum_{t=t_i}^{t=t_f}(E_{D\_el})_t} \quad (12)$$

where $E_{RES,el}$ is obtained from equation (11) and E_{D_el} (in W) is the electricity demand of the heat pump at a given time t, i.e. $E_{D\_el} = HP = ALM\_gMD1\_Pel\_powerHP\_[W]$.

The self-sufficiency data for the representative week is shown in Figure 58. These showed an average value of 0.58, with the highest value (0.63) on Monday 9.07. The results obtained show that the HYBUILD system manages to cover more than 50% of the cooling demand of the building with energy generated by the system itself. Furthermore, HYBUILD's electrical energy storage capabilities were used to increase the share of renewable energy consumed by the system as discussed in Section 3.1.3.12.

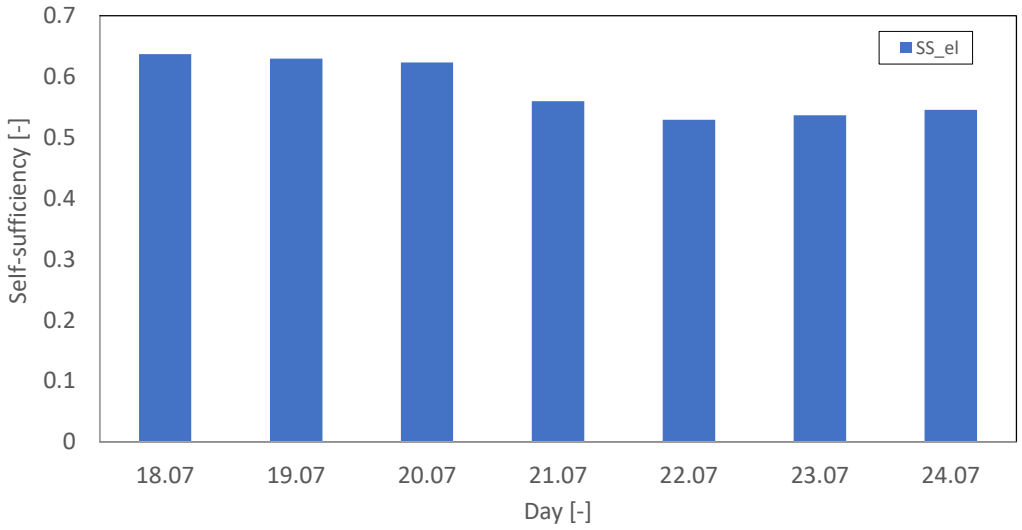

Figure 58. Almatret electric self-sufficiency during summer representative week

3.1.3.12 Share of renewables (SR_{el})

Share of renewables (SR_{el}) is a KPI similar to self-sufficiency, but in this case also the renewable energy fraction of the energy taken from the grid is considered in the calculations. This KPI represents the ratio between the overall renewable energy consumed (coming from both PV and battery, plus the renewable part of the electricity coming from the grid) and the total electricity demand, according to equation (13). The share of renewables also considers the electricity consumption of the auxiliaries.

$$SR_{el} = \frac{\sum_{t=t_i}^{t=t_f}(E_{RES*\_el})_t}{\sum_{t=t_i}^{t=t_f}(E_{D*\_el})_t} \quad (13)$$

where E_{RES*_el} (in W) is the energy produced by PV and directly consumed by the load or stored into the battery plus the renewable energy fraction coming from the grid at a given time t, while E_{D*_el} (in W) represents, in this case, the total energy demand (heat pump electrical consumption plus the consumption of all auxiliaries).

The total energy demand (E_{D*_el}) is obtained from equation (14):

$$E_{D*\_el} = ALM\_gMD1\_Pel\_powerHP\_[W] + ALM\_STP\_Pel\_Pel\_solar\_[W] + ALM\_HP\_Pel\_Pel\_sorption\_[W] + ALM_{aux}\_controller\_Pel\_Pel\_aux\_[W] \quad (14)$$

The renewable energy consumed by the system at time t (E_{RES*_el}) is given by equation (15):

$$E_{RES*\_el} = E_{RES\_el} + f_{ren} \cdot G \quad (15)$$

where E_{RES_el} is obtained from equation (11), G is obtained from equation (10), and f_{ren} is the renewable fraction of energy coming from the grid, which depends on the energy mix at a given time.

Figure 59 shows the share of renewable energy consumed by HYBUILD during the representative week in blue bars, and in orange bars the share of renewable energy of the grid energy mix corresponding to Spain for the representative week. The HYBUILD system with the use of its storage capabilities managed to double the share of renewable energy consumed during the week.

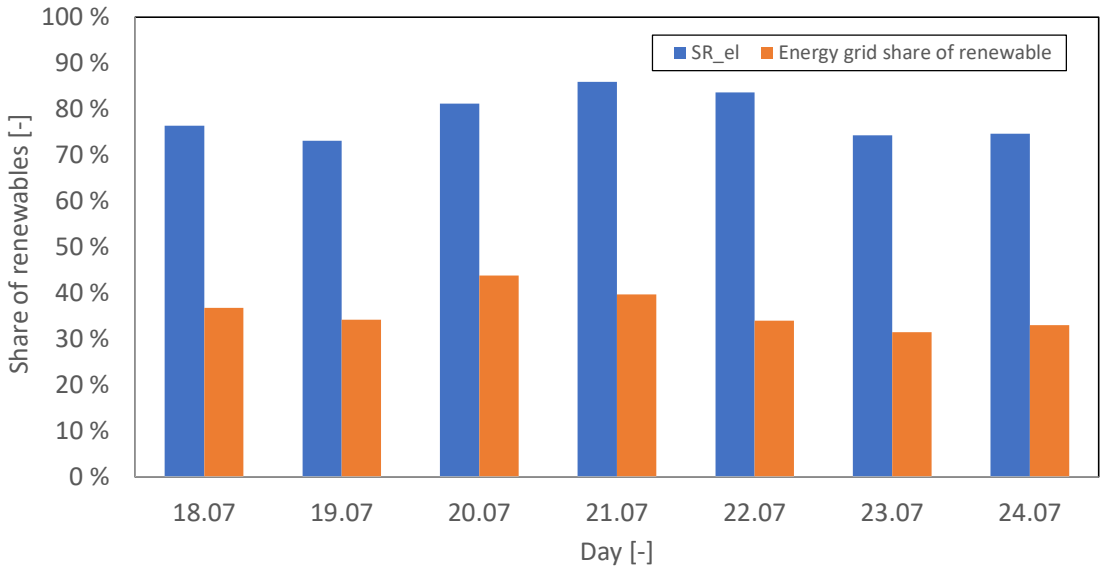

Figure 59. Almatret electric share of renewable during summer representative week

3.2 Aglantzia demo site

3.2.1 General scheme and sensors

In this section the overall system of Aglantzia demo site is described and all the sensors installed are presented. Figure 60 presents the P&ID diagram of the HYBUILD system installed, with all the sensors connected to the auxiliary controller (PLC) and the Master controller.

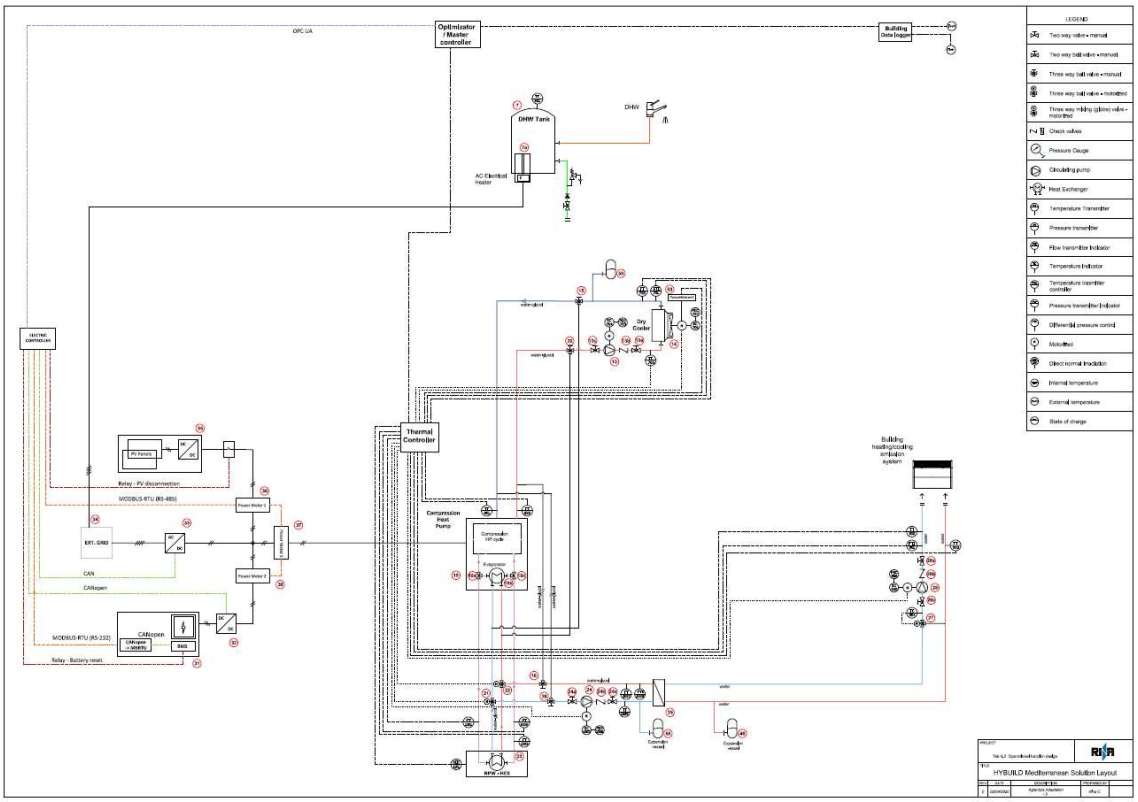

Figure 60. P&ID diagram of HYBUILD system of Aglantzia demo

Figure 61Figure 62 show the various parts of the system, as it is installed, and all the sensors that are connected to each component of the system. Figure 61 presents the dry cooler with the temperature and flow sensors related to this part. Furthermore, the circulating pump of the dry cooler (pump 13) is presented as well. In addition, Figure 61 presents the two of four manual 3-way valves which are responsible for switching from cooling mode to heating mode.

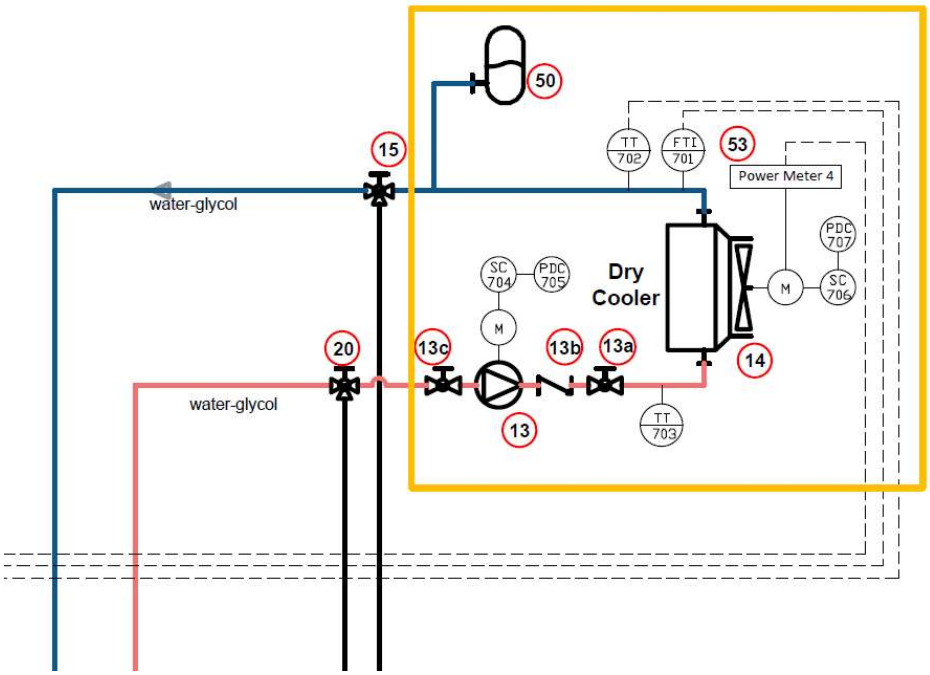

Figure 61. Connections and sensors of dry cooler

Figure 62 presents the compression Heat Pump with all the sensors connected to this module. These sensors include water temperature at the input and output of the condenser, temperature of the refrigerant gas at the evaporator and condenser input and output, and the pressure of the refrigerant gas circuit.

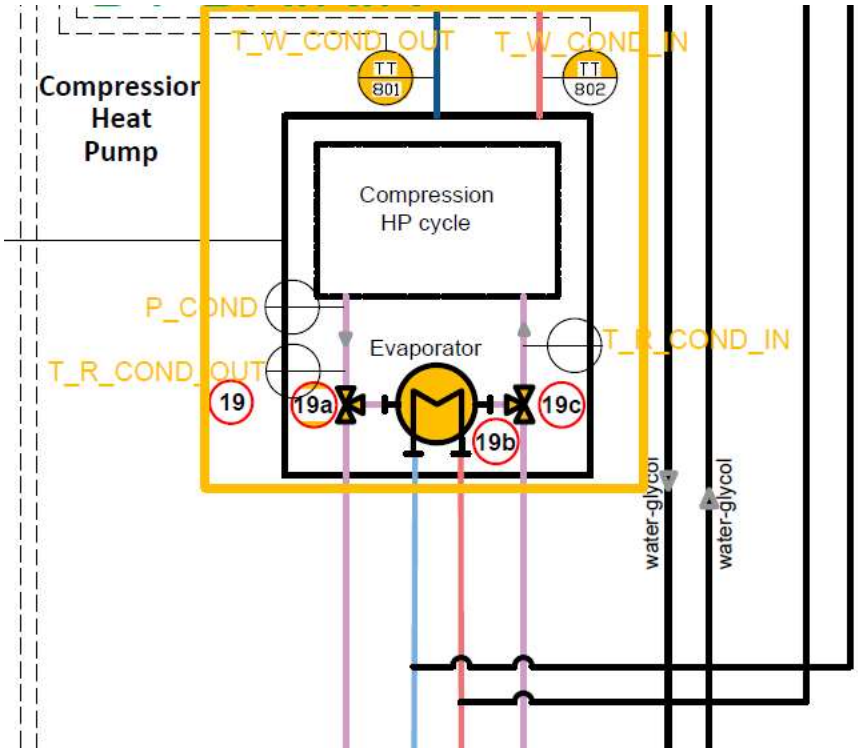

Figure 62. Connections and sensors of compression heat pump system

Figure 63 presents the RPW-HEX system (PCM latent storage) and its connections with the heat exchanger for the indoor distribution system. All the connected sensors on this part are presented as well. It should be noted here that due to a technical problem from the refrigerant gas leak that occurred inside the RPW-HEX, the RPW-HEX had to be bypassed for the time being until a suitable solution to this problem can be found.

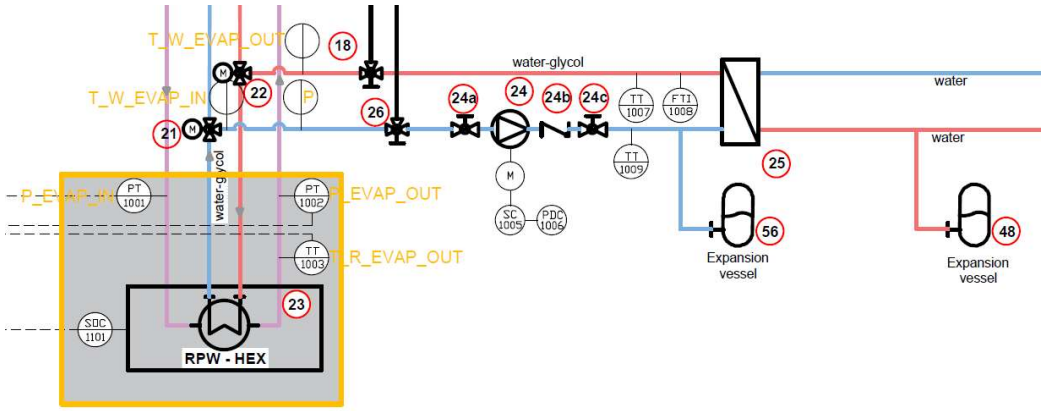

Figure 63. Connections and sensors of RPW-HEX and heat exchanger for the indoor distribution system

Figure 64 presents the indoor distribution system supplying the fan coil units with hot or cold water depending the selected operation mode. Furthermore, flow and temperature sensors connected on the from and to the fan coil units are presented.

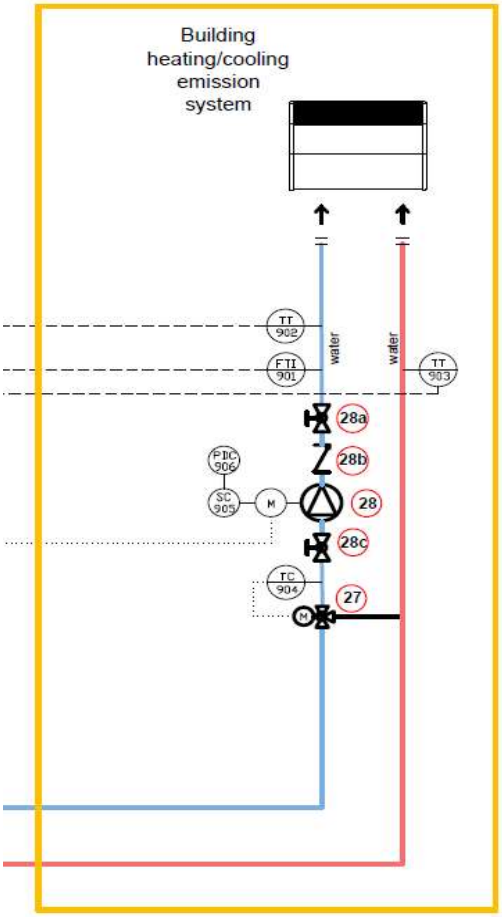

Figure 64. Connections and sensors of the indoor distribution system

Finally, Figure 65 presents the electric controller with the DC bus system and power meters connected on the circuit. The electric system consists of a 5 kWp photovoltaic system, a DC/DC string optimizer, a bidirectional AC/DC converter for the connection with the AC distribution grid, and a battery storage system with a battery management system in order to store electricity when there is surplus to use it at a later stage.

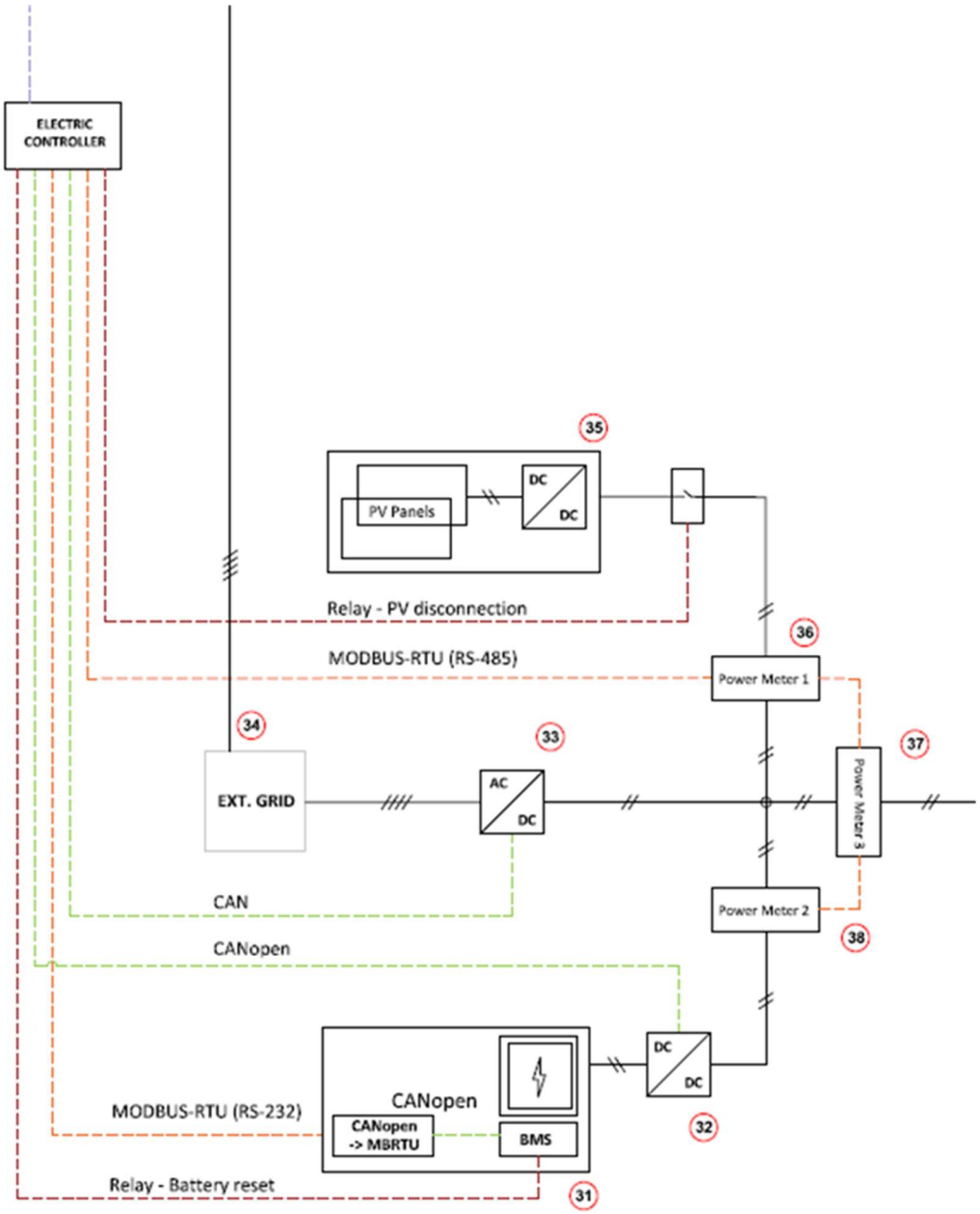

Figure 65. The DC bus system

3.2.2 Operational modes

According to deliverable D4.2, the system installed at the Aglantzia demo site can operate in different modes such as cooling, heating, and charging mode. These modes are described below and summarized in Table 5. For now, the only available modes are cooling mode 2 and heating mode 1 due to the leakage in RPW-HEX as it was mentioned earlier.

Cooling Mode 1 (Not working as RPW-HEX bypassed)

- Cooling provided by RPW-EX

Cooling Mode 2

- Cooling provided by the Compression HP
- RPW-HEX Bypassed
- Electricity to compression HP (19) provided by Electric sub-system

Cooling Mode 3 (Not working as RPW-HEX bypassed)

- Cooling provided by the Compression HP
- RPW-HEX charged/discharged simultaneously
- Electricity to compression HP provided by Electric sub-system

Heating Mode 1

- Heating provided by the Compression HP
- RPW-HEX bypassed
- Electricity to compression HP provided by Electric sub-system

Charging Mode (Not working as RPW-HEX bypassed)

- RPW-HEX (23) charging
- Compression HP (19) mode on
- Electricity provided by Electric sub-system

Table 5. Operational modes of Aglantzia demo site system

OPERATIONAL MODE	MAIN COMPONENTS OPERATIONS	ACTUATORS MODE
COOLING Mode 1	• Cooling provided by RPW-EX (23)	• Valves (21)(22) open 'RPW-HEX - User' circuit; • Pumps (24) (28) mode on; • Pump (13) mode off;
COOLING Mode 2	• Cooling provided by Compression HP (19); • RPW-HEX (23) Bypassed • Electricity to compression HP (19) provided by Electric sub-system	• Valves (21) (22) open 'Compression HP - User circuit'; • Valves (19a) (19c) open standard Evaporator (19b) circuit; • Valves (15) (20) close 'Compression HP Heating mode - Dry cooler' circuit • Valves (18) (26) close 'Compression HP Heating mode - User' circuit • Pumps (24) (28) mode on; • Pumps (13) mode on; • Electric Controller open external grid

		circuit (33) (34) or electric battery circuit (31) (32) or PV panel Circuit (35)
COOLING Mode 3	• Cooling provided by Compression HP (19); • RPW-HEX (23) charged/discharged simultaneously • Electricity to compression HP (19) provided by Electric sub-system	• Valves (21) (22) open 'RPW-HEX - User circuit'; • Valve (19a) (19c) bypass standard Evaporator (19b) circuit; • Valves (15) (20) close 'Compression HP Heating mode - Dry cooler' circuit • Valves (18) (26) close 'Compression HP Heating mode - User' circuit • Pumps (24) (28) mode on; • Pump (13) mode on; • Electric Controller open external grid circuit (33) (34) or electric battery circuit (31) (32) or PV panel Circuit (35)
CHARGING Mode 1	• RPW-HEX (23) charging ; • Compression HP (19) mode on; • Electricity provided by Electric sub-system	• Valves (21) (22) open 'RPW-HEX - User circuit'; • Valves (19a) (19c) bypass standard Evaporator (19b) circuit; • Valves (15) (20) close 'Compression HP Heating mode - Dry cooler' circuit • Valves (18) (26)close 'Compression HP Heating mode - User' circuit • Pumps (24) (28) mode off; • Pump (13) mode on; • Electric Controller open external grid circuit (33) (34) or electric battery circuit (31) (32) or PV panel Circuit (35)
HEATING Mode 1	• Heating provided by Compression HP (19); • RPW-HEX (23) bypassed; • Electricity to compression HP (19) provided by Electric sub-system	• Valves (18) (26)open 'Heating mode Compression HP - User' circuit • Valves (15) (20) open 'Heating mode Dry Cooler - Compression HP' circuit • Valves (19a) (19c) open standard Evaporator (19b) circuit; • Valves (21) close 'Compression HP - User circuit'; • Valve (22) close 'Compression HP - RPW-HEX' circuit'; • Pumps (28) mode on; • Pump (13) mode on; • Pumps (24)mode off; • Electric Controller open external grid circuit (33) (34) or electric battery circuit (31) (32) or PV panel Circuit (35)

3.2.3 Measurements collected and selection of reference periods (summer)

As has been described earlier in this document, there are various sensors used for the monitoring of the operation and for the evaluation of the efficiency of the HYBUILD system. For the analysis of the thermal part of the system the main parameters evaluated are the temperatures (*T*), indoor and outdoor.

In addition, regarding the electrical part, the main parameters evaluated are:

- PV system performance (*η_PV*)
- Battery Energy Storage System (BESS) performance
- The interaction of the system with the external electricity network

Finally, for the evaluation of the overall system, the main parameters used are:

- Self-consumption (SC_{el})
- Self-sufficiency (SS_{el})
- Share of renewables (SR_{el})

In order to analyse the behaviour of these KPIs in a quick and consistent way and to be able to adjust the control, if necessary, the concept of representative week is established. Following this approach, the week of 1-7 August was selected as the representative week to analyse the HYBUYILD system for Mediterranean climate in the Aglantzia demo site.

3.2.3.1 Temperature measurements

The outdoor ambient temperature trend for the representative summer week of the HYBUILD system in Aglantzia can be seen in Figure 66. The figure shows that the ambient temperature varies from 26,4 to 37,1 °C. Considering the values of the outdoor temperature for the specific week, we can calculate the comfort zone for the indoor temperature. According to the calculations carried out it follows that the upper and lower thresholds for 90% acceptability are 25 to 30 °C, while the upper and lower thresholds for 80% acceptability are 24 to 31 °C.

Figure 67 shows the fluctuation of the internal temperature of the building. The blue line shows the indoor temperature distribution, the red dashed lines show the upper and lower thresholds for 90% acceptability, while the green dashed lines show the upper and lower thresholds for 80% acceptability. As can be seen from the graphical representation of the indoor temperature, for the first three days of the specific week, 1 – 3/08/2022, during which the system was in operation, the indoor temperature was remained more or less stable with small fluctuations and within the thresholds of 90% acceptability. For the rest of the week, during which the system was not in operation, the indoor temperature of the building rises above the upper threshold of 90% acceptability, however remains within the thresholds of 80% acceptability.

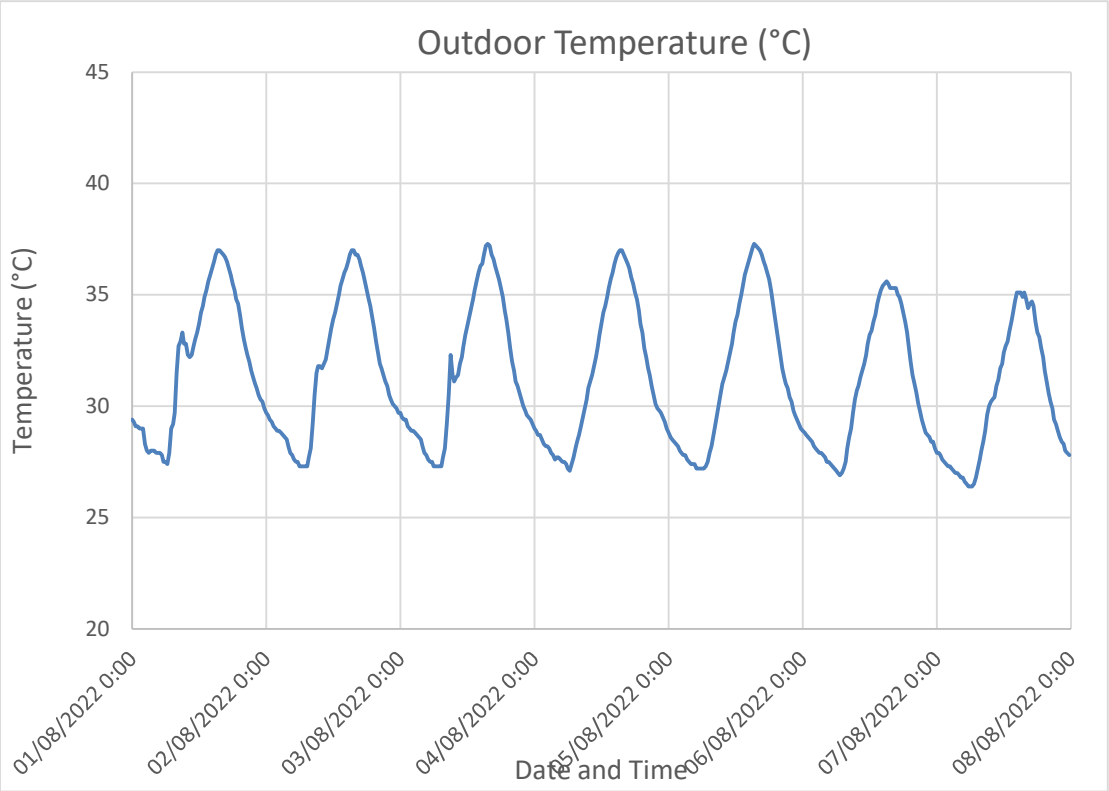

Figure 66. Ambient outdoor temperature in Aglantzia, Cyprus

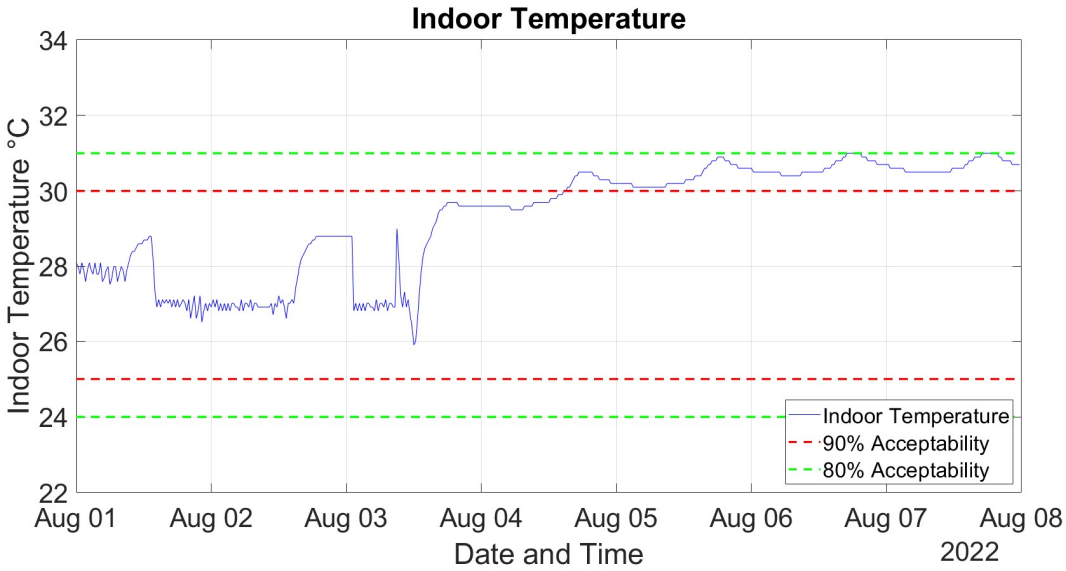

Figure 67. Indoor temperature of the building with thermal comfort zones

3.2.3.2 PV system performance

The PV system performance (η_PV) refers to the amount of energy (electricity) supplied by the PV panels to the DC bus in relation to the total amount of solar radiation incident on a horizontal surface (global horizontal irradiance) having the same area as the total PV panels surface area. Since the surface of the PV panels is not horizontal, this variable is different from the standard PV efficiency and it should reflect the influence of the tilt angle of the PV panels on the electricity generation in different periods of the year. So, this KPI can be calculated according to the following equation:

$$\eta_{PV} = \frac{Q_{PV}}{Q_{solar}} = \frac{\sum_{t=t_i}^{t=t_f}(AGL\_gMD1\_Pel\_powerPV\_[W])_t}{\sum_{t=t_i}^{t=t_f}(AGL\_STP\_IR\_Pyra\_[W/m2])_t \cdot 26}$$

where Q_{PV} is the total electricity generated by the PV system during a given time period, and Q_{solar} is the total amount of solar radiation incident on a horizontal surface having the same area as the total PV panels surface area. The factor 26 refers to the total surface area m^2 of PV panels installed.

For the representative week, the PVs delivered to the DC-bus approximately 16 - 19 kWh per day with an average efficiency of 11,45%. The average production and efficiency of the PV system is quiet low mostly due to the orientation of the PV system which is not the optimal (the system is looking South - East) and the small inclination of the PV panels.

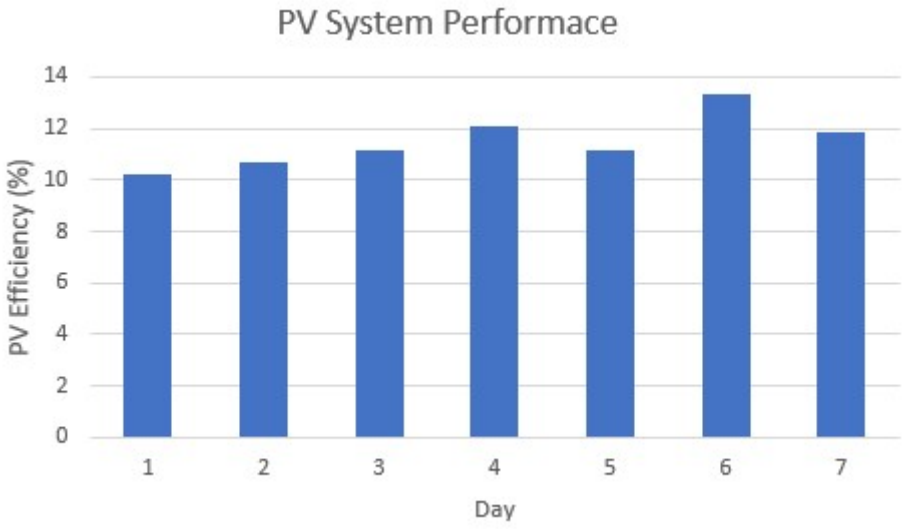

Figure 68. Aglantzia photovoltaic efficiency during summer representative week

3.2.4 Electrical system analysis

The operation of the electrical part of the system is evaluated through different analysis. In the first part, the evaluations about the electrical energy fluxes between PV, BESS, grid and HP (also called load) are presented. In this section, it is highlighted the contribution of the photovoltaic and battery system to cover the load. In the second part, the Self-sufficiency ($SS_{(el)}$) and Self-consumption ($SC_{(el)}$) indexes are used to analyse the energy-related performances of the system. If the first part about electrical energy fluxes analysis is basically a qualitative analysis, the calculation of the indexes in the second part give instead quantitative indications about the amount of electrical energy consumption that is covered through PV+BESS ($SS_{(el)}$) and about the amount of energy consumed with respect to PV production ($SC_{(el)}$). In addition to these indexes also the Share of renewables ($SR_{(el)}$) is evaluated. This indicator is calculated as the ratio between the electrical energy consumed on site coming from renewables (including also renewable fraction of the energy coming from the grid) and the total system electrical consumption.

3.2.4.1 Electrical energy from PV and BESS and interaction with external grid

The installed power of the PV system of Aglantzia is 5 kWp. The PV system consists of 16 PV panels of 300 Wp each connected in two strings with 8 panels per string. The PV panels are installed on the roof of the building and are South-East oriented and 12° tilted. Figure 69 presents the production of the PV system of Aglantzia during the first week of August 2022. As can be seen from the figure, the production curves are similar for almost all the days with some fluctuations due to weather or other events.

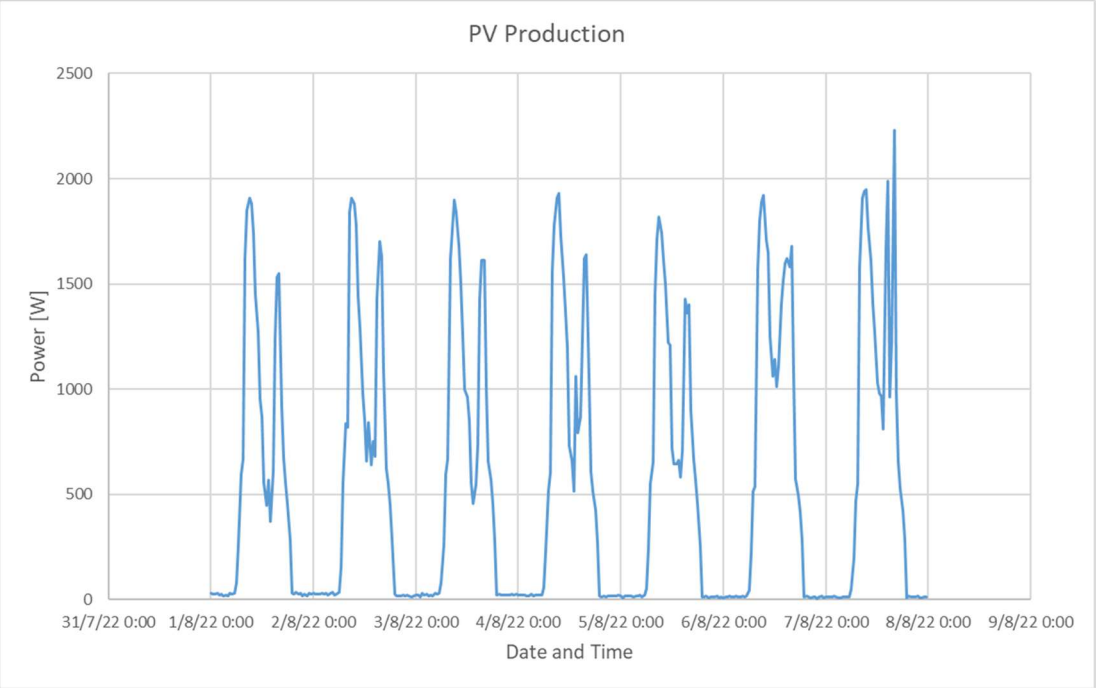

Figure 69. Production of the PV system in Aglantzia demo site during the first week of August

Regarding the BESS, positive energy fluxes indicates that the BESS is charged by the PV system in case of surplus of PV production with respect to the load, and negative when part of the load is covered by the BESS. Figure 70 presents the charging and discharging power of BESS during the first week of August. As has been mentioned earlier in this document, the first 3 days of the week, from 1st to 3rd of August the HYBUILD system and the building was in operation so we can see the results during the operating hours and compare them with the results when the system is not working.

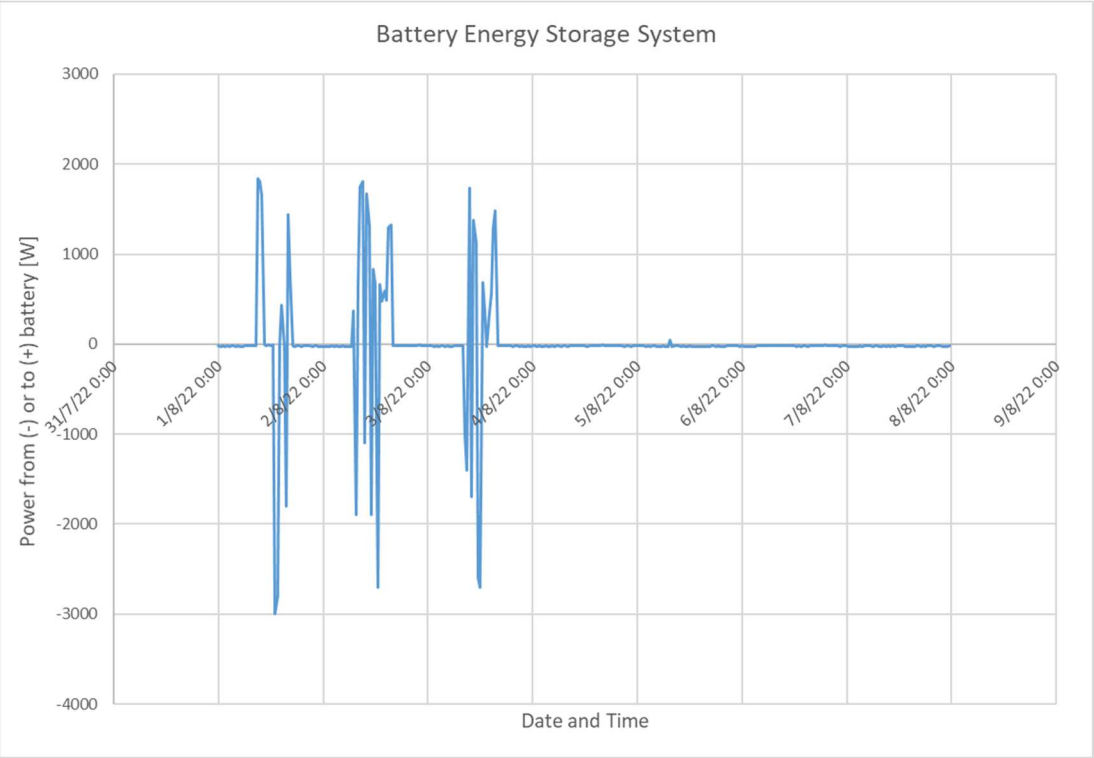

Figure 70. Charging (+) and discharging (-) power of the BESS

As for the BESS, also for the grid the energy fluxes can be positive or negative indicating that energy is taken (+) or is sent (-) to the grid. Figure 71 shows the interaction of the HYBUILD system with the external electricity network. The positive power indicates the power imported from the external grid in order to cover the loads when the production of the PV and the BESS are not able to cover the full load of the building. On the other hand, negative power indicates the surplus power produced from the PV and exported to the external electricity network.

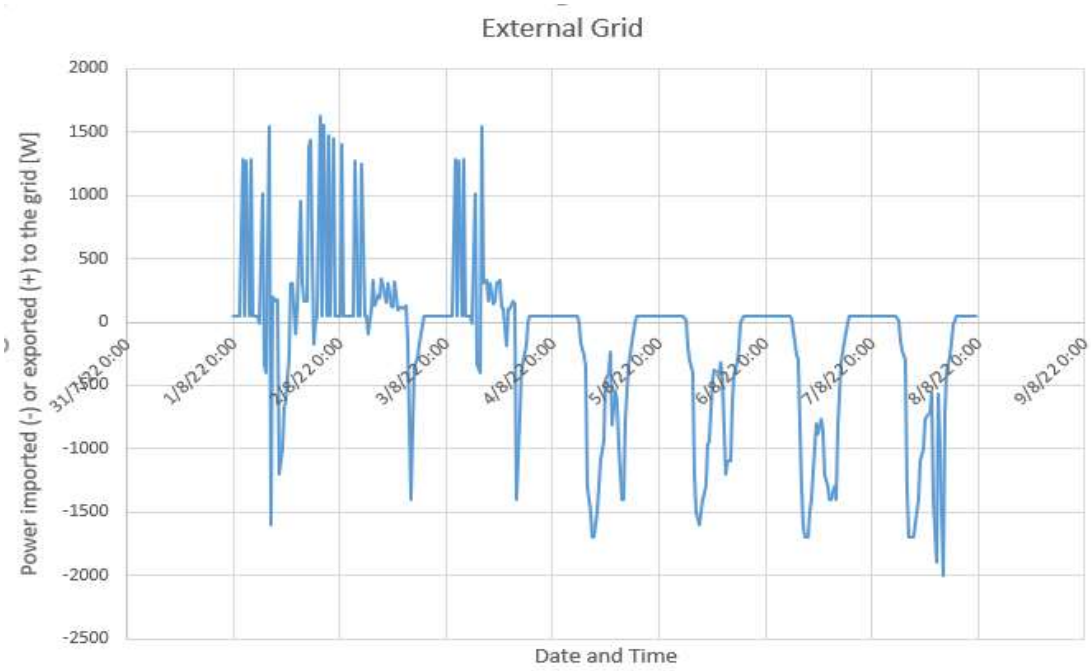

Figure 71. Imported (+) and exported (-) power to the external electricity network

Further to the results analysis, the amount of the produced energy from the PV system which consumed by the load or by the BESS and the produced power exported to the external electricity network can be calculated. Figure 72 shows the amount of PV production that is self-consumed (instantaneously or temporarily stored in the BESS and consumed by the HP in a second moment) and the amount of PV production that is exported to the grid.

As can be seen from the graph regarding the PV production of the first week of August, during the days when the system was in operation, most of the energy production was self-consumed on site, while a small portion of the produced energy was exported to the grid.

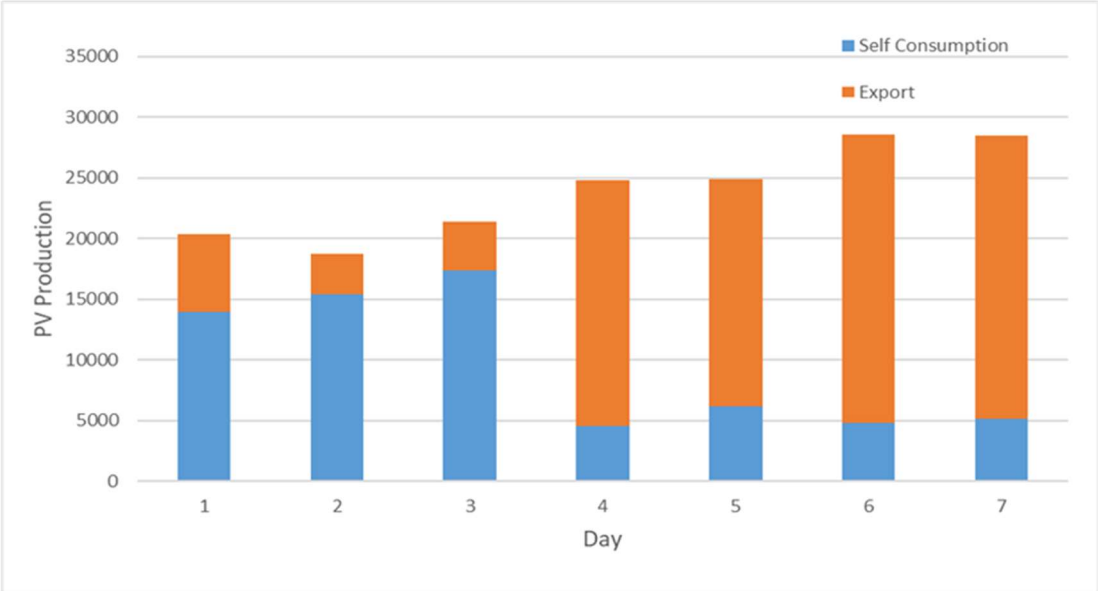

Figure 72. The self-consumed and the exported production of the PV system

3.2.4.2 Self-sufficiency and Self-consumption

Self-sufficiency is calculated, over the considered period, using the following formula:

$$SS_{(el)} = \frac{E_{RES\ (el)}}{E_{D\ (el)}}$$

Where:

- $E_{RES\ (el)}$ is the energy produced by PV and directly consumed by the HP or produced by PV, stored in the BESS and consumed by the HP in a second moment
- $E_{D\ (el)}$ is, in this case, the HP electrical energy consumption

On the other hand, Self-consumption is calculated, over the considered period, using the following formula:

$$SC_{(el)} = \frac{E_{RES\ (el)}}{E_{RES-TOT\ (el)}}$$

Where:

- $E_{RES-TOT\ (el)}$ is the PV production

Figure 99 presents the daily values of Self Sufficiency $SS_{(el)}$ for the first week of August. As can be seen in the chart, the $SS_{(el)}$ for the days that the system was in operation was near 100% with an average $SS_{(el)}$ for these days equal to 91%. For the rest of the week, when the building was closed, the $SS_{(el)}$ was higher than 150% and the reason is that the most of the produced energy from the PV system exported to the grid. On the other hand, Figure 74 presents the daily values of Self Consumption $SC_{(el)}$ during the same period as before. As can be seen, the $SC_{(el)}$ of the system during the operating days was very high (near 90%) which is a very positive result and achievement of the system bringing various benefits for the system and the external grid operation as well. On the contrary, during the days when the building was not in operation, the $SC_{(el)}$ was very low (less than 40%) because the most of the energy produced by the PV system exported to the grid.

Figure 73. Daily values of Self Sufficiency of the system

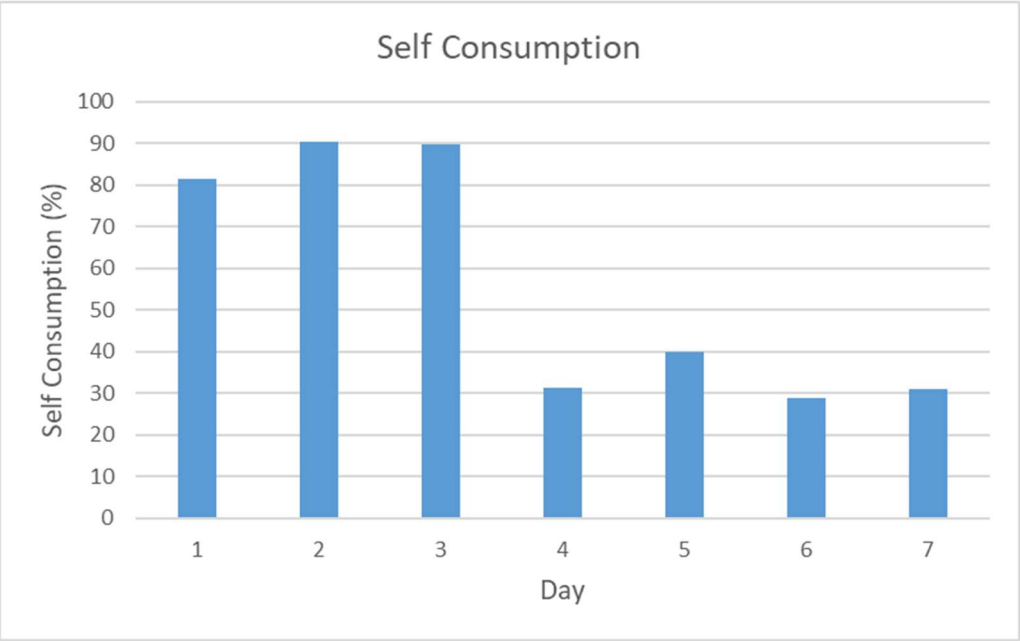

Figure 74. Daily Self Consumption of the building during the first week of August

3.2.4.3 Share of renewables

Share of renewables is calculated, over the considered period using the following formula:

$$SR_{(el)} = \frac{E_{RES*(el)}}{E_{D\ (el)}}$$

Where:

- $E_{RES*(el)}$ is the sum of energy produced by PV and directly consumed by the HP or produced by PV, stored in the BESS and consumed by the HP in a second moment and of the renewable fraction of the energy coming from the grid (calculated considering the renewable fraction in the electrical energy mix of Cyprus, wich was equal to 12,4% for year 2020 according to https://ec.europa.eu/eurostat/web/energy/data/shares).
- $E_{D\ (el)}$ is, in this case, the total electrical consumption. Here, in addition to HP consumption also the consumption of the auxiliaries is considered.

For the days that the system was in operation mode during the first week of August 2022, the share of renewables was really high because of the high self-sufficiency and self-consumption of the system. More specifically, the average $SR_{(el)}$ for these days was over 85%.

Table 6. Share of renewables (SR) over the 3rd representative winter week

Share of renewables ($SR_{(el)}$)
85.1%

3.3 Langenwang demo site

As already stated in section 2.4.3 the HYBUILD system installed at the Langenwang demo is running from end of year 2020. Nevertheless, as reported in the same section, different problems related to system operation and in some cases to specific components and measurements have been occurred and have been solved. The next sections report the description of the data collected and the analysis of some components starting from the identification of the sensors used to perform the various analysis.

3.3.1 General scheme and sensors

The general scheme of the system installed at the demo has been already presented in section 2.4.1. The following part reports instead simplified schematics of the system with the focus on the sensors used to monitor plant operations and to evaluate system performances. Figure 75 shows the main sensors used to evaluate HP+RPW-HEX operations. The thermal energy delivered by the generation system (where the term generation system in this context indicates the HP+RPW-HEX) is evaluated through the sensor K3MB5 that measures the thermal energy entering the hydraulic separator. To have an additional check on this measurement, also the thermal energy exiting the hydraulic separator is measured (using sensor K3MB6). Regarding the HP also the water temperature entering and exiting the HP condenser, as well as the HP compressor speed and the HP electrical consumption are measured. Regarding instead the RPW-HEX, its temperature, as well as its status is evaluated. The RPWHEX status is a variable that can assume three different values: 0, 1, 2 where 0 indicates that the RPW-HEX is not fully charged (RPW-HEX temperature $<$ 70 °C), 1 indicates that the RPW-HEX is empty and the system is working to charge the decentralized DHW tanks with only the HP, 2 indicates that the RPW-HEX is fully charged (RPW-HEX temperature $\geq$ 70 °C) and can be used to charge the decentralized DHW tanks.

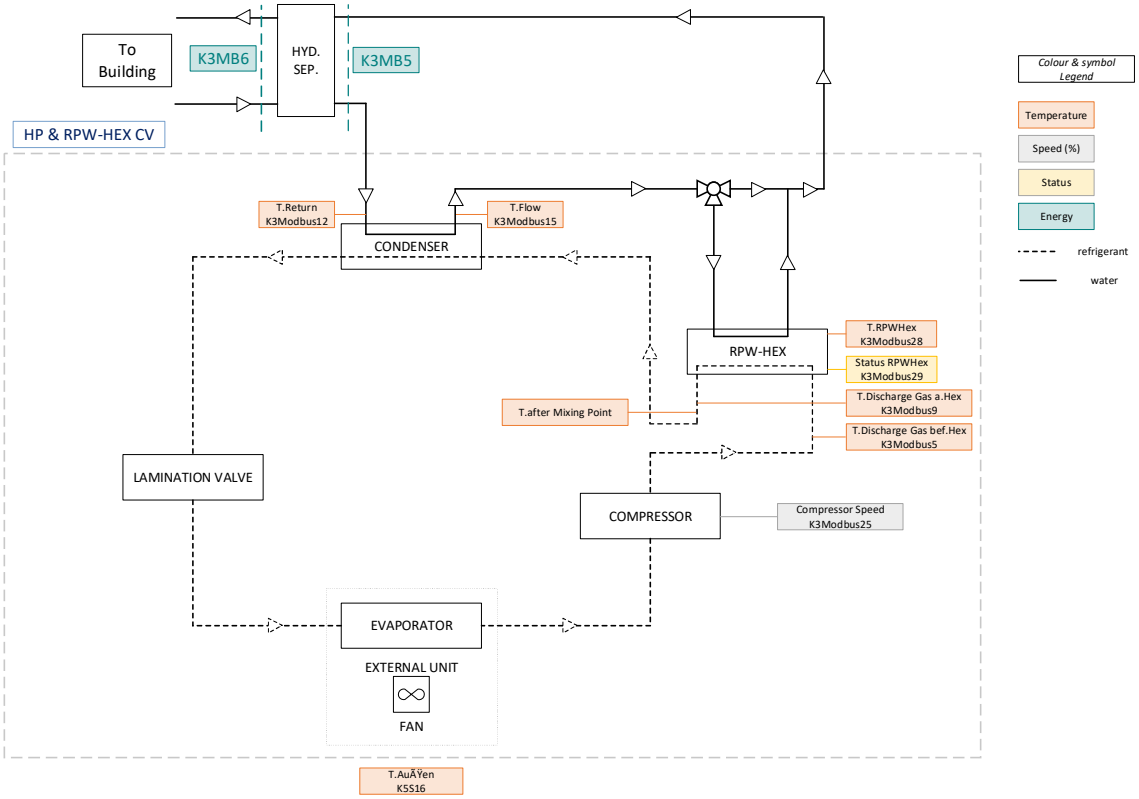

Figure 75. Simplified schematic of the HP and RPW-HEX part of the system with the main sensors used to evaluate system operations

Figure 76 shows instead the sensors used to measure the thermal energy entering (sensors K*MB1) and exiting (sensors K*MB3) the three decentralized DHW tanks and the thermal energy delivered from the various enerboxxes 01, 02, 03 for SH (sensors K*MB2). In this context, the symbol * refers to the respective enerboxx (* is equal to 6, 24, 43 for respectively enerboxx01, 02, 03). These thermal energy sensors internally calculate the thermal energy ($E_{(th)}$) measuring the mass flowrate (m), inlet and outlet temperatures (T_{inlet} and T_{outlet}) and knowing the water specific heat ($cp_{water} = 4.186 \frac{kJ}{kg \cdot K}$) through the following formula:

$$E_{(th)} = m \cdot cp_{water} \cdot (T_{inlet} - T_{outlet})$$

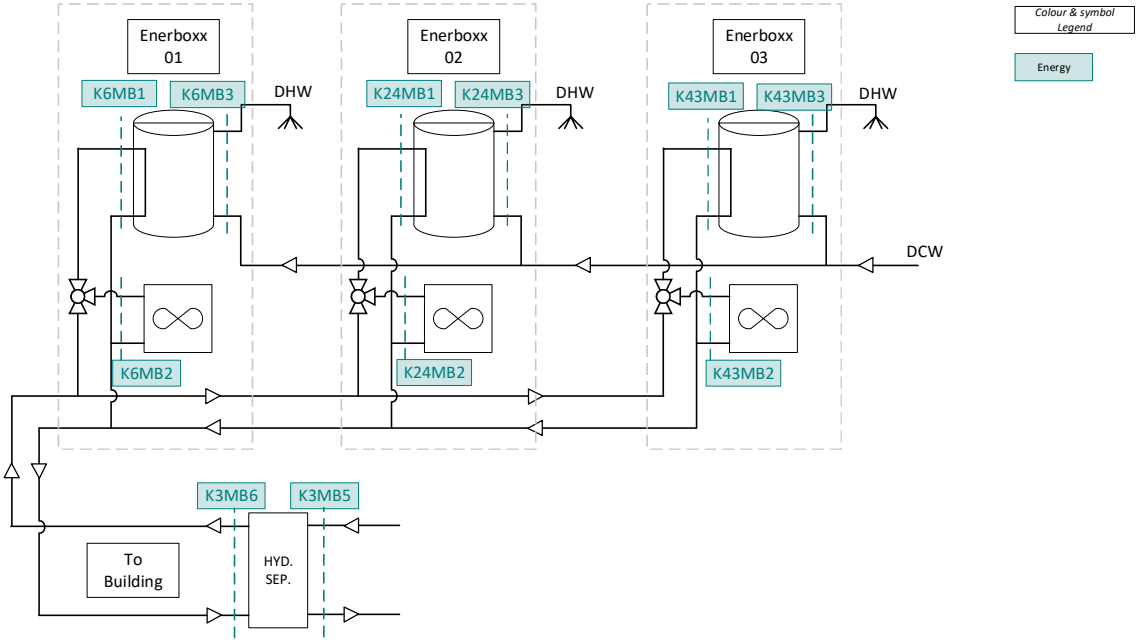

Figure 76. Simplified schematic of the distribution and user part of the system with the main sensors used to evaluate system operations

A simplified schematic of the electrical system is reported in Figure 77. This figure reports the energy sensors used to evaluate electrical energy fluxes. More specifically, gSM1.power(BESS) is the sensor used to evaluate energy fluxes to or from the BESS (this variable could be positive or negative to indicate respectively periods in which the BESS is charged or discharged). The sensor gSM2.power(PV) measures the PV production. Last, the sensor gSM3.power(HP) measures the HP consumption. The last two measurements, the PV production and the HP consumption present values always ≥ 0.

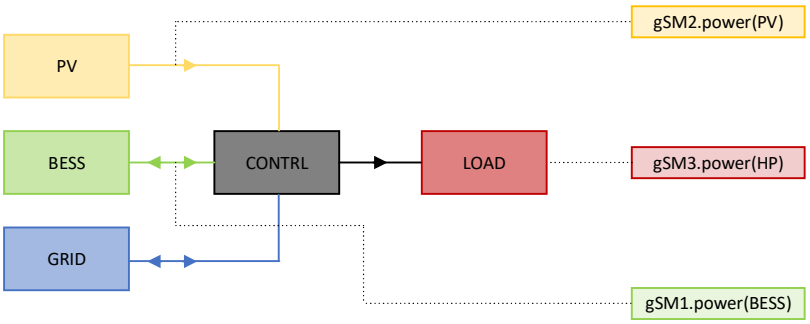

Figure 77. Simplified schematic of the electrical part of the system with the main sensors used to evaluate system operations

3.3.2 Measurements collected and selection of reference periods (summer and winter)

As can be seen in the previous figures (Figure 75, Figure 76, Figure 77) there are many sensors used to monitor system operations. For the analysis of the thermal part of the system the main quantities evaluated are:

- Temperature
- Mass/volume flowrate
- Thermal Power
- Thermal Energy

Regarding instead the electrical part, the main quantities evaluated are:

- Electrical Power
- Electrical Energy
- BESS SoC

All the measurements are acquired from end of 2020. However, for different reasons related to system problems and also to gaps in the data recorded from both thermal and electrical part of the system, it is not possible to extrapolate, analysing all data available, reliable indications about seasonal system performances. For this reason, it has been decided to define the concept of "representative week". The representative week is a week in which the system is working as expected and all (or almost all) data needed for the system performance analysis are available.

Following this approach, after having checked the data available in the period April-October 2021, the period 23 – 29 October 2021 has been selected as the first representative week of system operations in winter season. However, as reported in section 2.4.3, after the analysis of the monitored data of this first representative winter week it has been found that the system was not working exactly as expected. In fact, the RPW-HEX was never fully discharged. After various analysis to identify the reasons of this behaviour, some problems have been detected and solved and, a second representative winter week has been defined to evaluate system operation with the RPW-HEX that was completely discharged during system operations. This second representative winter week has been identified between March 10th and March 16th of year 2022.

After the analysis of this second representative winter week, some further modifications have been introduced. The modifications regard the control logic used to manage the decentralized DHW tanks charging. In fact, until March 17th the control logic used considered two predefined periods during the day in which the decentralized DHW tanks were charged without taking into consideration the RPW-HEX SoC and its possible contribution. This control logic was implemented with the aim to:

- Ensure that the decentralized DHW tanks are fully charged just before the moments in the day in which the user DHW demand is typically higher (these moments are generally the early morning, from 7 a.m. to 9 a.m. and the late afternoon, from 5 p.m. to 9 p.m. as visible in Figure 24. DHW draw-offs on a one-day basisFigure 24. DHW draw-offs on a one-day basis.)
- Limit as much as possible the periods of the day in which the system is working to charge the decentralized DHW tanks. This is related to the fact that the HYBUILD CON system can work in SH/SC mode to cover building SH/SC demand or in DHW mode charging the decentralized DHW tanks. It follows that during decentralized DHW tanks charging the system is not available to cover SH/SC building demand and this could lead to not ensure the comfort conditions inside the building.

However, from the analysis of the second winter representative week it emerged that the RPW-HEX contribution, although notably higher with respect to the period before March 10th could be still increased as the RPW-HEX is charged well above 70 °C. This value (70 °C) represents the temperature at which the RPW-HEX is considered fully charged. For this reason, it has been decided to act modifying the control logic that manages the decentralized DHW tanks charging. More specifically, from March 18th the decentralized DHW tanks charging does not occur only in the two predefined periods in a day but also each time the following two conditions are contemporaneously verified:

- RPW-HEX is fully charged (hence RPW-HEX temperature > 70°C)
- In the last 4 hours the system didn't work to charge the decentralized DHW tanks

The period 18 – 24 March 2022 is used as the third representative winter week to evaluate system performances with this new control logic.

For the sake of clarity, in the following Table 7 a summary of the three representative winter weeks with their characteristics is reported.

The system performance analysis presented in the following is based on the data of the third representative winter week as this period is the most representative of expected system operation and is characterized by the maximum exploitation of RPW-HEX thermal energy.

Table 7. Summary of the characteristics of the three winter representative weeks considered

Representative week	Period	Characteristics
First representative week	23–29 /10/2021	RPW-HEX never fully discharged due to incorrect mode of operation
Second representative week	10-16/03/2022	RPW-HEX fully discharged but DHW tanks charged only in two predefined periods per day
Third representative week	18-24/03/2022	RPW-HEX fully discharged and DHW tanks charged also as soon as the RPW-HEX is fully charged

The following figures (Figure 78, Figure 79, Figure 80) shows the RPW-HEX temperature trend respectively in the first, second and third representative winter week to highlight the differences in the management of RPW-HEX. More details about the RPW-HEX in terms of thermal energy contribution and duration of this contribution will be presented in section 3.3.4.6.

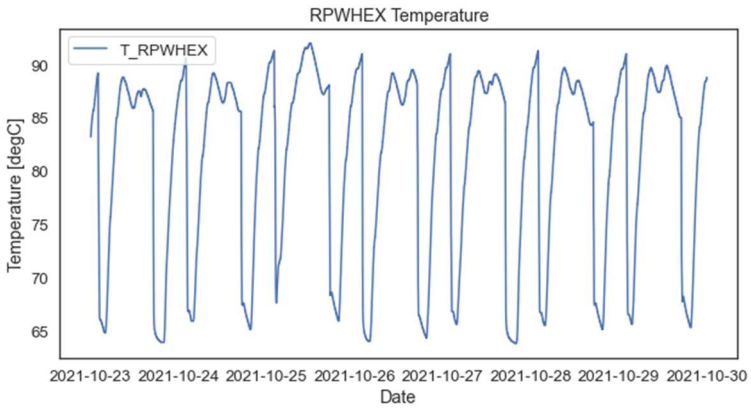

Figure 78. RPW-HEX temperature trend, 1st winter representative week

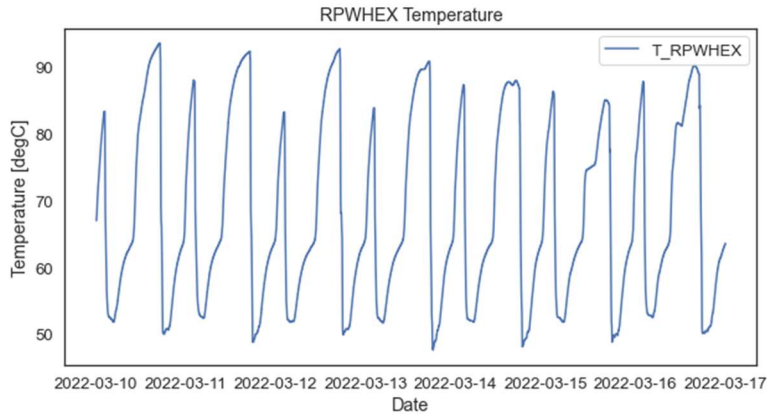

Figure 79. RPW-HEX temperature trend, 2nd representative winter week

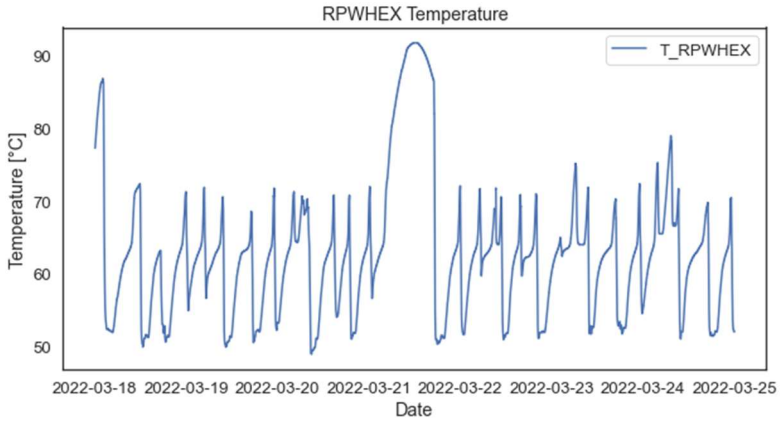

Figure 80. RPW-HEX temperature trend, 3rd representative winter week

Regarding instead the summer period it has not been possible to define a representative week in which the system works as expected as some problems have been solved only in March 2022 (see section 2.4.3). In the following section only results about system operation in the winter period through the analysis in the third representative winter week are reported.

It is considered useful to remind here that the focus of the HYBUILD CON system is to cover SH and DHW demand of buildings located in the European Continental climate, where building space heating demand is predominant.

3.3.3 Operational modes

The HYBUILD CON system is developed to cover different thermal energy needs of the building. To cover thermal energy needs of the building the system can work in the following four operational modes:

- SH: the HP works to cover building SH demand and at the same time can charge the RPW-HEX
- DHW with RPW-HEX: the HP and RPW-HEX work in series to charge the decentralized DHW tanks
- DHW without RPW-HEX: the HP works to charge the decentralized DHW tanks (the RPW-HEX is empty or in any case cannot be used)
- SC: the HP works to cover building SC demand and at the same time can charge the RPW-HEX

It is important to underline that, as already mentioned in previous section, the HYBUILD CON system can work alternatively in SH/SC mode or in DHW (with or without RPW-HEX) mode,

therefore, when the system is operating to charge the decentralized DHW tanks it is not available to cover SH/SC building demand and vice-versa.

3.3.4 Thermal system analysis

Thermal system analysis is presented in the following sections. First, the external ambient temperature and the temperature in the various zones inside the building connected to HYBUILD system are presented. Then, the subsequent sections report some evaluation about thermal energy delivered to the user to cover user DHW and SH needs and a comparison between thermal energy delivered by the generation system (HP+RPW-HEX) and delivered to the user to assess system thermal losses. The analysis of thermal part of the system concludes with a specific assessment of RPW-HEX operation analysing the contribution in terms of thermal energy delivered by this component and duration of this contribution.

3.3.4.1 External ambient temperature

The external ambient temperature trend in the 3rd representative winter week can be seen in Figure 81. From this figure it can be noted that in the considered period this temperature varies from -2 to 16 °C. In the same figure it is possible to see also a sudden increase followed by a sudden decrement of external air temperature in the days characterized by high external temperature. This behaviour occurs in all the cases just after reaching the peak external ambient temperature around noon and is probably due to the position of the sensor. These events are not representative of the real external ambient temperature trend. Considering that these events are in any case very short in time their presence can be accepted and their effect neglected in the following analysis.

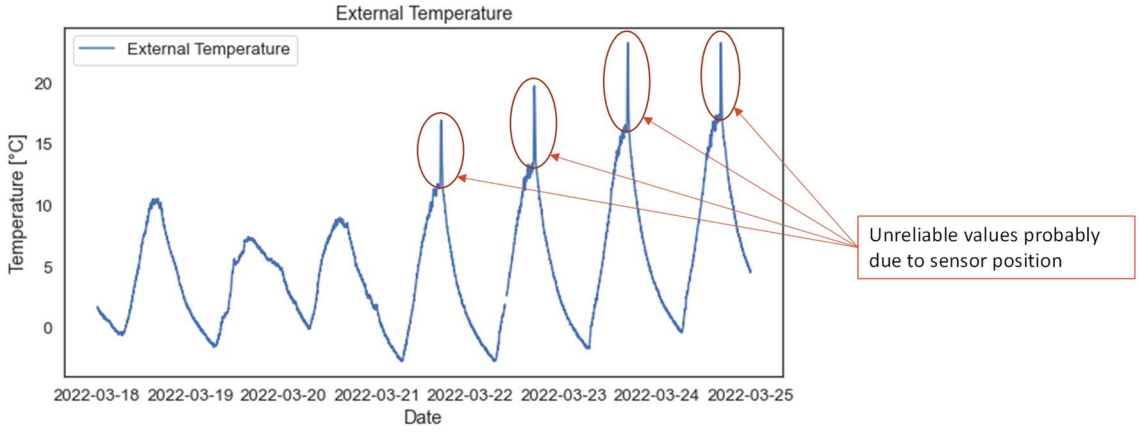

Figure 81. External ambient temperature trend during 3rd representative winter week

3.3.4.2 Internal temperature of the various zones

The internal temperature of the various zones connected to the HYBUILD system in the 3rd representative winter week are reported in this section. As can be seen in Figure 82 the temperature of all the monitored zones is between 19 and 27-28 °C and for most of the time in the range 20 – 24 °C. After a check it has been assessed that the high values in the last days of the 3rd representative winter week in some zones (temperature values up to 27- 28 °C) are reliable and due to solar radiation entering the windows of the considered zones. The values analysed indicate that the HYBUILD system almost always ensure the minimum internal comfort temperature (considered in this context equal to 20 °C) during the 3rd representative winter week. Figure 83 instead shows the internal temperature of the various zones connected to the HYBUILD system against the external ambient temperature. From Figure 83 it can be observed that a limited correlation is present between internal and external temperature. This indication confirms that, in the considered period, the HYBUILD system is able to almost always ensure the desired internal setpoint temperature independently from the external ambient temperature.

In addition, it is interesting to note the presence of a limited number of internal temperature measurements in the right part of the graph (in correspondence to high external ambient temperature). These values are associated to the peaks of external ambient temperature occurring just after noon already discussed in the previous section and, as already explained previously, should not be considered.

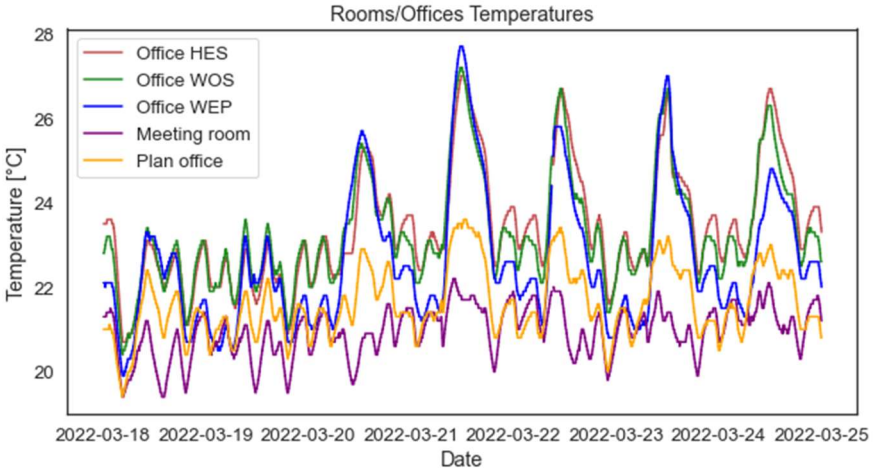

Figure 82. Internal temperature of the various zones connected to HYBUILD system, 3rd representative winter week

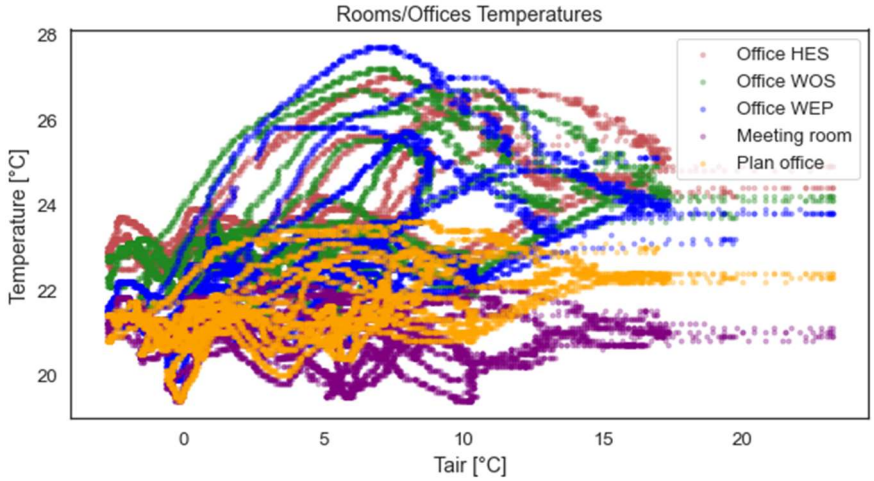

Figure 83. Internal temperature of the various zones connected to HYBUILD system during the 3rd representative winter week against external ambient temperature

3.3.4.3 DHW thermal energy analysis

This section reports an analysis of the thermal energy entering (from HP+RPW-HEX) and exiting (to the user) the decentralized DHW tanks (called also enerboxxes) in the 3rd representative winter week. As already mentioned in section 2.4.1 three decentralized DHW tanks are installed at the demo. Thermal energy entering and exiting the three enerboxxes are evaluated using respectively sensors K6MB1, K6MB3, K24MB1, K24MB3, K43MB1, K43MB3, all visible in Figure 76. Figure 84 shows the daily energy used to charge these decentralized DHW tanks coming from the HP+RPW-HEX. As can be noted in Figure 84 there are some differences (in the range of 2 kWh/day) in the daily thermal energy entering the three decentralized DHW tanks in the various days of the 3rd representative winter week. These differences are in any case limited and can be considered in an acceptable range. These differences are due to different factors. First, the different thermal energy delivered to the user in the various days. In fact, although the DHW daily users draw-off is constant, the delivered water temperature, and hence the thermal energy delivered to the users, could present some differences as it depends on the temperature at the

top of the decentralized DHW tanks. Second, the management of decentralized DHW tanks charging depends on the status of the RPW-HEX. Depending on the RPW-HEX availability the number of decentralized DHW tanks charging events could be different in the various days leading to differences in the thermal energy entering these tanks in the various days of the 3rd representative winter week. Regarding instead the thermal energy entering the three different decentralized DHW tanks in the 3rd representative winter week, this presents limited differences, and these differences can be considered in an acceptable range. In the 3rd representative winter week, the daily thermal energy entering the three decentralized DHW tanks is in the range 5 - 7 kWh/day.

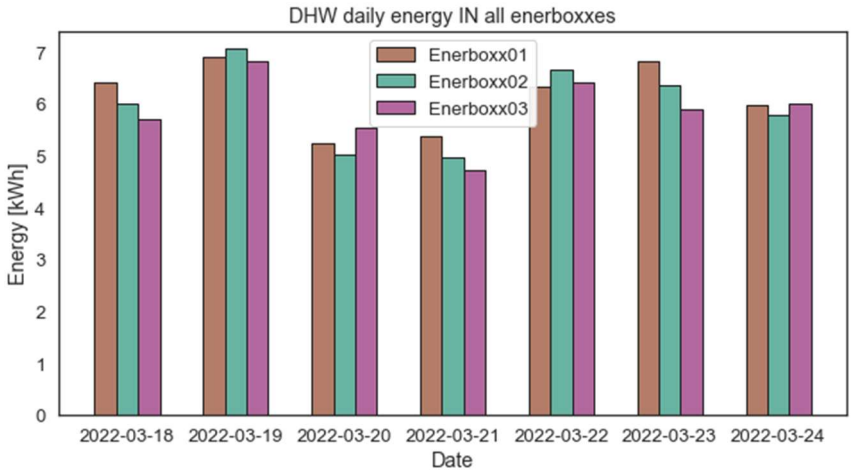

Figure 84. Daily thermal energy entering the three enerboxxes (enerboxxes01, 02, 03) in the 3rd representative winter week

Figure 85 instead shows the daily energy entering, exiting, and their difference for one of the DHW decentralized tanks (enerboxx01) in the 3rd representative winter week. As can be noted in Figure 85 the daily thermal energy entering the considered decentralized DHW tank is in the range 5 – 7 kWh/day, while the daily thermal energy exiting the same tank and delivered to the user is in the range 4-5 kWh/day. This last quantity (4-5 kWh/day) is aligned to indications from standard SIA 2024[1] that considers a DHW energy demand from the user of around 4 kWh/day considering the same boundary conditions in the calculation. In addition to these indications, the green columns in Figure 85 represent the difference, over the considered day, between the energy entering and exiting the decentralized DHW tank. This value represents the thermal losses of the decentralized DHW tank and, as can be seen in Figure 85, this value is generally in the range 1 – 2.5 kWh/day. This means that thermal losses of the DHW decentralized tank are equal to around 20 – 30% of the thermal energy entering the same DHW decentralized tank.

[1] Standard SIA 2024:2015. In this standard the user DHW daily demand for a dwelling of a s-MFH is calculated using the formula En=n.pers*m*cp,water*(Twater,out-Twater,in), where n.pers is the number of inhabitants of the dwelling (2 in the considered case), m is the DHW daily demand of one person (35 l/pers/day of water at 60°C), Twater,out is considered equal to 60°C and Twater,in is considered equal to 10°C

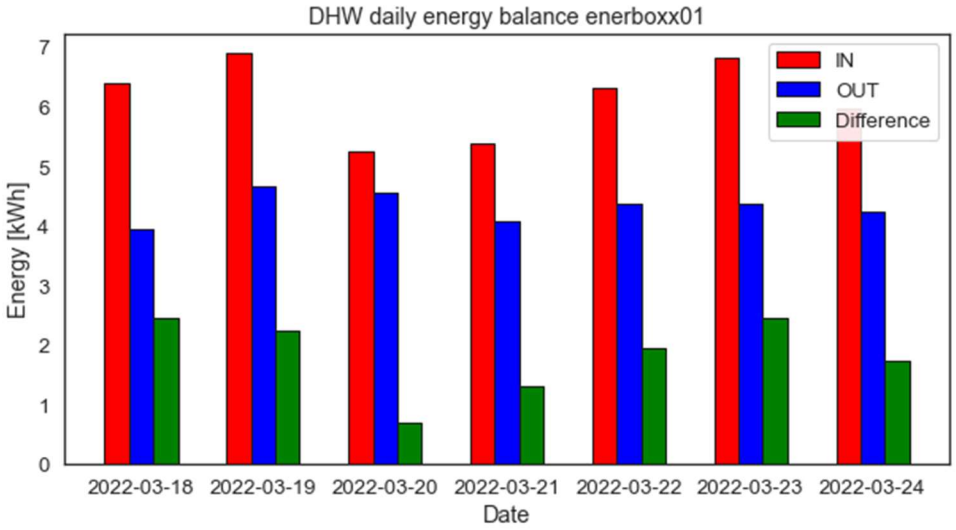

Figure 85. Daily thermal energy entering (IN) and exiting (OUT) one of the enerboxxes considered (enerboxx01). In addition, the difference between energy entering and exiting (quantity that represents the thermal losses of the DHW decentralized tank) is plotted in green (Difference). Period considered: 3rd representative winter week

3.3.4.4 Space heating thermal energy analysis

The SH thermal energy delivered to the various zones through the three enerboxxes in the 3rd representative winter week is reported in Figure 86. This quantity is evaluated, for the three enerboxxes 01, 02, 03, with the measurements of the sensors K6MB2, K24MB2, K43MB2 respectively. All these sensors are visible in Figure 76. Although the daily thermal energy distributed by the three enerboxxes is slightly different, this difference is considered within the acceptable range. The daily SH thermal energy delivered by the various enerboxxes is in the range 40 – 55 kWh/day. As can be noted visualizing together Figure 86 and Figure 87

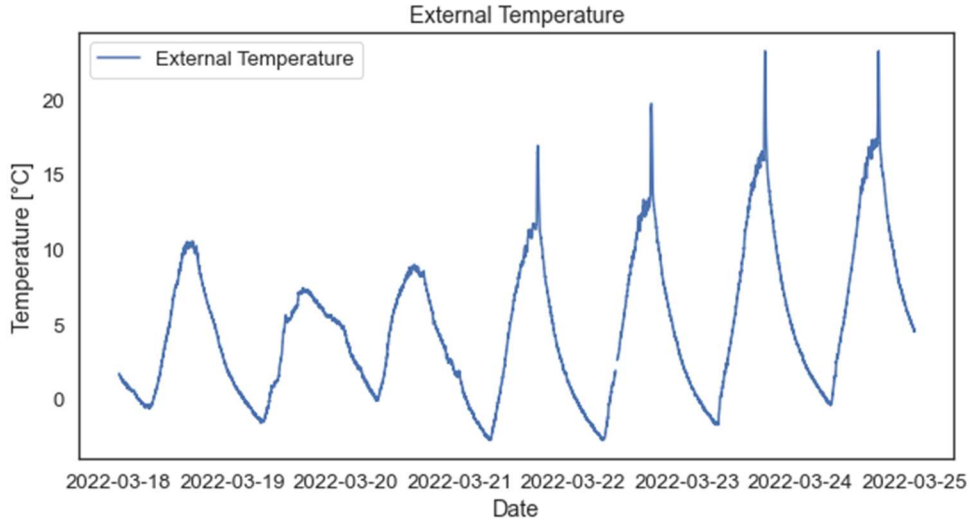

Figure 87, as expected, the highest values of SH thermal energy delivered by the three enerboxxes occurred in the second and third day of the 3rd representative winter week, in correspondence of slightly lower external air temperature.

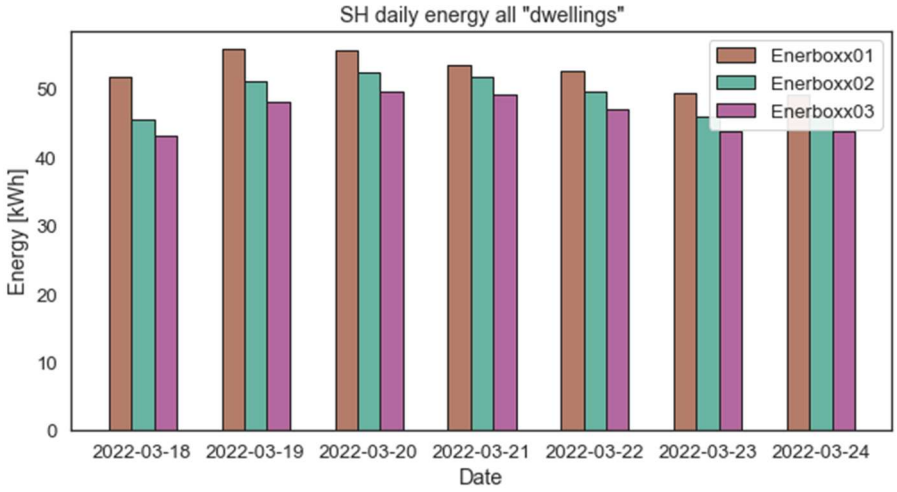

Figure 86. Daily thermal energy delivered for SH to the various zones through enerboxxes01, 02, 03 in the 3rd representative winter week

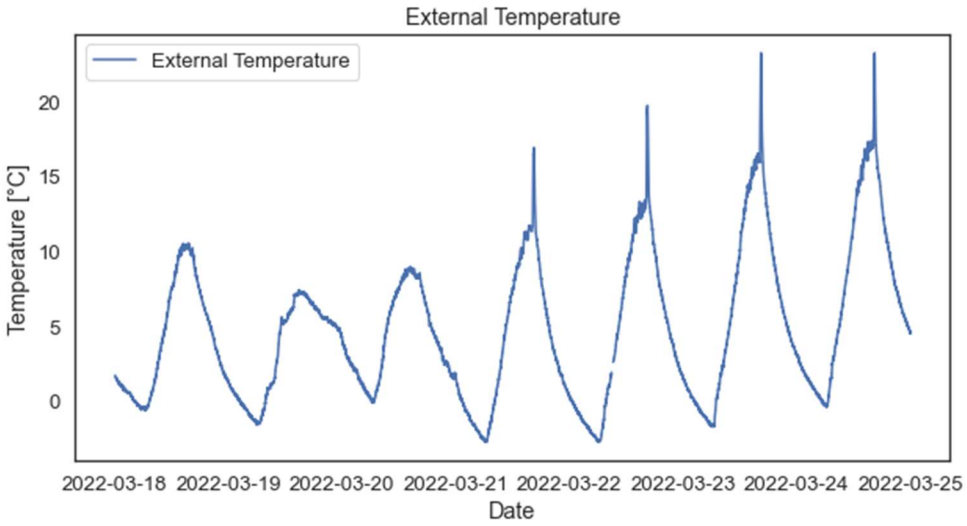

Figure 87. External ambient temperature trend during 3rd representative winter week

3.3.4.5 *Thermal energy delivered by the generation system and delivered to the user*

In this section the daily thermal energy delivered by the generation system (where in this context the term generation system refers to HP+RPW-HEX) and the daily thermal energy delivered to the user are compared. With this analysis it is possible to have an estimation about the thermal losses in the distribution circuit and about the thermal losses of the DHW decentralized tanks. The thermal energy delivered by the generation system is evaluated as the thermal energy entering the hydraulic separator and measured by sensor K3MB5 (visible in Figure 75). To check that this measure is not affected by important errors also the energy exiting the hydraulic separator (measured by sensor K3MB6, visible again in Figure 75) is evaluated and, as can be noted in Figure 88 the two measurements are basically the same for all the days of the 3rd representative winter week.

This is aligned to expectations as the hydraulic separator, in general but also in this case, is a small element with limited volume and is not characterised by important thermal losses. In addition to these two energy measurements, Figure 88 shows also the daily thermal energy entering the enerboxxes. This is the sum of the measurements of sensors K*MB1 and K*MB2 visible in Figure 76, where * refers to the specific enerboxx considered (6, 24, 43 for respectively

enerboxx01, 02, 03). The difference between the thermal energy entering the enerboxxes and the thermal energy delivered by the generation system is due to thermal losses in the distribution circuit. As can be noted the distribution circuit thermal losses are in the range 10-20 kWh/day (this range correspond to around 10 – 15% of the energy delivered by the generation system) and this value is basically constant in the various days of the 3rd representative winter week. The last column in Figure 88 represents instead the thermal energy delivered to the user. This quantity is the sum of the measurements of sensors K*MB3 and K*MB2 visible in Figure 76, where, again, * refers to the specific enerboxx considered (6, 24, 43 for respectively enerboxx01, 02, 03). The difference between the thermal energy entering the enerboxxes and the one delivered to the user is due to thermal losses of the decentralized DHW tanks. From Figure 88 this difference is limited and equal to 4 – 8 kWh/day, value aligned to what is reported in Figure 85 that shows that for one enerboxx (enerboxx01) the value of thermal losses (difference in Figure 85) is in the range 1 – 2.5 kWh/day.

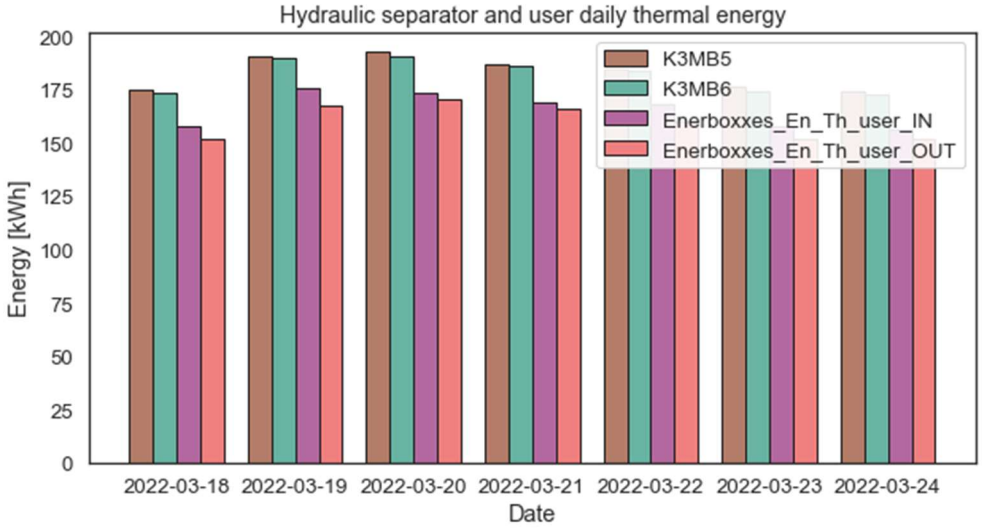

Figure 88. Daily thermal energy entering (brown) and exiting (green) the hydraulic separator, entering the enerboxxes (purple) and delivered to the user (orange) in the 3rd representative winter week

3.3.4.6 RPW-HEX contribution

This section reports a specific evaluation of RPW-HEX contribution to decentralized DHW tanks charging. As explained in section 3.3.2, three different winter representative weeks have been defined. These winter representative weeks are characterized by differences in the control logic used to manage the decentralized DHW tanks charging and the RPW-HEX contribution.

In the 1st representative winter week (23-29 October 2021) the RPW-HEX was basically never fully discharged (temperature always > 65°C, while the material phase change temperature is in the range 60 – 64 °C). The RPW-HEX temperature trend in this period is reported in Figure 89. In these conditions the RPW-HEX contribution to decentralized DHW tanks charging was limited to 1 – 2 kWh per each of the two decentralized DHW tanks charging events in a day, resulting in an RPW-HEX daily contribution to decentralized DHW tanks charging in the range 2 – 4 kWh/day (as visible in the figure on the left of Figure 90). As can be noted instead in the figure on the right of Figure 90 the duration of RPW-HEX contribution varies in the range 5 – 20 min per each of the two decentralized DHW tanks charging events in a day, resulting in a daily duration of the RPW-HEX contribution of around 25 min/day. Figure 91 shows the daily contributions to decentralized DHW tanks charging. As can be noted in Figure 91, in the 1st representative winter week, for the reasons explained above, most of the thermal energy used to charge the decentralized DHW tanks comes from the HP when it works not coupled with the RPW-HEX (purple part of the columns in Figure 91). The contribution of RPW-HEX is limited (green part of the columns in Figure 91) and still lower is the contribution of the HP when it works coupled with the RPW-HEX

(brown part of the columns in Figure 91). Figure 92 instead shows the daily duration of decentralized DHW tanks charging with HP and RPW-HEX working in series (green part of the columns in Figure 92) and with HP only (purple part of the columns in Figure 92).

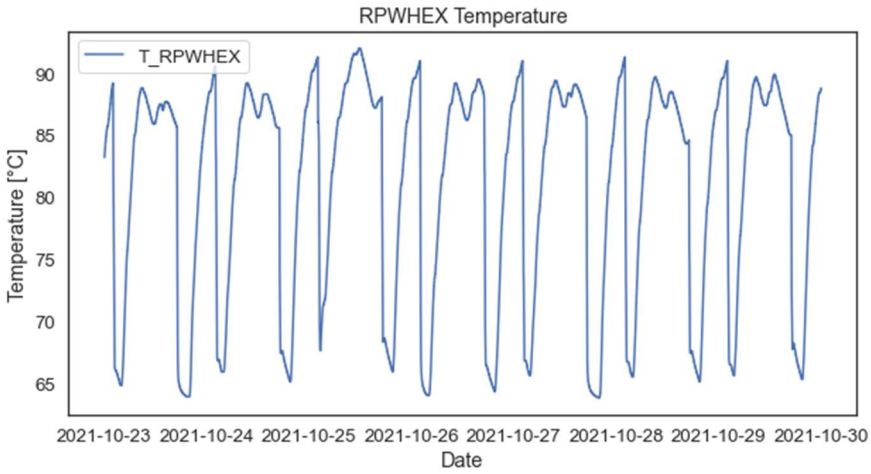

Figure 89. RPW-HEX temperature in the 1st representative winter week

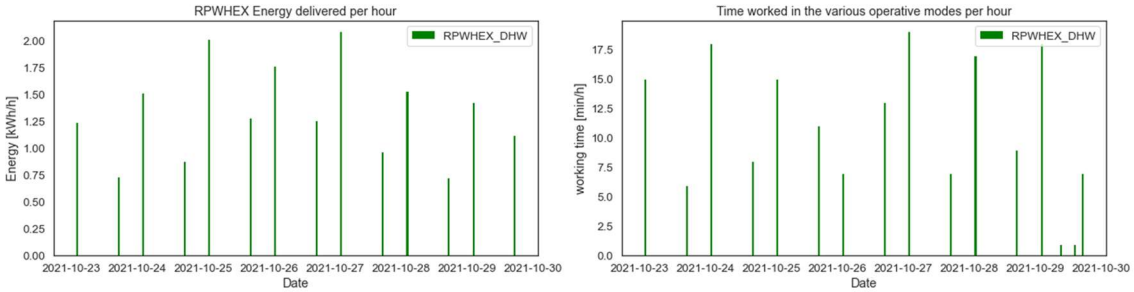

Figure 90. RPW-HEX energy contribution to decentralized DHW tanks charging (left) and duration of RPW-HEX contribution to DHW tanks charging (right) in the 1st representative winter week

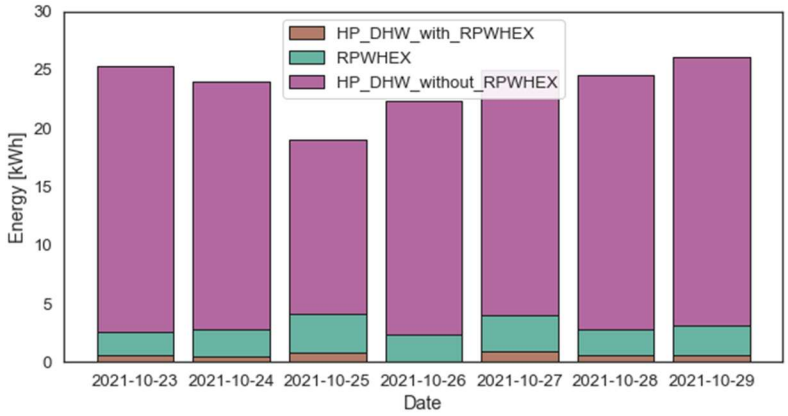

Figure 91. Daily energy contributions to decentralized DHW tanks charging: HP contribution when it works in series with RPW-HEX (brown), RPW-HEX contribution (green) and HP contribution when it works without the RPW-HEX (purple) in the 1st representative winter week

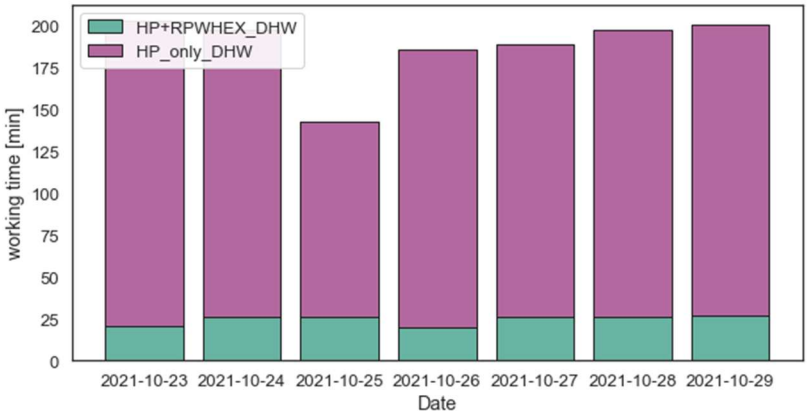

Figure 92. Daily duration of decentralized DHW tanks charging with HP that works in series with RPW-HEX (green) and without RPW-HEX (purple) in the 1st representative winter week

In the 2nd representative winter week (10-16 March 2022) the RPW-HEX was fully discharged and its contribution to decentralized DHW tanks charging is notably higher. The RPW-HEX temperature after its discharging in the 2nd representative winter week reaches values around 50 °C as shown in Figure 93 indicating that in this representative winter week also the latent contribution of the RPW-HEX is exploited. As can be seen in the figure on the left of Figure 94 the RPW-HEX contribution to decentralized DHW tanks charging is in the range 5 - 8 kWh per each of the two decentralized DHW tanks charging events in a day, resulting in a daily RPW-HEX contribution in the range 10 – 15 kWh/day. From the figure on the right in Figure 94 it can be noted instead that the duration of RPW-HEX contribution is in the range 40 – 50 min per each of the two decentralized DHW tanks charging events in a day, resulting in a daily duration of RPW-HEX contribution around 80 – 120 min/day. Figure 95 shows instead the energy contribution to decentralized DHW tanks charging coming from the HP when it works in series with RPW-HEX (purple part of the columns in Figure 95) from the RPW-HEX (green part of the columns in Figure 95) and from the HP when it works without the RPW-HEX (brown part of the columns in Figure 95). Figure 96 instead shows the daily duration of decentralized DHW tanks charging with HP and RPW-HEX working in series (green part of the columns in Figure 96) and with HP only (purple part of the columns in Figure 96). In this 2nd representative winter week, the RPW-HEX contribution is notably higher than the one in the 1st representative winter week (compare Figure 91**¡Error! No se encuentra el origen de la referencia.** and Figure 95). Also, the duration of the RPW-HEX contribution in the 2nd representative winter week is notably higher in comparison to the 1st representative winter week as can be noted comparing Figure 92 and Figure 96.

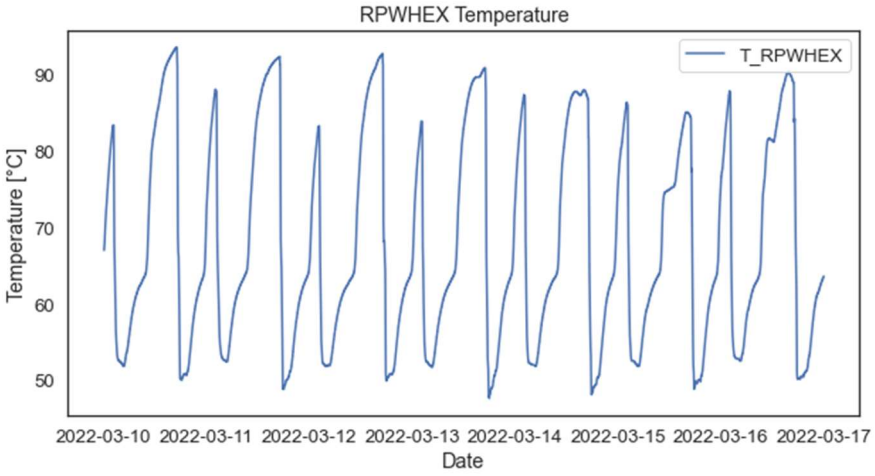

Figure 93. RPW-HEX temperature in the 2nd representative winter week

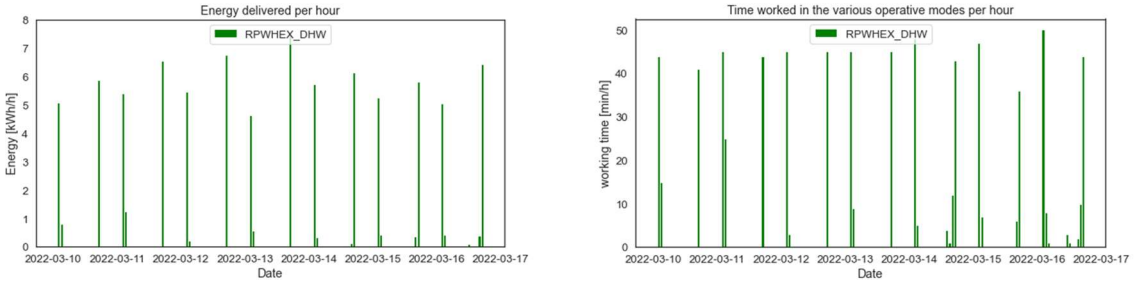

Figure 94. RPW-HEX energy contribution to decentralized DHW tanks charging (left) and duration of RPW-HEX contribution to DHW tanks charging (right) in the 2nd representative winter week

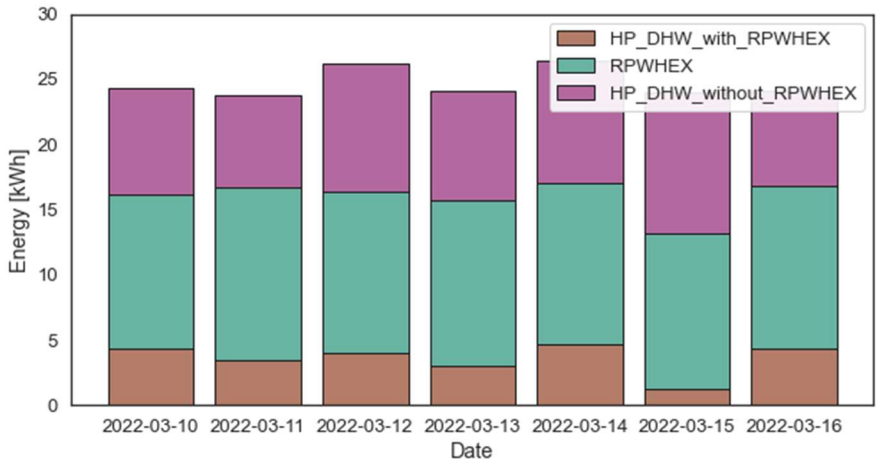

Figure 95. Daily energy contributions to decentralized DHW tanks charging: HP contribution when it works in series with RPW-HEX (brown), RPW-HEX contribution (green) and HP contribution when it works without the RPW-HEX (purple) in the 2nd representative winter week

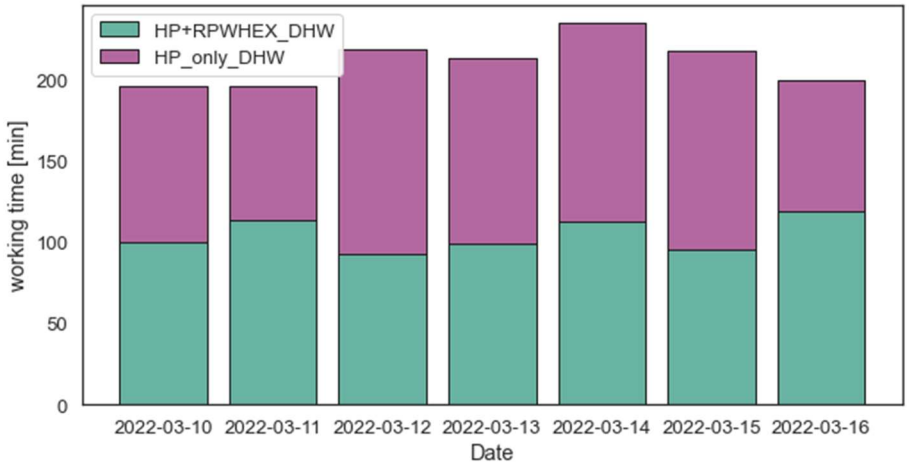

Figure 96. Daily duration of decentralized DHW tanks charging with HP that works in series with RPW-HEX (green) and without RPW-HEX (purple) in the 2nd representative winter week

In the 3rd representative winter week, the RPW-HEX is fully discharged and in addition to the two predefined periods in a day, decentralized DHW tanks are charged also when the RPW-HEX is considered fully charged (RPW-HEX temperature > 70°C). The number of daily DHW tanks charging events in a day with this new control logic passes from 2 to 3-4.

As can be seen in Figure 97, a part for two exceptions on March 18th and on March 21st that are explained better in the following, the RPW-HEX temperature is limited to 70 °C. After the decentralized DHW tanks charging event (and hence after RPW-HEX discharging) the RPW-HEX temperature is in most of the cases in the range 50 – 55 °C indicating that the RPW-HEX has been fully discharged as occurred in the 2nd representative winter week. Nevertheless, in some

cases, the RPW-HEX temperature after discharging (points after a steep decrement of RPW-HEX temperature in Figure 97) results higher and in the range 55 – 60 °C. This higher RPW-HEX temperature after RPW-HEX discharging is due to the fact that in these cases the three decentralized DHW tanks results completely charged in short time and before the RPW-HEX temperature decreases to values in the range 50 – 55 °C. This is also related to the fact that the decentralized DHW storages are charged more frequently in the 3rd representative winter week in comparison to what occurred in the 2nd representative winter week. More frequent charges of the DHW storages means that their average temperature is higher, hence also the return temperature from them is higher and finally it is not always possible to reach RPW-HEX temperature lower than 55 - 60 °C. Regarding the high RPW-HEX temperature at the beginning of the 3rd representative winter week (on March 18th), this value is due to the fact that on that morning the control logic has been changed from the logic used in the 2nd representative winter week (decentralized DHW tanks charged only in two predefined periods in a day regardless the RPW-HEX status) to the one used in the 3rd representative winter week (decentralized DHW tanks charged also as soon as the RPW-HEX is available, hence its temperature is higher than 70 °C).Regarding instead the high RPW-HEX temperature values on March 21st these are due to the fact that, contrarily to the control logic applied, for some hours on that day the decentralized DHW tanks charging phase didn't started although the RPW-HEX temperature was higher than 70°C and the last decentralized DHW tanks charging was more than 4 hours before. This condition can be observed in Figure 98 that shows the mass flowrate entering the decentralized DHW tanks for their charging in the 3rd representative winter week. Being this event an exception its presence is considered acceptable.

As can be seen in the figure on the left of Figure 99 the RPW-HEX contribution to decentralized DHW tanks charging is in the range 4 - 6 kWh per each decentralized DHW tanks charging event. This value appears lower than the same quantity obtained in the 2nd representative winter week and this is due to the lower RPW-HEX sensible contribution to decentralized DHW tanks charging due to the fact that RPW-HEX temperature at the beginning of the RPW-HEX discharging phase in the 3rd representative winter week (around 70 °C) is lower in comparison to the same quantity in the 2nd representative winter week (around 90 °C). However, the fact that more charging events occurred in a day increases the duration of RPW-HEX contribution to decentralized DHW tanks charging at daily level to around 120 – 150 min/day. Figure 100 shows instead the energy contribution to decentralized DHW tanks charging coming from the HP when it works in series with RPW-HEX (purple part of the columns in Figure 100) from the RPW-HEX (green part of the columns in Figure 95) and from the HP when it works without the RPW-HEX (brown part of the columns in Figure 100). Last, Figure 101 shows the daily duration of decentralized DHW tanks charging with HP and RPW-HEX working in series (green part of the columns in Figure 101) and with HP only (purple part of the columns in Figure 101).

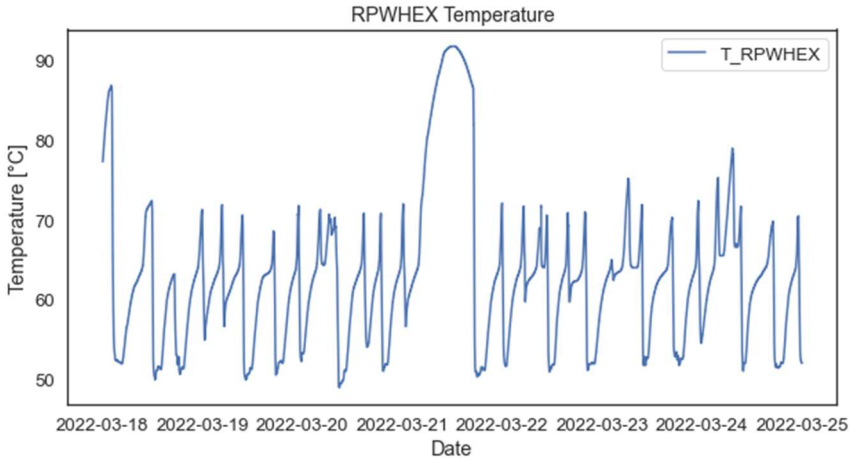

Figure 97. RPW-HEX temperature in the 3rd representative winter week

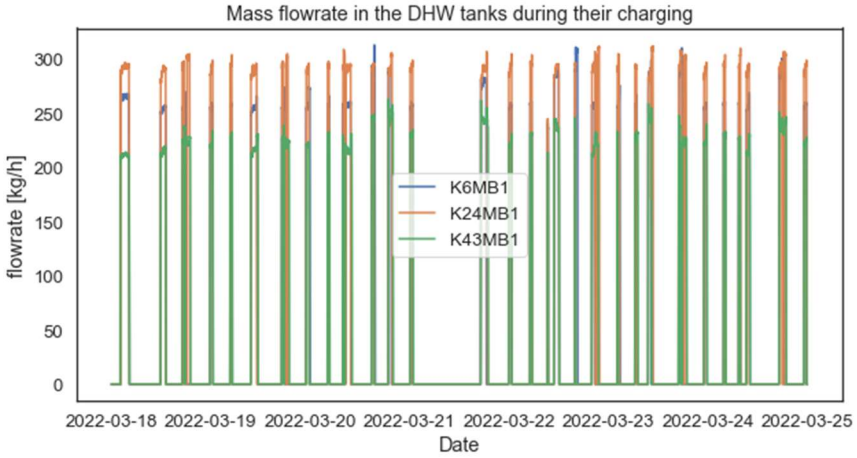

Figure 98. Mass flowrate used to charge the three decentralized DHW tanks in the 3rd representative winter week

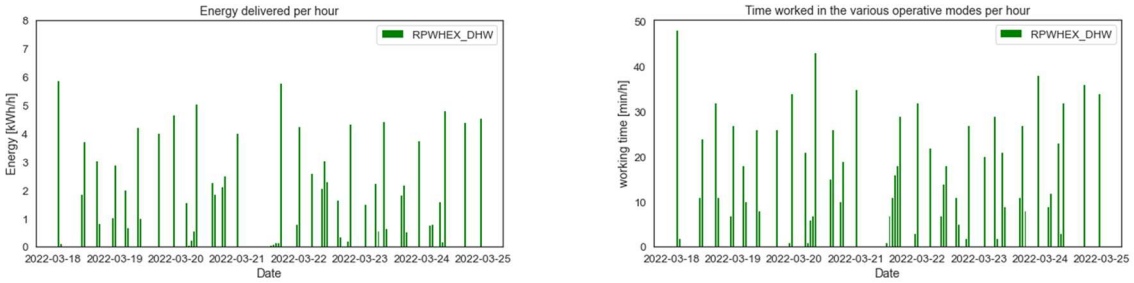

Figure 99. RPW-HEX energy contribution to decentralized DHW tanks charging (left) and duration of RPW-HEX contribution to DHW tanks charging (right) in the 3rd representative winter week

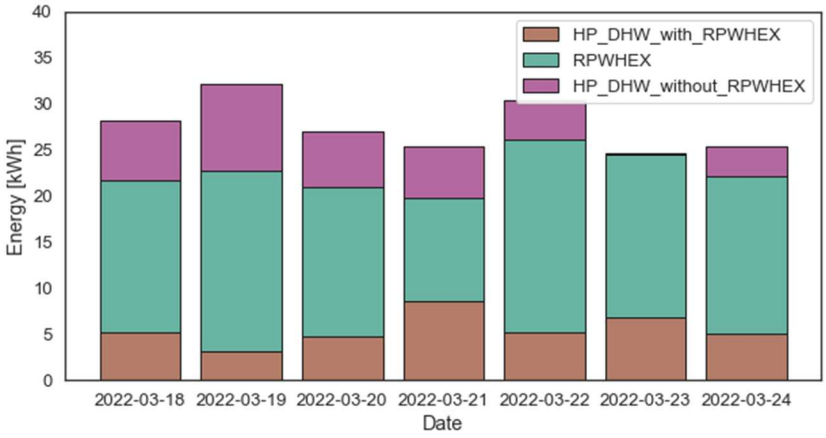

Figure 100. Daily energy contributions to decentralized DHW tanks charging: HP contribution when it works in series with RPW-HEX (brown), RPW-HEX contribution (green) and HP contribution when it works without the RPW-HEX (purple) in the 3rd representative winter week

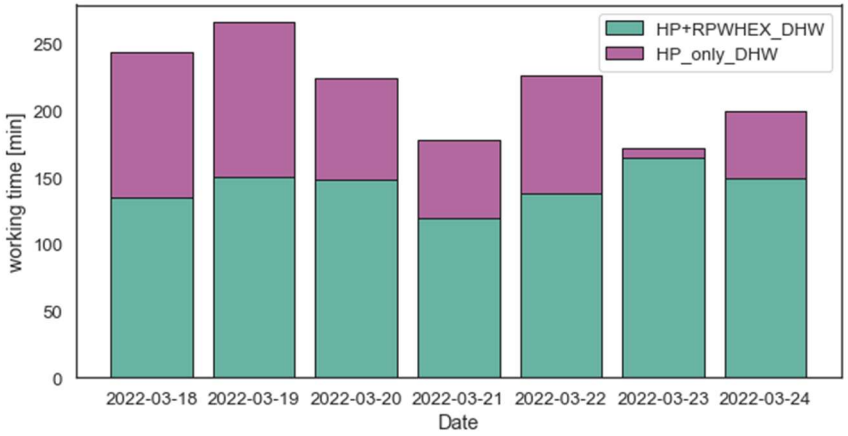

Figure 101. Daily duration of decentralized DHW tanks charging with HP that works in series with RPW-HEX (green) and without RPW-HEX (purple) in the 3rd representative winter week

In conclusion, with the new control logic applied on 3rd representative winter week the RPW-HEX contribution to decentralized DHW tanks charging is increased both in terms of thermal energy delivered by the latent storage and in terms of duration of this contribution. The improvement can be observed comparing Figure 95 with Figure 100 (in terms of thermal energy) and Figure 96 with Figure 101 (in terms of duration of RPW-HEX contribution). The control logic applied during the 3rd representative winter week therefore represents the once that allows the highest exploitation of RPW-HEX.

It is also important to note that, although the number of decentralized DHW tanks charging events in the various days of the 3rd representative winter week is higher in comparison to the same quantity in the 1st and 2nd representative winter week, this is not associated to an increment of discomfort in the various zones connected to HYBUILD system. In fact, the indoor temperature during the 3rd representative winter week is almost always higher than the comfort value (considered equal to 20 °C) as visible in Figure 82.

3.3.5 Electrical system analysis

The operation of the electrical part of the system is evaluated through different analysis. In the first part, the evaluations about the electrical energy fluxes between PV, BESS, grid and HP (also called load) are presented. In this section, it is highlighted the contribution of the photovoltaic and battery system to cover the load. In the second part, the Self-sufficiency ($SS_{(el)}$) and Self-consumption ($SC_{(el)}$) indexes are used to analyse the energy-related performances of the system. If the first part about electrical energy fluxes analysis is basically a qualitative analysis, the calculation of the indexes in the second part give instead quantitative indications about the amount of electrical energy consumption that is covered through PV+BESS ($SS_{(el)}$) and about the amount of energy consumed with respect to PV production ($SC_{(el)}$). In addition to these indexes also the Share of renewables ($SR_{(el)}$) is evaluated. This indicator is calculated as the ratio between the electrical energy consumed on site coming from renewables (including also renewable fraction of the energy coming from the grid) and the total system electrical consumption.

3.3.5.1 Electrical energy fluxes from PV, to and from BESS, to and from grid and to load

The PV system installed at the Continental demo has a nominal power of 6.2 kWp. Figure 102 shows the PV production in the various hours of the day and for the different days of the 3rd representative winter week. As expected from the modules orientation (25° tilted, South-East oriented), the PV production is concentrated in the hours of the day around noon. The PV production is similar for almost all the days of the 3rd representative winter week with the

exception of the second day (March 19th), where, due to probably cloudy weather conditions, the PV production during the entire day is much lower.

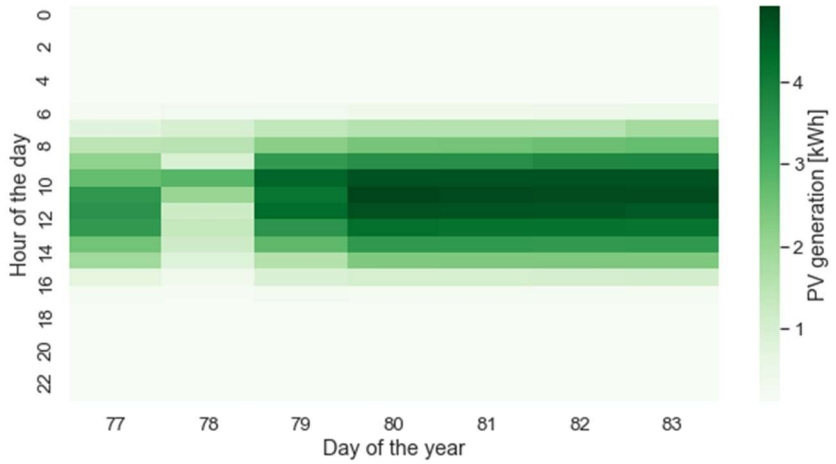

Figure 102. PV production in the various hours of the day in the various days of the 3rd representative winter week

Regarding the BESS, positive energy fluxes indicates that the BESS is charged by the PV system in case of surplus of PV production with respect to the load, and negative when part of the load is covered by the BESS. Figure 103 shows that the BESS is generally charged in the morning and is discharged typically in the afternoon when PV production becomes lower than the load.

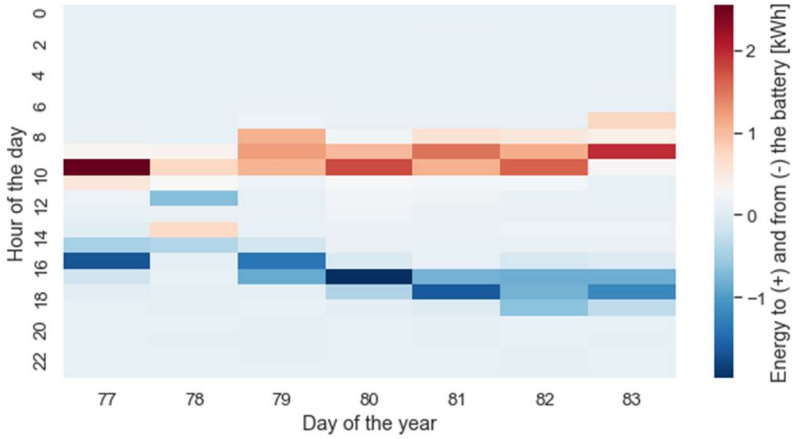

Figure 103. Electrical energy to (+) and from (-) BESS in the various hours of the day for the various days of the 3rd representative winter week

As for the BESS, also for the grid the energy fluxes can be positive or negative indicating that energy is taken (+) or is sent (-) to the grid. Figure 104 shows the energy fluxes to and from the grid in the various hours of the day and for the different days of the 3rd representative winter week. As can be noted from Figure 104 between 8 a.m. and 4 p.m. the PV and BESS are able to cover the load in almost all the days of the 3rd representative winter week, with the exception of the second day (March 19th) for the reasons already explained before. In addition, Figure 104 shows that in the central hours of the day there is also in the winter period a PV production surplus that cannot be stored in the BESS as this component is already fully charged. Therefore the surplus is sent to the grid.

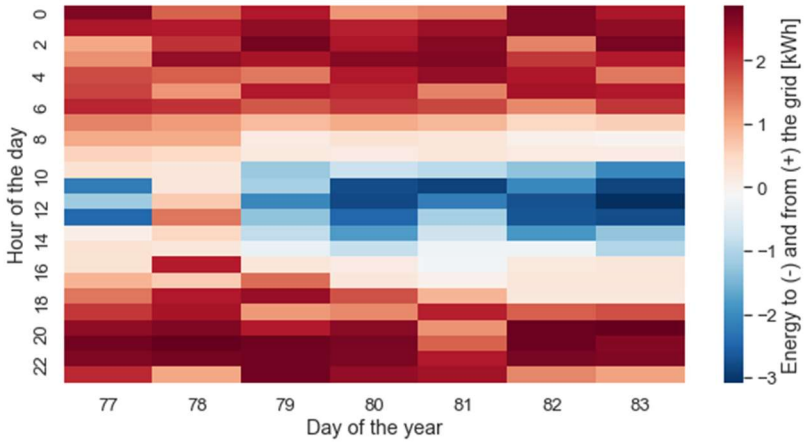

Figure 104. Electrical energy to (-) and from (+) the grid in the various hours of the day for the various days of the 3rd representative winter week

Regarding the relation between PV production and load, the upper plot in Figure 105 shows the amount of PV production that is self-consumed (instantaneously or temporarily stored in the BESS and consumed by the HP in a second moment) and the amount of PV production that is sent to the grid. In almost all the days of the 3rd representative winter week there is a part of the PV production that is not used on-site and is sent to the grid. The lower plot in Figure 105 shows instead how much of the energy consumed by the load comes from PV+BESS (self-consumption in Figure 105, lower figure) and how much comes from the grid. From this lower figure it can be noted that, on a daily base, the energy from the grid is generally higher that the PV+BESS contribution that is for most of the days of the 3rd representative winter week around 40% of the HP consumption.

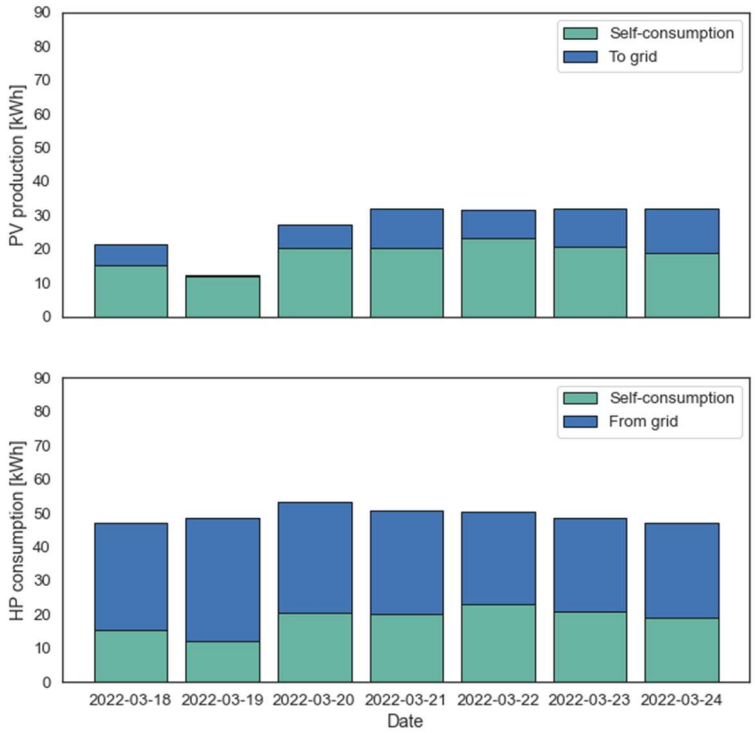

Figure 105. The upper figure shows the energy produced by PV and self-consumed on site (green) and the energy produced by PV and sent to the grid (blue). The lower figure shows instead the HP consumption covered through energy coming from PV+BESS (green) and from the grid (blue) in the 3rd representative winter week

For a more in-deep view, the trend of energy from PV, to/from BESS, to/from grid and to the load are reported in the upper figure of Figure 106 for one day of the 3rd representative winter

week (March 22nd). In this figure it can be noted that the PV production is generally centred around noon. Contemporary to the peak of PV production, also the PV surplus becomes relevant. In the morning, the surplus is used first to charge the BESS (positive values of the variable "BESS" in Figure 106) and then the exceeding energy is sent to the grid (negative values of the variable "Grid" in Figure 106). The BESS is instead discharged (negative values of the variable "BESS" in Figure 106) in the afternoon/evening when the PV production becomes lower than the load and this situation continues until the BESS is completely discharged. After this point the load is covered with electricity coming totally from the grid (values of variables "HP" and "Grid" in Figure 106 are overlapped). The bottom plot in Figure 106 reports instead the BESS SoC. Aligned to the upper figure, the BESS SoC increases in the morning when the PV production becomes greater than HP consumption and decreases in the afternoon/evening when the opposite situation occurs.

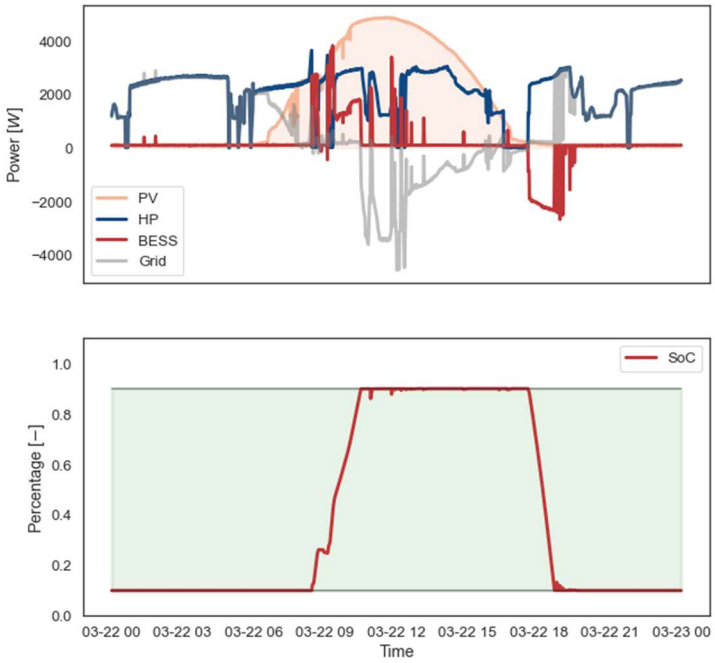

Figure 106. The upper figure shows the PV production, energy to (+) and from (-) the BESS, energy to (-) and from (+) the grid and energy to the load. The lower figure shows the BESS SoC. Both figures are obtained in one day of the 3rd representative winter week (March 22nd)

3.3.5.2 Self-sufficiency and Self-consumption

Self-sufficiency is calculated, over the considered period, using the following formula:

$$SS_{(el)} = \frac{E_{RES\,(el)}}{E_{D\,(el)}}$$

Where:

- $E_{RES\,(el)}$ is the energy produced by PV and directly consumed by the HP or produced by PV, stored in the BESS and consumed by the HP in a second moment
- $E_{D\,(el)}$ is, in this case, the HP electrical energy consumption

On the other hand, Self-consumption is calculated, over the considered period, using the following formula:

$$SC_{(el)} = \frac{E_{RES\,(el)}}{E_{RES-TOT\,(el)}}$$

Where:

- $E_{RES-TOT\ (el)}$ is the PV production

As can be seen in Figure 107 the daily values of $SS_{(el)}$ around 40% for most of the days of the 3rd representative winter week), while the daily values of $SC_{(el)}$ during the same period are relatively high (around 60%). These values are aligned to expectations. In fact, in the considered period (18 – 24 March 2022), due to the weather conditions the PV production is limited and, at the same time, HP consumption is quite high to ensure the coverage of building thermal needs. These two opposite effects lead to relatively low values of $SS_{(el)}$, indicating that only part of HP consumption is covered by energy coming from PV+BESS. On the contrary $SC_{(el)}$ is relatively high, indicating that most of the PV production is consumed by the HP and is not sent to the grid. As already mentioned in previous sections, the low value of $SS_{(el)}$ on March 19th is due to the unfavourable weather conditions that are responsible of very low PV production on this day.

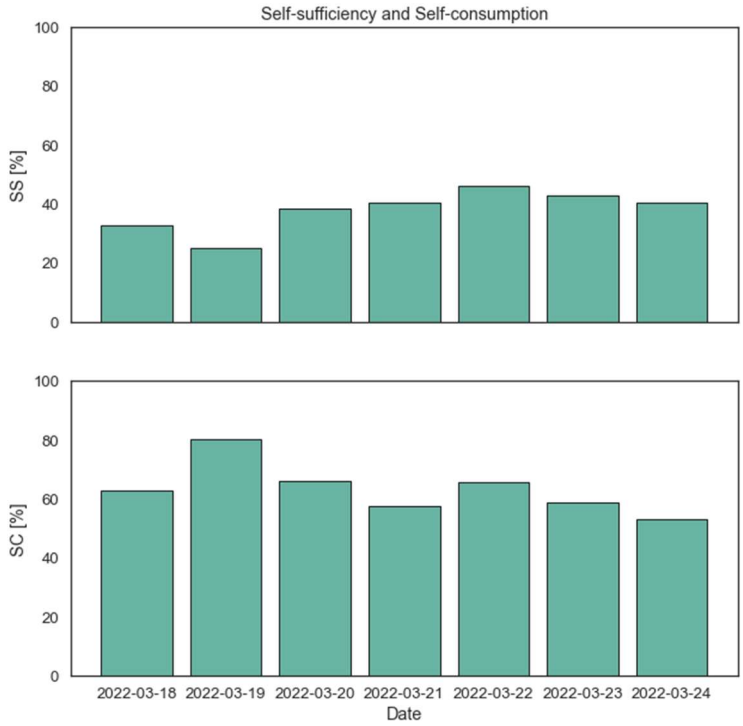

Figure 107. Daily Self-sufficiency (SS) and Self-consumption (SC) values during the 3rd representative winter week

The values of $SS_{(el)}$ and $SC_{(el)}$ for the 3rd representative winter week are calculated weighting the daily values based on the daily HP energy consumption ($SS_{(el)}$) and based on the daily PV production ($SC_{(el)}$). These values are reported in **¡Error! No se encuentra el origen de la referencia.**.

Table 8. Self-sufficiency (SS) and Self-consumption (SC) over the 3rd representative winter week

Self-sufficiency ($SS_{(el)}$)	Self-consumption ($SC_{(el)}$)
39%	62%

3.3.5.3 Share of renewables

Share of renewables is calculated, over the considered period using the following formula:

$$SR_{(el)} = \frac{E_{RES*(el)}}{E_{D\ (el)}}$$

Where:

- $E_{RES*(el)}$ is the sum of energy produced by PV and directly consumed by the HP or produced by PV, stored in the BESS and consumed by the HP in a second moment and of the renewable fraction of the energy coming from the grid (calculated considering the renewable fraction in the Austrian electrical energy mix, value equal to 75.07% for year 2019 according to https://ec.europa.eu/eurostat/web/energy/data/shares).
- $E_{D\ (el)}$ is, in this case, the total electrical consumption. Here, in addition to HP consumption also the consumption of the auxiliaries is considered.

As can be seen in Figure 108 the share or renewables ($SR_{(el)}$) is relatively high for all the days of the considered winter representative week although the values of $SS_{(el)}$ are, as reported in section 3.3.5.2, relatively low (32%). This is due to the high fraction of electrical energy produced through renewable energy sources in the electrical energy mix of the considered country (Austria).

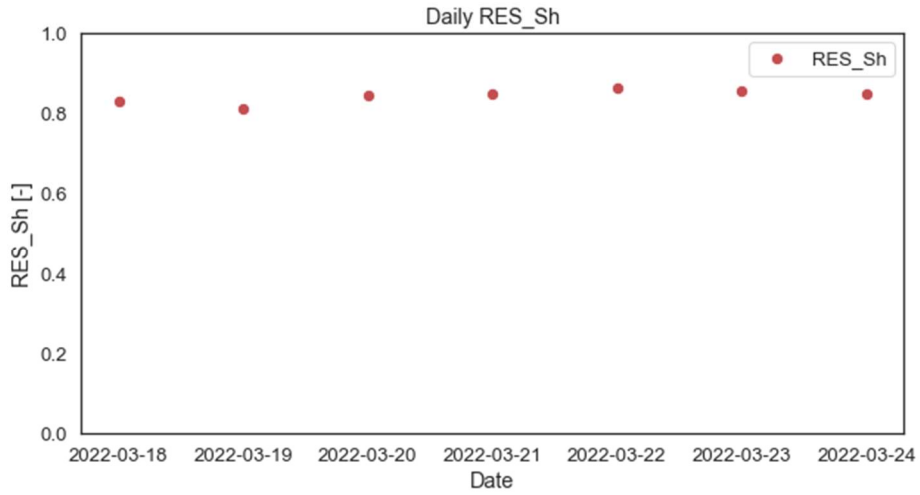

Figure 108. Daily Share of renewables (SR or RES_Sh) during the 3rd representative winter week

The $SR_{(el)}$ over the 3rd representative winter week is calculated as the weighted average of daily values weighting the daily contribution with respect to the daily total electrical energy consumption. Table 9 reports the $SR_{(el)}$ over the 3rd representative winter week.

Table 9. Share of renewables (SR) over the 3rd representative winter week

Share of renewables ($SR_{(el)}$)
84%

3.3.6 Global system analysis

After the analysis of thermal and electrical part of the system separately, in this section some evaluations that regards the whole system (thermal + electrical) are reported. In the first part of this section the quantities analysed are the system PCOP (system COP over the considered period) and the system PPF (system Performance factor over the considered period). In the second part of this section, instead, the Final Energy and Primary Energy consumption, as well as the CO2eq emissions are calculated. These last three quantities are also compared with the same quantities obtained considering that the thermal energy delivered by the HYBUILD system in the 3rd representative winter week is delivered by the reference system. In this context, the term “reference system” indicates the system generally present in the buildings in the EU CON

climate as better specified in the following sections. This allows to assess which would have been the FE consumption, PE consumption and CO2eq emissions if the same thermal energy had been provided by the reference system. Comparing the results in terms of PE consumption and CO2eq emissions of the reference and HYBUILD systems it is possible to also assess PE savings and CO2 emissions savings associated to the use of HYBUILD system.

3.3.6.1 System PCOP

The system PCOP represents the system COP over the considered period. Typically, this index is evaluated over the winter season and the name of this index is SCOP (Seasonal COP). In this work the name has been changed to system PCOP (Period COP) to clarify that the indicator is calculated only over the 3rd representative winter week. The system PCOP represents the ratio between the thermal energy delivered by the generation system (HP+RPW-HEX) measured at the entrance of hydraulic separator through the sensor K3MB5 (see Figure 75) and the HP electrical consumption. This indicator is calculated using the following formula:

$$SYS\_PCOP = \frac{E_{HP+RPW-HEX\ (th)}}{E_{D\ (el)}}$$

Where:

- $E_{HP+RPW-HEX\ (th)}$ is the thermal energy delivered by HP+RPW-HEX
- $E_{D\ (el)}$ is, in this case, the HP electrical energy consumption

As shown in Figure 109 the daily system PCOP is similar for all the days of the 3rd representative winter week and relatively high (in the range 3.5 - 4).

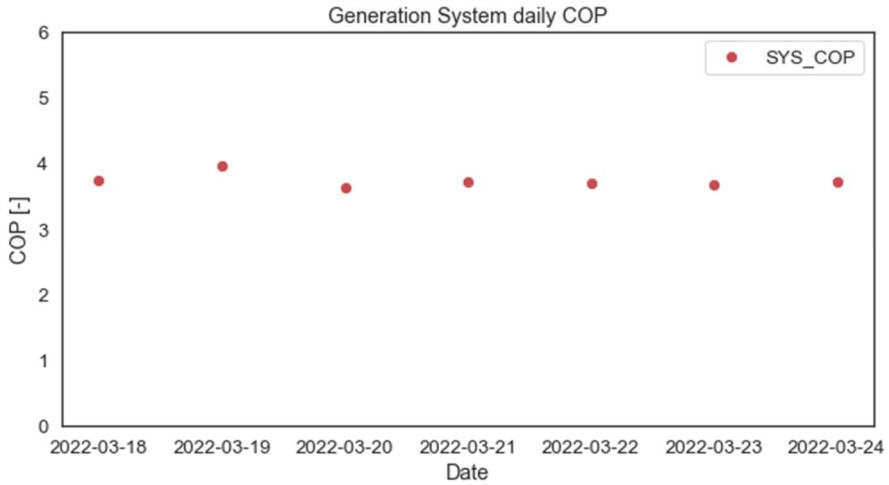

Figure 109. Daily System PCOP during the 3rd representative winter week

The system PCOP over the entire 3rd representative winter week is calculated as the integral of the daily thermal energy delivered by HP+RPW-HEX divided by the integral of the daily values of HP electrical consumption. The system PCOP over the 3rd representative winter week is reported in Table 10.

Table 10. System PCOP over the 3rd representative winter week

SYS_PCOP
3.7

3.3.6.2 System PPF

The system PPF represents the system performance factor over the considered period. Similar to system COP, also this index is generally evaluated over the winter season and the name of this index is SPF (Seasonal Performance Factor). In this work the name has been changed to system PPF (Period Performance Factor) to clarify that the indicator is calculated only over the 3rd representative winter week. The system PPF is calculated as the ratio between the thermal energy delivered to the user to cover SH and DHW user demand and the system electrical consumption. The thermal energy delivered to the user for SH and DHW is measured respectively by sensors K*MB2 and K*MB3, where the symbol * indicates the number associated to each enerboxx (6 for enerboxx01, 24 for enerboxx02, 43 for enerboxx03 as visible in Figure 76). In this context the system electrical consumption considers not only the HP consumption but also the consumption of the auxiliaries. This indicator is calculated using the following formula:

$$SYS\_PPF = \frac{E_{SH+DHW\ delivered\ to\ user\ (th)}}{E_{D\ (el)}}$$

Where:

- $E_{SH+D\quad delivered\ to\ user\ (th)}$ is the thermal energy delivered to the user to cover SH and DHW user demands
- $E_{D\ (el)}$ is, in this case, the total electrical consumption. Here, in addition to HP consumption also the consumption of the auxiliaries is considered.

Figure 110 shows the daily system PPF in the 3rd representative winter week and, as can be noted, the system PPF is almost constant for the various days and in the range 3 - 3.5.

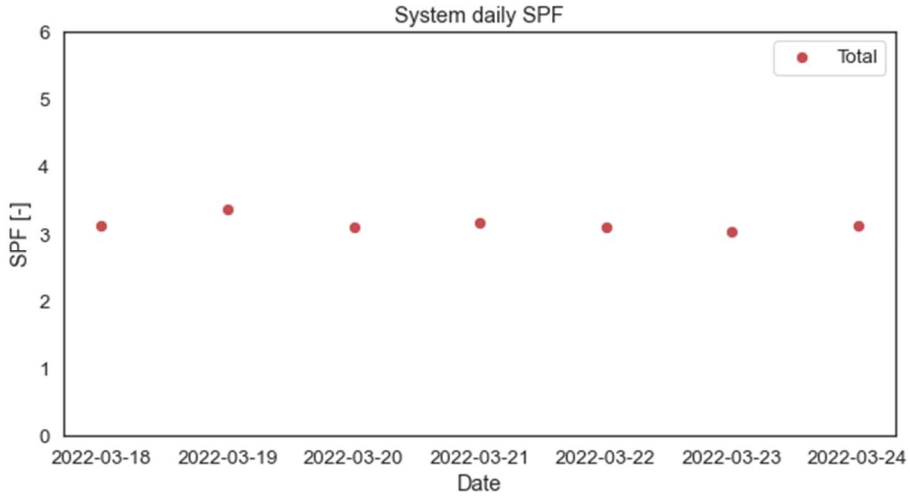

Figure 110. Daily System PPF during the 3rd representative winter week

The system PPF over the entire 3rd representative winter week is calculated as the integral of thermal energy delivered to the user to cover SH and DHW user demand divided by the integral of system electrical consumption. The system PPF over the 3rd representative winter week is reported in Table 11.

Table 11. System PPF over the 3rd representative winter week

SYS_PPF
3.1

3.3.6.3 Final Energy consumption, Primary Energy consumption and CO2 emissions

Before the installation of HYBUILD system, the thermal needs of Langenwang demo building were covered through thermal energy coming from the local DHN. This District Heating System is fed by biomass. A District Heating System fed by biomass cannot be considered representative of the most common heating system adopted in the buildings of EU CON climate. Considering that one of the goals of this analysis is to calculate, in addition to FE consumption, PE consumption and CO2eq emissions also the related savings guaranteed by the adoption of the HYBUILD system, a reference system for the comparison must be assumed. Having stated that the Biomass District Heating System present at the demo before the installation of the HYBUILD system is not representative of the most common technology used to cover thermal needs in buildings in EU CON climate it has decided to consider, as reference system, a gas boiler. This is also in accordance with the assumptions about reference system considered in other WPs for buildings in EU CON climate. For this reason, in this section, the calculations of savings are performed comparing the HYBUILD system to a reference one that foresees the presence of a gas boiler.

FE consumption is evaluated for the 3rd representative winter week from measurements at the demo. In this period the HYBUILD system delivered 1281 kWh of thermal energy. The measured electrical consumption of HYBUILD system to deliver this thermal energy (1281 kWh) is equal to 346 kWh. Part of this electrical consumption comes from PV+BESS (131 kWh), while the remaining part comes from the electrical grid (215 kWh). The HYBUILD system total FE consumption, therefore, results equal to 346 kWh. Knowing the primary energy factor for electricity from the grid (value equal to 1.63 from https://www.oib.or.at/sites/default/files/richtlinie_6_12.04.19_1.pdf) and from PV+BESS (the electrical energy from PV+BESS is considered totally renewable and the primary energy factor is assumed equal to 1.00) it is possible to calculate the PE consumption of the HYBUILD system as the sum of the respective FE consumption (215 kWh from the grid and 131 kWh from PV+BESS) multiplied by the respective primary energy factor (1.63 for the grid and 1.00 for the PV+BESS). In this way, the PE consumption of the HYBUILD system results equal to 481 kWh. The CO2eq emissions of the HYBUILD system in the 3rd representative winter week is instead equal to 49 kgCO2eq. This value is calculated multiplying the part of the FE consumption coming from the grid (215 kWh) by electrical grid emission factor (equal to 277 gCO2eq/kWh from https://www.oib.or.at/). For the sake of simplicity, it is assumed that the electrical energy produced on-site and self-consumed (131 kWh) is neutral in terms of CO2eq emissions (hence the emission factor of electrical energy coming from PV+BESS is equal to 0 gCO2eq/kWh).

As stated before, the reference system considered in this analysis is a gas boiler. This kind of system presents a primary energy factor equal to 1.10 (value from https://www.oib.or.at/), while the emission factor is considered equal to 247 gCO2eq/kWh from https://www.oib.or.at/. To deliver the same thermal energy to the building (1281 kWh) the FE consumption of the reference system should be increased to consider the thermal losses in the generation and distribution part of the system. For the sake of simplicity, an overall efficiency of the reference system equal to 0.8 has been assumed. In this way, the delivering of 1281 kWh to the user implies a FE consumption equal to 1601 kWh. The PE consumption is obtained multiplying the FE consumption (1601 kWh) times the primary energy factor of gas (1.10), resulting in a PE consumption for the reference system equal to 1761 kWh. Finally, the CO2eq emission of the reference system is calculated multiplying the FE consumption (1601 kWh) times the emission factor for gas (247 gCO2eq/kWh) resulting in the emission of 396 kgCO2eq in the 3rd representative winter week.

Table 12 summarizes the FE and PE consumption of the reference and HYBUILD system, as well as the CO2eq emissions. As can be noted the PE consumption of the HYBUILD system is notably lower that the same characteristic for the reference system, indicating that an important

decrement in terms of PE consumption can be reached using the HYBUILD system. In addition to that, also the CO2eq emissions of HYBUILD system are sensibly lower than the same quantity for the reference system.

Table 12. Final Energy (FE) consumption, Primary Energy (PE) consumption and CO2eq emissions of reference and HYBUILD system in the 3rd representative winter week

Characteristic	Unit	Reference system	HYBUILD system
Final energy (FE) from el. grid	kWh	-	215
Final energy (FE) Total	kWh	1601	346
Primary energy (PE) Total	kWh	1761	481
CO2eq emissions	kgCO2eq	396	49

4 KPIs: results and discussion

4.1 Almatret demo site

4.1.1 Thermal Energy Storage Density

According to deliverable D1.3 - Requirements: key performance indicators, system components and performance targets, the thermal energy storage density ($ED_{thermal}$) is a KPI that measures the amount of thermal energy that can be stored in a certain available volume. This KPI can be calculated at two different levels: thermal energy storage material and component/module levels.

The thermal energy density at component/module level was evaluated for this report since this level is more relevant from a practical point of view. This KPI is defined as the ratio between the amount of thermal energy storage capacity ($ESC_{thermal}$) and the component/module volume (V_{module}), as shown in the following equation:

$$ED_{thermal} = \frac{ESC_{thermal}}{V_{module}}$$

The thermal energy storage capacity ($ESC_{thermal}$) estimates the total amount of thermal energy that a system can store at nominal conditions and considers both the storage capacity of the material and the sensible heat that can be stored in the components/materials that are in contact with the TES material. Therefore, the thermal energy storage capacity is calculated according to the following equation:

$$ESC_{thermal} = ESC_{mat} + ESC_{comp}$$

where the thermal energy storage capacity of the material (ESC_{mat}) and the thermal energy storage capacity of all system components (ESC_{comp}) are calculated below:

$$ESC_{mat} = ED_{mat} \cdot \frac{m_{mat}}{\rho_{min}}$$

$$ESC_{comp} = \sum_{1}^{x} \left(c_{p.comp.x} \cdot m_{comp.x}\right) \cdot \Delta T_{op}$$

where $\rho_{min.mat}$ [$kg \cdot m^{-3}$] is the minimum density of the TES material, $c_{p.comp,x}$ [$kJ \cdot kg^{-1} \cdot K^{-1}$] is the average specific heat of component "x", $m_{comp,x}$ [kg] is the mass of component "x", ΔT_{op} is the operation temperature range, which is defined as the range of nominal temperature conditions at which the material will be maintained during the operation of the system between a minimum temperature (T_{min}) and a maximum temperature (T_{max}).

Although the system installed at the Almatret demo site includes three TES technologies, only sensible and latent technologies are actually used in practice, being the sorption module not used as a TES component, but rather as a chiller in cascade with the heat pump to increase its cooling efficiency. Therefore, the TES capacity was only evaluated for the buffer tank (sensible TES component) and for the RPW-HEX (latent TES component).

Starting with the sensible TES component (buffer tank), the main materials to be considered in the evaluation are the TES material (800 L of water) and the container material (95 kg of stainless steel). All other materials such as insulation and sensors were neglected in the analysis. The maximum operation temperature (T_{max}) is fixed by the maximum temperature supplied by the

Fresnel solar field (95 ºC), while the minimum temperature (T_{min}) is the one that should allow to preheat the return water from the heating system (50 ºC was assumed).

With all these assumptions, a TES storage capacity of the buffer tank of 151.4 MJ was obtained. The actual volume of the buffer tank (V_{module}) is the volume occupied by the whole component, including insulation material, which was estimated to be equal to 1.9667 m^3. Therefore, the TES density of the buffer tank was estimated to be $ED_{thermal,buffer} = 76.98$ MJ·m^{-3}.

Next, the latent TES component energy density was evaluated. For the RPW-HEX, an operation temperature range between -2 ºC and 9 ºC was assumed as the minimum and maximum temperatures levels at which the PCM can effectively be charged and discharged, respectively. In this case, the TES material consists of 40 kg of PCM (RT-4 from Rubitherm company [5]), which is a paraffin that stores cold by solidification at a temperature around 4 ºC. The thermo-physical properties of the TES material were evaluated by the University of Lleida and presented in a scientific paper [6]. Moreover, energy can also be stored in the other components of the RPW-HEX as sensible energy, being the casing material (148 kg of aluminium) and the heat transfer fluid (5 kg of mixture of 70% water by 30% glycol) the most relevant ones.

With the above-mentioned assumptions, a TES storage capacity of the RPW-HEX of 7.35 MJ was obtained. The actual volume of the RPW-HEX (V_{module}), including insulation material, was estimated to be equal to 0.47 m^3. Therefore, the TES density of the latent storage module (RPW-HEX) was estimated to be $ED_{thermal,RPW-HEX} = 15.64$ MJ·m^{-3}. The results of the thermal energy storage density calculated for the Almatret demo site components are summarised in Table 13.

Table 13. Thermal energy storage density for HYBUILD Almatret demo

Component	Energy density [MJ·m^{-3}]
$ED_{thermal,buffer}$	76.98
$ED_{thermal,RPW-HEX}$	15.64

4.1.2 Seasonal energy performance, share of renewable, and self-consumption

Seasonal energy performance (SPF_{th} , SPF_{el}), share of renewables ($SR_{(el)}$), and self-consumption ($SC_{(el)}$) have been calculated in Section 3.1.3. Table 14 summarizes the values obtained for these KPIs over the representative summer week.

Table 14. Seasonal energy performance, share of renewable, self-sufficiency, and self-consumption for Almatret demo

KPI	Value
Thermal seasonal performance factor	0.48
Electric seasonal performance factor	4.64
Self-consumption	0.82
Self-sufficiency	0.58
Share of renewables	75%

4.1.3 Energy savings and CO_2 emission saving

To analyse the energy savings and CO_2 emissions savings the HYBUILD Mediterranean reference system described on D1.1 was employed. Energy savings and especially CO_2 emissions savings

are key performance indicators of particular interest. They show the feasibility of the HYBUILD system to contribute to the fulfilment of the sustainable development objectives set in Europe.

Figure 111 shows the energy savings for both natural gas and electricity consumption of the HYBUILD system. As shown in the figure, there is an increase in electricity consumption due to the change of the HYBUILD energy system matrix from natural gas to grid electricity.

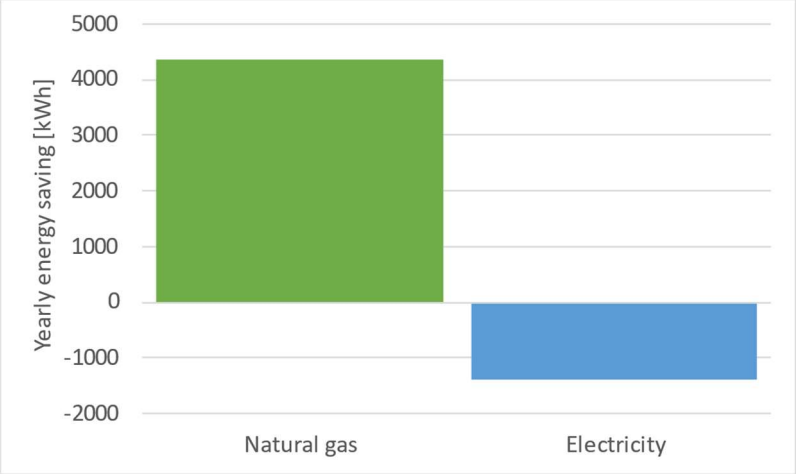

Figure 111. HYBUILD primary energy savings

Figure 112 shows the CO_2 emissions savings corresponding to the HYBUILD Mediterranean system. For the emissions estimation, the conversion factors proposed by the European Commission (0.1757 tonnes CO_2e/MWh Electricity, 0.202 tonnes CO_2e / MWh natural gas) were used. These factors are based on the COMMISSION DELEGATED REGULATION (EU) 2018/2066 of 19 December 2018, annex VI (https://ec.europa.eu). The results show considerable savings in CO_2 emissions, avoiding the emission of 0.63 tons of CO_2 per year into the atmosphere.

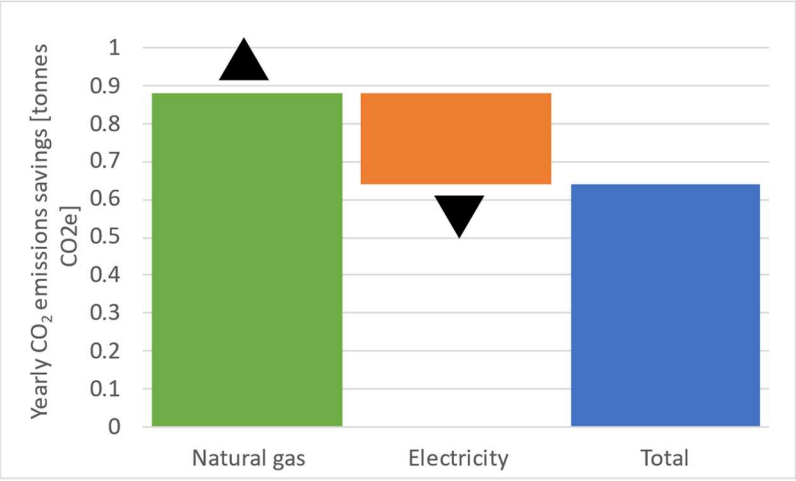

Figure 112. HYBUILD Mediterranean system CO_2 emissions savings

4.1.4 Compactness

As defined in deliverable D1.3 - Requirements: key performance indicators, system components and performance targets, the compactness is defined at component level as the ratio of the volume occupied by a component on a functional unit. The volume occupied is defined as the volume of a virtual parallelepipedal shape into which the component can be placed, and it should also include any security or service space specified in the component installation guidelines. The choice of a parallelepipedal shape is necessary because it is the easiest shape for integration into a building (along walls, on the floor, in a corner, …).

The functional unit dependents on the type of component considered. For a component that produces or transfers energy such as heat pumps, boilers, heat emitters, etc., the functional unit will be the power in kW. For a storage component such as electric batteries, sensible storage, or PCM storage, the functional unit will be the energy storage capacity in kWh.

This compactness is a key indicator that is easy to use to compare systems that provides the same level of energy services. The HYBUILD system installed at the Almatret demo site was designed to provide heating, cooling, and DHW to the building. Therefore, as explained in D1.3, the functional unit was defined as the sum of the energy needed for space heating and cooling, and for DHW along a full year, and the compactness of the system can be defined as below:

$$\frac{V_{HP} + V_{PCM\ sto} + V_{W\ sto} + \cdots}{E_{Heat} + E_{Cool} + E_{DHW}}$$

where V_{HP} is the volume occupied by the heat pump, $V_{PCM\ sto}$ is the volume occupied by the PCM storage unit, $V_{W\ sto}$ is the volume occupied by the water storage unit, $E_{Heat} = 7742.6$ kWh/year is the yearly heating energy demand, $E_{Cool} = 2606.6$ kWh/year is the yearly cooling energy demand, and $E_{DHW} = 2471.6$ kWh/year is the yearly energy demand for DHW production.

The building energy demand for space heating and DHW was obtained during the pre-intervention monitoring period, and the results were consistent with the ones obtained from simulations. However, since the building did not have any cooling system installed previous to the HYBUILD system, the energy demand for cooling could not be monitored. Therefore, the overall energy demand should be evaluated from the same building energy simulations reported in deliverable D4.1 - Smart system algorithms.

The following components that are placed in the technical room were considered in the evaluations of the compactness: electric rack (including DC bus and electric battery), heat pump, latent storage (RPW-HEX), sorption module, buffer and DHW tanks, solar field hydraulic unit, filling unit, expansion vessels, and heat exchangers. The volumes of each component and the energy demand for heating, cooling, and DHW are shown in Table 15.

Table 15. Volume of the components in the technical room of the Almatret demo system

Component	Volume (m^3)
Electric rack	0.97
Heat pump	2.25
Latent storage (RPW-HEX)	0.47
Sorption module	9.93
Buffer tank	2.50
DHW tank	0.52
Solar field hydraulic unit	0.14

Filling unit	0.28
Expansion vessels	0.3
Heat exchangers	0.04
Total	17.4

With this, the compactness of the system installed in the technical room of the Almatret demo site was evaluated to be equal to $1.36 \cdot 10^{-3}$ $m^3 \cdot year \cdot kWh^{-1}$.

The remaining two KPIs defined in the project, i.e. flexibility and return on investment, were not be reported in this deliverable. The BEMS (Building Energy Management System) installed at the Almatret demo is not configured to exploit services to the local electrical grid like flexibility. For this reason, this KPI cannot be calculated for this demo. Regarding the return on investment, since this KPI is strongly related to the economic aspects of the HYBUILD system, the results of this KPI were presented in the corresponding deliverable (D1.3) associated to Task 1.3 for the potentially commercial HYBUILD system (reference Mediterranean system). Since the energy consumption obtained during the pre-intervention monitoring period didn't include energy consumption associated to the cooling demand (no cooling system was available before the installation of the HYBUILD system), any attempt to calculate this KPI for the current system installed at the demo site wouldn't make much sense. Moreover, the results would be very strongly affected by the initial cost of the system, which is very different from the cost of serial production of the commercial HYBUILD system.

4.2 Aglantzia demo site

4.2.1 Thermal Energy Storage Density

Thermal energy storage density is the amount of energy that can be supplied from a storage technology per unit weight (measured in Watt-hours per kg, Wh/kg) or per volume Wh/m^3. The installed thermal energy storage technology for Aglantzia demo site is the latent heat thermal energy storage (TES). However, after the installation and the commissioning of the system, an issue with thermal energy storage system (RPW-HEX) was found. Therefore, after discussions with the consortium, we decided to bypass this component for the current stage in order to proceed with the commissioning of the rest of the HYBUILD system.

4.2.2 Seasonal energy performance

The coefficient of performance (COP) defined the efficiency of the heat pump. It is defined as the ratio between the heat output from the condenser (Q_{SH}) and the power supplied to the compressor (W_{SH}). In case, the ratio is calculated based on the average seasonal values both thermal and electric are given by:

$$SCOP_{DHW} = {Q_{DHW}}/{E_{DHW}}$$

$$SCOP_{SH} = {Q_{SH}}/{W_{SH}}$$

$$SCOP_{tot} = {(Q_{DHW} + Q_{SH})}/{(E_{DHW} + E_{SH})}$$

The performance of the heating and cooling system can be evaluated at all hierarchical levels, component/module level, sub-system level and system level.

The Q_{SH} is the produced thermal energy for space heating, Q_{DHW} is the yearly produced energy for covering the DHW needs Q_{SC} is the seasonal thermal energy produced for covering the cooling loads. The energy E refers to the electricity used for producing the useful energy

Apart of the single components, the project studies the combination of more than one device whose interaction improves the performance of the single one studied alone. In the following, we define an indicator that represents a sort of efficiency of the whole sub-system (L2). Conceptually, it is the same as the one used for the component level, but the boundaries change.

For the case of the sub-system, we define the SPF Seasonal Performance Factor [kWh/kWh] over the year and obtained as the ratio of the delivered energy from the sub sub-system over the energy used to produce it.

For Aglantzia demo site, the total delivered energy consists of the cooling energy exiting the latent thermal storage or directly the chiller, and the heat provided for the DHW load. The Total consumed electricity is the electricity used for running the adsorption module, the dry cooler, the chiller, and all the auxiliaries.

In order to evaluate the performance of the whole system (L3), including renewable energy generation, thermal losses of the distribution system and storages, auxiliaries, distribution terminals in the building, we can calculate the Seasonal Performance Factor (SPF). Similarly, to the previous case, the SPF_{el} is the ratio between the useful energy required by the users for space heating, cooling and DHW, over the overall energy consumed for delivering it.

$$SPF_{el} = \frac{Total\ delivery\ energy}{Total\ consumed\ electricity}$$

$$SPF_{th} = \frac{Total\ delivery\ energy}{Total\ consumed\ thermal\ energy}$$

Looking at the whole system, building and user included, this indicator gives an estimation of the real energy system behaviour. Compared with a "reference" case where a common reversible heat pump coupled with a centralized thermal storage , the SPF for the studied cases should be higher. The SPF_{el} is presented in Table 16 in chapter 4.2.3.

4.2.3 Share of renewable and self-consumption

According to deliverable D1.3 - Requirements: key performance indicators, system components and performance targets, one of the main goals of HYBUILD project is to optimize the use of the storage units to maximize the exploitation of renewable energy sources. At Aglantzia demo site only a photovoltaic system can be considered as a renewable energy source.

According to the energy typology there are different definition of share of renewable indicators [%]. Since, HYBUILD project is focused at building system level, the most common definition is given by the ratio between the energy demand cover by RES (E_{RES}) over the total energy demand E_D.

$$Share\ of\ renewables_{el} = \frac{E_{RES}}{E_D}$$

Where E_{RES} considered the energy from renewable energy sources (PV) directly consumed or stored in the storage system, and E_D is the total electric energy demand of the building. E_{RES} can include also the amount of energy imported from the main grid coming from RES.

Self-consumption

According to deliverable D1.3 another KPI related to the contribution of RES to the energy mix of the building is the self-consumption.

$$Self - Consumption_{el} = \frac{E_{RES}}{E_{RES-TOTAL}}$$

where E_{RES} considered only the energy from renewable directly consumed or stored to the storage unit, while $E_{RES-TOTAL}$ represents the total energy produced by RES.

Self-sufficiency

Another relevant KPI is the Self-sufficiency. Self-sufficiency is represented by the following equation.

$$Self - Sufficiency_{el} = \frac{E_{RES}}{E_D}$$

Electric seasonal performance factor (SPF_{el})

The definition of the electric seasonal performance factor (SPF_{el}) (at system level) expresses the ratio between the cooling or heating supplied to the building by the system ($Q_{cool/heat\_supply}$) and the total electricity consumption of the whole HYBUILD system (El_Energy_IN)

El_Energy_IN takes into account all electrical energy contributions: electricity consumed by the dry cooler, by the HP compressor, and by all pumps connected in between the dry cooler, the HP, and the indoor distribution circuit.

The SPF of the overall system is given by the following equation:

$$SPF_{el} = \frac{Q_{cool/hea\ \_supply}}{El\_Energy\_IN}$$

At a component level, the SPF of a heat pump is the ratio of annual heat generated to the annual electricity consumed for the operation of the heat pump.

As a formula this is calculated as:

$$SPF_{el} = \frac{\text{Total heat/cool output per annum}}{\text{Total electricity consumed per annum}}$$

The Table below presents the values of these KPIs calculated for the summer representative week, the first week of August.

Table 16: Key Performance Indicators for the system calculated for the summer representative week.

KPI	Value
Seasonal Performance Factor (SPF_{el})	4,3
Share of renewables	85,1%
Self Sufficiency	91%
Self Consumption	87%

4.2.4 Energy savings and CO_2 emission saving

Energy saving and reduction of CO2 emissions are among the most important key performance indicators of a system. The main purpose of the HYBUILD system is to help reduce these indicators by getting closer to achieving the sustainable development goals set by the European Union.

The system that was developed and installed in the demo site of Aglantzia is expected to contribute to the reduction of these parameters as it combines renewable energy sources (photovoltaic system) and electrical storage through the battery. These indicators can be calculated in the coming months since the commissioning of the system has just been completed by end of march 2022. Based on the production of the HYBUILD system and the calculations related to the first week of August which is the summer representative week for Aglantzia demo site, the CO2 emissions savings from the system during that week were about 99,2 tonnes.

4.2.5 Compactness

The overall description of the system of Aglantzia demo site is presented in depth in section 2.3.1. However, the final system that has been installed is very different from the HYBUILD Mediterranean reference system due to some modifications which had to be made for the licensing of the system and its proper operation after specific updates. More specifically, after the departure of FRESNEX from the project, it was decided not to install solar thermal and to increase the installed power of the photovoltaic system. Additionally, after a leak was detected in the RPW-HEX it was decided to bypass this component.

As a result, the system installed at Aglantzia demo site, is not 100% representative of the HYBUILD MED reference system.

4.2.6 Flexibility

This demo site, is not able to provide flexibility services to the local electricity network at this moment. However, this KPI can be considered as a next step of this work.

4.3 Langenwang demo site

4.3.1 Thermal Energy Storage Density

The Thermal Energy Storage Density is a KPI indicating the amount of thermal energy that is delivered by the storage (that is the RPW-HEX in the HYBUILD CON system) per each discharge,

with respect to the volume of the storage. This index is expressed in kWh/m3 and is calculated with the following formula:

$$ED_{thermal} = \frac{E_{delivered\ (th)}}{V_{storage}}$$

Where:

- $E_{delivered\ (th)}$ is the average thermal energy delivered by the storage (RPW-HEX) during decentralized DHW tanks charging phase (in the 2nd representative winter week this value is equal to 6.2 kWh, while it results equal to 4.3 kWh in the 3rd representative winter week)
- $V_{storage}$ is the storage volume that in this case is equal to 103 dm^3 (two modules with a volume of 51.5 dm^3 each).

Table 17 reports the thermal energy storage density calculated considering the average thermal energy delivered by RPW-HEX per each discharge in the 2nd and 3rd representative winter week. To have a comparison, from laboratory tests the thermal energy delivered by the RPW-HEX was 4.84 kWh per decentralized DHW tanks charging phase, resulting in a thermal energy storage density equal to 47 kWh/ m^3.

It is considered useful to report in this case both values obtained during 2nd and 3rd representative winter weeks to highlight some aspects. The average thermal energy delivered by RPW-HEX per each discharge during the 2nd representative winter week results equal to 6.2 kWh. This value is higher than the one obtained from laboratory tests and also to the one obtained in the 3rd representative winter week (4.3 kWh). The fact that the RPW-HEX contribution in the 2nd representative winter week is higher than the same quantity obtained during laboratory tests is due to the fact that in the 2nd representative winter week the used control logic foreseen only two charges of decentralized DHW tanks per day, while in laboratory tests the used control logic was more similar to the one considered in the 3rd representative winter week, where the charges of decentralized DHW tanks starts as soon as the RPW-HEX is fully charged (RPW-HEX temperature > 70 °C). The fact that in the 2nd representative winter week the RPW-HEX temperature reaches values higher than 70 °C implies that more energy is available in the subsequent discharging phase when the decentralized DHW tanks are being charged in comparison to laboratory test and also to 3rd representative winter week. On the contrary, the values obtained from laboratory tests and from 3rd representative winter week are considered similar (with a difference in an acceptable range).

Table 17. Thermal energy storage density from laboratory tests and obtained for the 2nd and 3rd representative winter week

Considered test or representative week	Thermal Energy Storage Density ($ED_{thermal}$) [kWh/m3]
Laboratory tests	47.0
2nd representative winter week	60.2
3rd representative winter week	41.7

4.3.2 Period Energy Performance

System PCOP and PPF are the KPIs used to assess system performance over the 3rd representative winter week. These two indicators have been calculated respectively in section

3.3.6.1 and 3.3.6.2. Table 18 reports the system PCOP and PPF over the 3rd representative winter week.

Table 18. System PCOP and PPF in the 3rd representative winter week

SYS_PCOP	SYS_PPF
3.7	3.1

4.3.3 Share of renewable and self-consumption

Share of renewables ($SR_{(el)}$) and Self-consumption ($SC_{(el)}$) have been calculated respectively in section 3.3.5.3 and 3.3.5.2. Table 19 summarizes the values over the 3rd representative winter week. As already explained in section 3.3.5.3, the ($SR_{(el)}$) results particularly high due also to the high fraction of renewables in the Austrian electrical energy mix (75.06% for year 2019 from https://ec.europa.eu/eurostat/web/energy/data/shares). Also ($SC_{(el)}$), calculated over the 3rd representative winter week is relatively high, as reported in section 3.3.5.2. This is because the PV production in the winter period is typically low and, at the same time, HP consumption to cover building thermal needs is high. This leads to consume trough the HP almost all the energy produced by PV.

Table 19. Share of renewables (SR) and Self-consumption (SC) over the 3rd representative winter week

Share of renewables ($SR_{(el)}$)	Self-consumption ($SC_{(el)}$)
84%	62%

4.3.4 Energy savings and CO_2 emission saving

The details about the calculation of FE consumption, PE consumption and CO2eq emissions of reference and HYBUILD system over the 3rd representative winter week are reported in section 3.3.6.3. Here Table 20 summarizes these quantities and reports also the related savings (in absolute and percentage terms) guaranteed by the HYBUILD system in comparison to the reference one. Considering that the reference and HYBUILD system use different energy carriers to ensure the coverage of building thermal needs, the evaluation of energy savings can be performed only with respect to PE consumption. As can be noted in the Table 20, the PE consumption of the HYBUILD system is around 1/3 of the PE consumption of the reference system. In addition, the HYBUILD system ensures the coverage of building thermal needs with notably lower (around 1/8) CO2eq emissions in comparison to the reference system.

Table 20. Final Energy (FE) consumption, Primary Energy (PE) consumption and CO2eq emissions for reference and HYBUILD system in the 3rd representative winter week. In addition, also PE savings and CO2eq emissions savings guaranteed by the HYBUILD system are reported

Characteristic	Unit	Reference system	HYBUILD system	Savings	Savings %
Final energy (FE) from el. grid	kWh	-	215	-	-
Final energy (FE) Total	kWh	1601	346	-	-
Primary energy (PE) Total	kWh	1761	481	1280	73%
CO2eq emissions	kgCO2eq	396	49	347	88%

4.3.5 Compactness

As presented in section 2.4.1, the HYBUILD system installed at the Langenwang demo presents important differences in comparison to the HYBUILD CON reference system. In fact, the HYBUILD CON reference system is meant to cover thermal energy needs of a s-MFH with 10 dwellings having a net floor area of 50 m² each in the EU CON climate.

If on one hand the operation of the HYBUILD CON reference system and that of the system installed at the Langenwang demo is the same, this cannot be considered about the number of components. In fact, one aspect in which the two systems differ is the number of some components (e.g. the number of decentralized DHW tanks). Considering that the Compactness indicator provides indications about the volume occupied by a system and the energy that is delivered by the same system, the calculation of this index for the HYBUILD CON demo cannot be considered representative of the effective Compactness of the HYBUILD CON system.

4.3.6 Flexibility

The BEMS (Building Energy Management System) installed at the Langenwang demo is not configured to exploit services to the local electrical grid like flexibility. For this reason, this indicator cannot be calculated for this demo.

4.3.7 Return on Investment

As presented in section 2.4.1, the HYBUILD system installed at the Langenwang demo presents important differences in comparison to the HYBUILD CON reference system that is designed to cover thermal energy needs of a s-MFH with 10 dwellings having a net floor area of 50 m² each in the EU CON climate.

As already mentioned in previous sections, if on one hand the operation of the HYBUILD CON reference system and that of the system installed at the Langenwang demo is the same, this cannot be stated about the number of components. The fact that the two systems differ, for example, in the number of some components (e.g. the number of decentralized DHW tanks) leads to different estimation of the initial cost of the two systems. Being the ROI calculation strongly affected by the initial cost of the system, the calculation performed considering the system installed at the Langenwang demo cannot be considered representative of the effective ROI of the HYBUILD CON system.

5 CONCLUSIONS

On the **Mediterranean demonstrator site in Almatret**, the installation and commissioning started during summer 2021 and adjustments were made until the beginning of the summer season. Monitoring data were obtained during summer 2022, which could allow to evaluate system performance during one representative week. The Almatret demo site is mostly identical to the general layout of the Mediterranean HYBUILD system: Fresnel solar collectors, PV panels, low temperature storage tank with PCM linked to the evaporator of the heat pump, a sorption thermal storage system connected to the solar thermal collectors. Several issues faced previous and during system installation and commissioning (such as material shortage, leakage on Fresnel components, adjustments required on the controller of the solar field, motor failures in the solar field, anomalies on the electric system, etc.) were overcome and the system is currently running correctly.

For the HYBUILD system installed at the **Almatret demo site**, several **KPIs** were calculated, based on theoretical calculations and numerical model simulations when necessary. The TES density of the buffer tank was estimated to be $ED_{thermal,buffer} = 76.98$ MJ·m^{-3}, while the TES density of the latent storage module (RPW-HEX) was estimated to be $ED_{thermal,RPW-HEX} = 15.64$ MJ·m^{-3}. Moreover, energy and CO_2 emissions savings were also estimated and the results showed that the HYBUILD system can avoid the emission of 0.63 tons of CO_2 per year. The compactness of the system installed in the technical room of the Almatret demo site was evaluated to be equal to $1.36 \cdot 10^{-3}$ m^3·year·kWh^{-1}. Other KPIs were evaluated for a representative week during summer period, showing satisfactory results in terms of thermal and electrical seasonal performance factor (0.48 and 4.64, respectively), self-consumption (82%), self-sufficiency (58%), and share of renewables (75%).

The **Mediterranean demonstrator in Aglantzia** has been installed during summer – autumn 2021 and commissioned during March 2022. Adjustments were needed during Winter 2021 – 2022 in order to bypass the RPW-HEX as indicated in previous sections. The system has been commissioned and is in operation mode since March 2022. The demonstrator in Aglantzia does not include a solar thermal system, mainly due to the lower DHW demand based on the type of use of the building. For the analysis and the evaluation of the performance of the system, the first week of August has been selected as the summer representative week. The most important **KPIs** were calculated for this demo site such as the seasonal electrical performance factor, the self consumption, the self sufficiency and the share of renewables. From the results can be concluded that the system is very efficient with high SC and SS rates (87% and 91% respectively).

Furthermore, after the analysis of the results, the system shows very satisfactory results in terms of share of renewables (85,1%) thus contributing to the significant reduction of CO_2 emissions.

On both Mediterranean demonstrator sites, the full monitoring plan has been deployed and the operation modes have been defined and implemented, as described in section 3. The demonstrators have then collected representative data during spring and summer 2022.

The **Continental demonstrator in Langenwang** has been deployed and commissioned in late 2020, and then finetuning has been carried out to get the system operative by summer 2021. However, due to different problems, errors in some measurements and the need of adjustments in the control logic, the system operates as expected only in the last month (March 2022). For this reason, the concept of “representative winter week” has been introduced. The representative winter week is defined as a week in the winter period in which the system is operating as expected and all (or almost all) the monitored data are available and reliable. The analysis of system performances over the 3rd representative winter week is the most reliable indication of what can be achieved with the current state of the proposed technology. The system delivers thermal energy for space heating and DHW (with a load created artificially to

ensure a sufficient demand level). The system includes various components: PV plant, RPW-HEX, HP, decentralized DHW tanks, hydraulic and electric connections, cooling/heating ceiling, district heating back-up connection.

For the **continental HYBUILD concept**, several key performance indicators have been calculated.

The **thermal energy storage density** is slightly higher than the value from the tests, **60.2 kWh/m³** during the 2nd representative week instead of **47 kWh/m³**. This last value (47 kWh/m³) is calculated starting from results obtained in laboratory tests. On the contrary, the same quantity calculated over the 3rd representative winter week (**42 kWh/m³**) is more aligned to the one calculated starting from results obtained in laboratory tests (47 kWh/m³). As mentioned in section 4.3, the results in both cases are deeply linked with the operating logic adopted (e.g. conditions on charge/discharge set on temperature threshold).

The **coefficient of performance** (ratio between the thermal output of the generation system and its electrical consumption) and the **performance factor** (ratio between the thermal energy actually delivered to the user and the system electrical consumption) have been calculated for the 3rd representative winter week. These KPI values are respectively **3.7** and **3.1**.

The values for the **share of renewables** and **self-consumption** in the 3rd representative winter week are very high: **84%** and **62%** respectively. Though it is improved by the HYBUILD system the share of renewables is highly dependent on the Austrian electrical energy mix, which is especially rich in renewables (typically 75%). The self-consumption is high due to the limited PV production in the 3rd representative winter week compared with the HP consumption used to cover building thermal needs, thus ensuring the self-consumption of most of the energy produced locally by PV system.

The energy savings depend on the reference system compared with. In the case of HYBUILD CON system, that considered as reference system a gas boiler, the **primary energy savings** are **73%** whereas **CO_2 equivalent emissions** are reduced by **88%**. These notably reductions are partly due to the differences in terms of components used to cover buildings thermal demands (HP + RPW-HEX in the case of HYBUILD solution, gas boiler in the reference system) and partly to the fact that a relevant amount (around 40%) of the electrical energy consumed by the HYBUILD system is covered through on-site renewable energy production through the PV system.

Some KPI such as compactness, flexibility and return on investment have not been calculated. As described in section 4, they have not been considered as relevant due to the context of this demonstration. They should be calculated when the technology will reach a status comparable with the reference HYBUILD CON system, and will offer representative KPI values.The results for the continental HYBUILD concept offer precious feedback and show promising results, even though the overall system is complex to set and operate in optimal conditions. While several TRL steps remain for the full hybrid technology to reach the market, several components will be improved through future initiatives. Deliverables D7.8 and D7.9 describe the future step in the development and exploitation of the results of the project.

6 REFERENCES

[1] David Palinkas, Merche Polo, Alvaro Picatoste and Sergio Costa, 2018 : Requirements for M&V plan for demo sites. Overview of IPMVP Methods. Report for HyBuild project, T6.1

[2] G. S. Brager et R. de Dear, *Center for the Built Environment*, 2001

[3] GIVOINI, Baruch, 1991 : Comfort, climate and building design guidelines, Energy and building, 18 (1992) 11-23.

[4] Vesterberg, Jimmy, Andersson, Staffan, 2016 : A single-variate building energy signature approach for periods with substantial solar gain In: Energy and Buildings, ISSN 0378-7788, E-ISSN 1872-6178, Vol. 122, p. 185-191

[5] Rubitherm RT-PCM. Available online: https://www.rubitherm.eu/en/index.php/productcategory/organische-pcm-rt (ac-cessed on 2 October 2019)

[6] Mselle, B.D.; Zsembinszki, G.; Vérez, D.; Borri, E.; Cabeza, L.F. A detailed energy analysis of a novel evaporator with latent thermal energy storage ability. Applied Thermal Engineering 201 (2022) 117844.